Outcome from stroke: bimanual coordination in daily living and role of mesial frontal cortex

Inaugural dissertation

for the attainment of the title of doctor
in the Faculty of Mathematics and Natural Sciences
at the Heinrich Heine University Düsseldorf

presented by

Jianghai Ruan

from Chongqin, P.R. China

Düsseldorf, 06. 2017

from Cécile and Oskar Vogt Institute of Brain Research
at Heinrich-Heine-Universität Düsseldorf

Published by permission of the Faculty of Mathematics and Natural
Sciences at Heinrich Heine University Düsseldorf

Supervisor: Prof. Dr. Rüdiger J. Seitz
Co-supervisors: Prof. Dr. Petra Stoerig
                Prof. Dr. Katrin Amunts

Date of oral examination: 23rd May 2017

Erklärung

Hiermit erkläre ich ehrenwörtlich, dass ich die vorliegende Dissertation mit dem Titel „Ergebnis aus Schlaganfall: bimanuelle Koordination im täglichen Leben und Rolle der mesialen frontalen Kortex" selbst angefertigt habe. Außer den angegebenen Quellen und Hilfsmitteln wurden keine weiteren verwendet. Diese Dissertation wurde weder in gleicher noch in abgewandelter Form in einem anderen Prüfungsverfahren vorgelegt.

Düsseldorf, den 07. 06. 2017

Jianghai Ruan

Acknowledgements

First of all, I would like to express my heartfelt thanks to Prof. Dr. Rüdiger J. Seitz for giving me this cherish opportunity and excellent working conditions and facilities to purse my doctoral study in Centre of Neurology and Neuropsychiatry, LVR-Klinikum Düsseldorf and Cécile and Oskar Vogt Institute of Brain Research at Heinrich-Heine University, Düsseldorf. His patient direction and help at my study and life allow me to finish doctoral work and enjoy a happy four years time in Germany.

I want to express my sincere appreciations to Prof. Dr. Petra Stoerig to help me improve my studies and dissertation. Also, her positive and careful working spirit will inspire me in the future academic careers.

I very much appreciated Prof. Dr. Katrin Amunts to help me carry out the study in the Cécile and Oskar Vogt Institute of Brain Research. Her patient directions are very important for me to finish my doctoral study.

I am deeply indebted to Dr. Sebastian Bludau for his unforgettable support and help to start the study in the Cécile and Oskar Vogt Institute of Brain Research.

My special thanks to Dr.Nicola Palomero-Gallagher for all of his precious help for discussion about the result of my research.

Acknowledgements

I sincerely thank Prof. Dr.Svenja Caspers and my colleague Dr. Benjamin Sigl for their enthusiastic help during my study period.

I would like to specially thank Prof. Dr.Simon Eickhoff and Mr.Diplom-Physiker Hartmut Mohl-berg for help me to calculate the probality maps and do the MACM analysis.

I also would like to express my sincerely appreciation to Mr. René Hübbers, Mr. Ul-rich Opfermann-Emmerich, Ms. Eleonore Sommerkorn for their well preparation for my research.

I thank all my colleagues in Centre of Neurology and Neuropsychiatry, LVR-Klinikum Düsseldorf and Cécile and Oskar Vogt Institute of Brain Research at Heinrich-Heine University.

I am very grateful to China Scholarship Council, Ministry of Education of China for the financial support during my study in Germany.

In the end, I express my greatest appreciation to my family for their encouraging and supporting me to finish this study.

To all of you, thank you very much!

Abstract

This study included two parts. The part I was oriented to explore the associations between spontaneous movement activity and focal abnormal slow wave activity in the patients with stroke and patients with suspected epilepsy. The part II focused on the cytoarchitecture, probability maps of the human mesial frontal cortex, and a coordinate based functional meta-analysis was performed using the created probabilistic maps of supplementary motor area (SMA) and presupplementary motor area (pre-SMA) as reliable seed regions.

Part I: Focal abnormal slow wave activity (1-4Hz, SWA) has been reported to be a marker of pathological stages rather than a process of healthy aging and the bimanual coordination in real daily living activity has not been studied yet. Using 24-hour video EEG and simultaneous bimanual actiwatch recordings, bimanual coordination was characterized by the Spearman's rank correlation coefficient (r_s), which was calculated from the movement counts of the two arms. The relative movement activity (RMA) between the two arms was calculated using the spontaneous movement counts of the two arms. The EEG pattern (SWA and epileptiform discharge activity) and sleep architecture were scored for individuals. Nine patients with stroke as compared to nine age- and sex-matched control patients with seizures but without vascular disease. It was found that the stroke subjects showed reduced sleep, a decreased r_s in daytime and far less spontaneous movement activity in the affected arm. These result suggested that stroke patients had significant reduced sleep, deficits in bimanual coordination and less spontaneous movement activity in affected arm.

The association between bimanual coordination and focal abnormal SWA was investigated in 153 patients with focal or generalized seizures. It was found that those patients with focal abnormal SWA had a decreased bimanual coordination assessed by r_s. The RMA between the two arms in the patients with focal abnormal SWA showed no significant differences with those patients without abnormal SWA. The SWAs were not related to age and interictal epileptiform discharge activity. In sum, a decreased function of bimanual coordination in real daily living activity was related to the occurrence of SWAs but not to interictal epileptic discharges. This kind of deficit in bimanual coordination was not apparent in neurological motor testing.

Abstract

Part II: The mesial frontal cortex has been subdivided into SMA and pre-SMA, which play an important role in human behaviour. Evidences from cytoarchitectonic, stimulation, and functional studies have found structural and functional divergences between the two subregions. However, a map obtained in a representative sample of brains in a stereotaxic reference space is still lacking. The present study showed that the mesial frontal motor cortex comprised of two structurally heterogeneous brain regions: area SMA and area pre-SMA. Area specific microstructural pattern were quantified using observer-independent cytoarchitectonic analysis based on reproducible cell architectonic and statistical features. Mappings of areas SMA and pre-SMA from ten individual brains were 3D reconstructed, and transferred to a common reference space. The probabilistic maps of areas SMA and pre-SMA were created by superimposing the individual delineations. A coordinate based functional meta-analysis was subsequently performed using the created probabilistic maps as reliable seed regions. It revealed that areas SMA and pre-SMA were strongly co-activated with precentral gyrus, supramarginal gyrus, superior frontal gyrus, rolandic operculum, thalamus, putamen and cerebellum. Moreover, both areas were related to motor functions, but area pre-SMA was related to more complex processes such as learning, cognitive process, perception. The here described subsequent analyses led to converging evidences which support the microstructural and functional segregation of areas SMA and pre-SMA.

Zusammenfassung

Diese Studie umfasste zwei Teile. Der Teil I war bestrebt, die Assoziationen zwischen spontaner Bewegungsaktivität und fokalen abnormen langsamen Wellenaktivitäten bei Patienten mit Schlaganfall und Patienten mit vermuteter Epilepsie zu untersuchen. Der Teil II konzentrierte sich auf die Cytoarchitektur, Wahrscheinlichkeitskarten der menschlichen mesialen frontalen Kortex und eine koordinationsbasierte funktionale Metaanalyse wurde mit den erzeugten probabilistischen Karten des Supplementär motorischen Area (SMA) und des Prä-supplementär motorischen Area (Prä-SMA) als zuverlässig durchgeführt Saatgutregionen

Teil I: Focal abnorme langsame Welle Aktivität (1-4Hz, SWA) wurde berichtet, dass ein Marker von pathologischen Stadien statt ein Prozess der gesunden Alterung und die bimanuelle Koordination in echten täglichen Lebenstätigkeit wurde noch nicht untersucht. Mit Hilfe von 24-Stunden-Video-EEG und simultanen Bimanual-Actiwatch-Aufnahmen war die Bimanual-Koordination durch den Rangkorrelationskoeffizienten (r_s) des Spearmans charakterisiert, der aus den Bewegungszählungen der beiden Arme berechnet wurde. Die Relativbewegungsaktivität (RMA) zwischen den beiden Armen wurde unter Verwendung der spontanen Bewegungszählungen der beiden Arme berechnet. Das EEG-Muster (SWA und epileptiforme Entladung Aktivität) und Schlaf-Architektur wurden für Einzelpersonen bewertet. Neun Patienten mit kortikalen oder subkortikalen Schlaganfall wurden mit neun alters- und geschlechtsbezogenen Kontrollpatienten mit Krampfanfällen, aber ohne Gefäßerkrankung, verglichen. Es wurde festgestellt, dass die Schlaganfall-Patienten reduzierten Schlaf, eine verringerte r_s in tagsüber und weit weniger spontane Bewegung Aktivität in den betroffenen Arm. Diese Ergebnisse schlugen vor, dass Schlaganfallpatienten signifikant reduzierten Schlaf, Defizite in der bimanuellen Koordination und weniger spontane Bewegungsaktivität im betroffenen Arm hatten.

Die Assoziation zwischen bimanueller Koordination und fokalen abnormen SWA wurde bei 153 Patienten mit fokalen oder generalisierten Anfällen untersucht. Es wurde festgestellt, dass diese Patienten mit fokalen abnormen SWA eine verminderte bimanuelle Koordination von rs. Die RMA bei den Patienten mit fokalen abnormen

Abstract

SWA zeigte keine signifikanten Unterschiede mit diesen Patienten ohne anormale SWA. Die SWAs waren nicht mit dem Alter und der interlimalen epileptiformen Entladung verbunden. In Summe war eine verminderte Funktion der bimanuellen Koordination in der realen täglichen Lebenstätigkeit mit dem Auftreten von SWAs verbunden, aber nicht mit interparalen epileptischen Entladungen. Diese Art von Defizit in der bimanuellen Koordination zeigte sich bei der neurologischen Motorprüfung nicht.

Teil II: Der mesiale frontale Kortex wurde in den SMA und Prä-SMA unterteilt, die eine wichtige Rolle im menschlichen Verhalten spielen. Evidenz aus zytoarchitektonischen, stimulierenden und funktionellen Studien haben strukturelle und funktionelle Divergenzen zwischen den beiden Teilbereichen gefunden. Jedoch fehlt noch eine Karte, die in einer repräsentativen Stichprobe von Gehirnen in einem stereotaxischen Referenzraum erhalten wird. Die vorliegende Studie zeigte, dass der mesiale frontale motorische Kortex aus zwei strukturell heterogenen Hirnregionen besteht: Bereich SMA und Bereich Prä-SMA. Das flächenspezifische Mikrostrukturmuster wurde mittels Beobachter-unabhängiger zytoarchitektonischer Analyse auf der Grundlage reproduzierbarer zellarchitektonischer und statistischer Merkmale quantifiziert. Mappings der Bereiche SMA und Prä-SMA aus zehn einzelnen Gehirnen wurden 3D rekonstruiert und auf einen gemeinsamen Referenzraum übertragen. Die probabilistischen Karten der Bereiche SMA und Prä-SMA wurden durch Überlagerung der einzelnen Abgrenzungen geschaffen. Eine koordinationsbasierte funktionale Metaanalyse wurde anschließend mit den erzeugten probabilistischen Karten als zuverlässige Saatgebiete durchgeführt. Es zeigte sich, dass die Bereiche SMA und Prä-SMA stark mit dem präzenten Gyrus, dem supramarginalen Gyrus, dem oberen frontalen Gyrus, dem rolandischen Operculum, dem Thalamus, dem Putamen und dem Cerebellum kooperiert wurden. Darüber hinaus waren beide Bereiche mit motorischen Funktionen verknüpft, aber Bereich Prä-SMA war mit komplexeren Prozessen wie Lernen, kognitiven Prozess, Wahrnehmung verbunden. Die hier beschriebenen analogen Analysen führten zu konvergierenden Beweisen, die die mikrostrukturelle und funktionelle Segregation der Bereiche SMA und Prä-SMA unterstützen.

Table of contents

Table of contents

Part I Outcome from stroke: bimanual coordination in daily living and role of mesial frontal cortex

1 Introduction

1.1 Outcome from stroke: Deficit in bimanual coordination

Bimanual movements are extremely important in most of our daily activities, e.g. the fork and knife for eating and lacing shoes. In activities, the two hands are used mostly together to execute bimanual tasks (Kilbreath and Heard 2005). During the process of executing, the relative direction of the moving limbs in external space may interact with muscular constraints to stabilize or destabilize coordination patterns (Temprado, et al. 2003). Bimanual coordination was found to be impaired in patients following stroke (Kilbreath, et al. 2006; Kantak, et al. 2016). The disruption of spontaneous inter-limb coordination patterns might be caused by the stroke-induced impairments in the neuro-musculo-skeletal system (Temprado, et al. 2007; Sleimen-Malkoun, et al. 2011). Bilateral training can improve unilateral paretic limb functions of the upper extremity after stroke (McCombe, et al. 2008). Moreover, compared with unilateral training, bilateral coordination recovery training was found to be important for functional rehabilitation of patients with cerebrovascular accidents (Cauraugh, et al. 2002).

The deficits in bimanual coordination could not be predicted by common clinical testing of paretic arm impairment (Kantak, et al. 2016). That means that patients who show impairments in bimanual coordination cannot be detected by normal neurological clinical testing. However, bimanual finger movements, drawer manipulandum and simple whole-hand movements (Kazennikov, et al. 2002; Koeneke, et al. 2004; Grefkes, et al. 2008) are comparatively simple. Tasks studies on complex and irregular bimanual actions of daily life are still lacking. The bimanual coordination in daily living is still unknown.

1.2 Cortical network involved in bimanual coordination

EEG and functional imaging studies have found that bimanual coordination relies on an extended neuronal network associated with primary sensorimotor cortices, lateral premotor cortex, mesial frontal cortex (pre-SMA and SMA), cingulate motor area, basal ganglia, and cerebellum (Cardoso de Oliveira 2002; Muller, et al. 2011). In the cortical network, the mesial frontal area plays a prominent role in promoting or suppressing activity in the cortical motor network driving uni- and bilateral hand movements (Grefkes, et al. 2008; Garbarini and Pia 2013) and the SMA participates in planning and execution of sequential unimanual and bimanual movements (Gerloff, et al. 1997; Tanji, et al.1988; Tanji and Shima, 1994; Toyokura, et al. 1999). The prominent corticospinal projection of SMA may subserve the functions of temporal and spatial sequencing for bilateral movements (Seitz, et al. 2000).

1.3 Focal abnormal SWA in patients with brain lesions

Slow wave rhythm is a normal characteristic involving to deep sleep (Rechtschaffen 1968). However, the focal abnormal slow wave activity (delta waves, 1-4Hz, SWA) occurs in patients with structural lesions including stroke, subdural hematomas, tumour (Bassetti and Aldrich 2001; Inui, et al. 2001; Vock, et al. 2002; Baayen, et al. 2003; de Jongh, et al. 2003; Chu, et al. 2015). SWAs were also found in mental disorders (schizophrenic, depressive) (Hoffmann, et al. 2000; Rockstroh, et al. 2007), degenerative neurological disorders including lewy bodies disease, Alzheimer disease, Parkinson's disease (Helkala, et al. 1991; Yener, et al. 1996; Lindau, et al. 2003; Chan, et al. 2004), as well as in toxic and metabolic encephalopathy (Smith 2005). Findings from electroencephalographic studies have attributed focal SWA to pathological or "dysfunctional" neural tissue and to predict poor recovery (Burghaus, et al. 2007; Leirer, et al. 2011; Chinoy, et al. 2014). In the diseases showing SWAs, a progressive increase in SWAs parallels the increasing severity of the brain disorder (Smith 2005). In patients with Alzheimer disease, the greater slowing of EEG pattern suggested more severe cognitive deficits (Helkala, et al. 1991; Elmstahl, et al. 1994; Strijers, et al. 1997; Locatelli, et al. 1998; Fernandez, et al. 2002; Jeong 2004).

Focal abnormal SWA exists also in some patients with epilepsy and seizure disorder (Hughes and Fino 2004). Not like the epileptiform discharge, SWAs are thought to be a type of non-epileptiform EEG abnormality but are non-specific (Ishibashi, et al. 2002;

Andraus and Alves-Leon 2011). In the stroke patients, studies have found that SWAs predict poor recovery of stroke and reflect the functional recovery of stroke (Reith, et al. 1997; Cyril Charlin 2000; Arboix, et al. 2003; Jordan 2004; Meinzer, et al. 2004; Burghaus, et al. 2007).

1.4 Focal SWA in subjects with no substantial brain lesions

Focal SWAs can also be found in normal aged subjects (Torres, et al. 1983; Visser, et al. 1987; Wienbruch 2007; Leirer, et al. 2011; Kolassa, et al. 2012; Chinoy, et al. 2014). Although the focal SWAs subgroup proved to perform poorly on some aspects of the function (Visser, Hooijer et al. 1987), these patients had no substantial brain lesions or other neurological diseases. The definite mechanism of SWAs is still unclear, the occurrence of focal abnormal SWAs is thought to be related to cortical atrophy (lower cortical gray matter volume) (Babiloni, Carducci et al. 2013) or loss of neurotransmitters (e.g. choline acetyltransferase) (Neufeld, et al. 1994; Briel, et al. 1999). Interestingly, use of cholinergic monoaminergic blockade can partially improve the EEG slowing pattern (Neufeld, et al. 1994; Dringenberg 2000; Osipova, et al. 2003). Therefore, the author tend to agree that occurrence of SWAs can be classified as a "dysfunctional state" or "pathological state" of the neuronal tissue (Lewine and Orrison 1995; Leirer, et al. 2011).

1.5 Objective of the study

Two trials were performed in this study. The first trial was designed to examine the function of bimanual coordination in the stroke patients in daily living activities and compare them with the age- and sex-matched patients without cerebral vascular disease and obviously motor dysfunction. The EEG patterns in the two groups were also detected. The second trial was carried out to assess bimanual coordination for the patients with seizures but no motor dysfunction in activities of daily living. Based on the assumption that the bimanual coordination may be indicated by the EEG patterns such as focal abnormal SWAs, it was hypothesized that bimanual coordination is related to the EEG pattern even in those patients who show no obvious differences on

neurological examination. In the two trials, the EEG pattern was explored. Thus, it allows us to detect the association between the bimanual coordination and EEG pattern.

2 Methods

2.1 Trial one: Reduced sleep and bimanual coordination in acute stroke

2.1.1 Patients with stroke

This prospective clinical study was performed from March 2013 until April 2014. Included into the study were 9 consecutive, right-handed patients who were treated in the Centre of Neurology and Neuropsychiatry of the LVR Klinikum Düsseldorf, aged 68.2±7.6 years presenting with acute ischemic stroke.

Inclusion criteria were:

1. Onset of hemipares is no more than 14 days before the 24-hour video EEG recording,

2. Acute ischemic infarct lesion assessed by diffusion weighted magnetic resonance imaging (MRI),

3. First-ever stroke with no prior brain lesions as detected by T2 weighted MRI,

4. Full capacity to comply with the task instruction.

Exclusion criteria were:

1. Severe systemic disease such as sepsis, myocardial infarct, etc. and past epilepsy or seizures,

2. Reduced consciousness,

3. Intracranial hemorrhage,

4. Sensory aphasia,

5. Anticonvulsive or sedative treatment.

During their stay in hospital, the patients received medical treatment with respect to their specific status according to the present stroke guideline (Jauch, et al. 2013). One stroke patient received systemic thrombolysis treatment with body-weight adjusted alteplase. All patients had a continuous 72-hour monitoring of heart rate, blood pressure, blood oxygen saturation, measurement of body temperature, and testing of blood samples including blood sugar levels. The score of the National Institutes of Health

Stroke scale (NIHSS) (Brott, et al. 1989) was assessed by experienced clinical observers on admission, at six hour intervals during the first 72 hours, and at discharge.

The 24-hour video-EEGs and concurrent actigraph recordings were performed at the time when the patients could be transferred out from the acute stroke unit to the video-EEG examination room. Informed consent was obtained from each patient before the investigation. The study was approved by the Ethics Committee of the Heinrich-Heine University, Düsseldorf (#4206).

2.1.2 Controls

Nine age- and gender-matched, right-handed patients clinically suspicious of epilepsy (two women, seven men) aged 68.2±11.7 years were investigated, while they were hospitalized in our department between March 2013 and April 2014 for work-up of presumptive seizure activity. They were neurologically normal and, in particular, had no motor deficit. Measurements with the 24-hour video-EEG and actiwatches were identical to those of the stroke patients (see below).

2.1.3 Accelerometry

Accelerometry by actiwatches is a well-established and validated method for recording spontaneous movement activity of arms or legs (Siekierka-Kleiser, et al. 2006; Seitz, et al. 2011). To invest the bimanual spontaneous movements continuously, recordings with actiwatches (Cambridge Neuro-technology, Cambridge, UK; http://camntech.co.uk) were done. The device, a small light-weight gadget the size of a wrist-watch, synchronously recorded arm movements for 24h in all three dimensions with movement-sensitive sensors. The actiwatches were placed on the both wrists of the subjects, respectively. Counts of activities were binned into one-minute-epochs in which the movement activity was integrated by each device (Actiwatch Activity &Sleep Analysis 5.42, Cambridge Neuro-technology). The sensitivity of the actiwatches calibrated. Thus, the counts per minute of the arm movements were acquired from actiwatchs. Data from the actiwatches were analyzed off-line using SPSS (version17.0; SPSS Inc.) software. The movement artefacts due to nursing were eliminated from the data. The relative arm movement activity were the mean activity of the affected arm divided by that of the unaffected arm in the stroke patients, and the mean activity of the left arm divided by that of the right arm in the control patients.

2.1.4 EEG data acquisition

EEGs were recorded using a nineteen-channel analogue recorder (Nihon Kohden EEG-1200) according to the international 10–20 system (American Clinical Neurophysiology 2006) consecutively for 24 hours. In addition, a video camera (Nihon Kohden) located on the ceiling above the patient recorded the behavioural data. EEG and video data were recorded in a time-locked fashion. The electrodes were placed using a quantified ruler and a marker pencil to mark strictly on the scalp by hand. The impedances of the electrodes were kept less than 10 kΩ. Filter settings were 0.3–40 Hz. Also, to score sleep stage accurately, electrooculographic channels were placed mainly following *The AASM Manual for the Scoring of Sleep and Associated Events: rules, terminology and technical specifications (AASM Manual)* (Iber C 2007). The EEG and video data were displayed simultaneously off-line on a personal computer for formal and statistical analysis. Two reviewers scored the sleep stages mainly based on *AASM Manual*. Reference montages (reference electrodes: Cz, average electrode) were used as well as bipolar montages (longitudinal: Fp2-F4, F4-C4, C4-P4, P4-O2; Fp2-F8, F8-T8, T8-P8, P8-O2 (accordingly on the left side) to assess sleep stages and epileptiform discharges and focal SWAs. Only when the two reviewers reached an agreement the data would be brought into the finally statistical analysis.

In this study, abnormal focal SWA was defined as in (Ahmed 1988; Burghaus, et al. 2007): Slow wave activity (1-4Hz) repeatedly presented asymmetrically in EEG electrodes during waking periods or non-deep sleep stage. In addition, sleep was graded according to the AASM manual. Specifically, the total sleep time (TST), the wake after sleep onset (WASO), the proportion of non-rapid eye movement sleep (NREM), and the proportion of rapid eye movement sleep (REM) were assessed from the EEG recordings.

2.2 Trial two: bimanual coordination in daily living and SWA activity in patients with focal or generalized seizures

2.2.1 Participants

This prospective clinical study was performed in the Centre of Neurology and Neuropsychiatry of the LVR Klinikum Düsseldorf from March 2013 until June 2016.

153 subjects who had focal or generalized seizures or were suspicious of having epileptic seizures participated in this study. The patients were treated with anti-epileptic drugs according to treatment guidelines of the International League against Epilepsy (Glauser, et al. 2006). They in particular, showed no dysfunction in daily living and motor deficit or psychiatric illnesses. All patients had monitoring of heart rate, blood pressure, blood oxygen saturation, measurement of body temperature, and testing of blood samples including blood sugar levels. According to the specific status of individuals, the patients received antiepileptic drugs treatment with levetiracetam, valproate, lamotrigin, lacosamid or lorazepam. All the patients received brain MRI examines after hospitalized.

2.2.2 Procedures

In addition to a routine 20-chanel EEG involving an episode of hyperventilation, the patients had a 24-hour video-EEGs concurrent with actigraphy recordings with actiwatches on both arms. Measurements with the 24-hour video-EEG and actiwatch recording were identical on all the patients. Informed consent was obtained from each patient before the investigation.

2.2.3 EEG and actigraphy data acquisition

The settings of EEG and actiwatches are same with the first trial. Abnormal focal SWA was defined as in (Ahmed 1988; Burghaus, et al. 2007): Slow wave activity (1-4Hz) repeatedly presented asymmetrically in EEG electrodes during waking periods or non-deep sleep stage. In addition, sleep was graded according to the AASM manual (Iber 2007). The actiwatches recorded the movements of the two arms synchronously and the counts of activities were binned into one-minute-epochs (counts/min.). The movement Spearman's rank correlation coefficient (r_s) between two arms is calculated by using the activity data obtained by bimanual actigraphy recording. Higher movement divergences between two arms will lead to a lower r_s of two arms. The r_s is used to quantitatively depict the spontaneous bimanual coordination (Fig. 2.2.3.1).
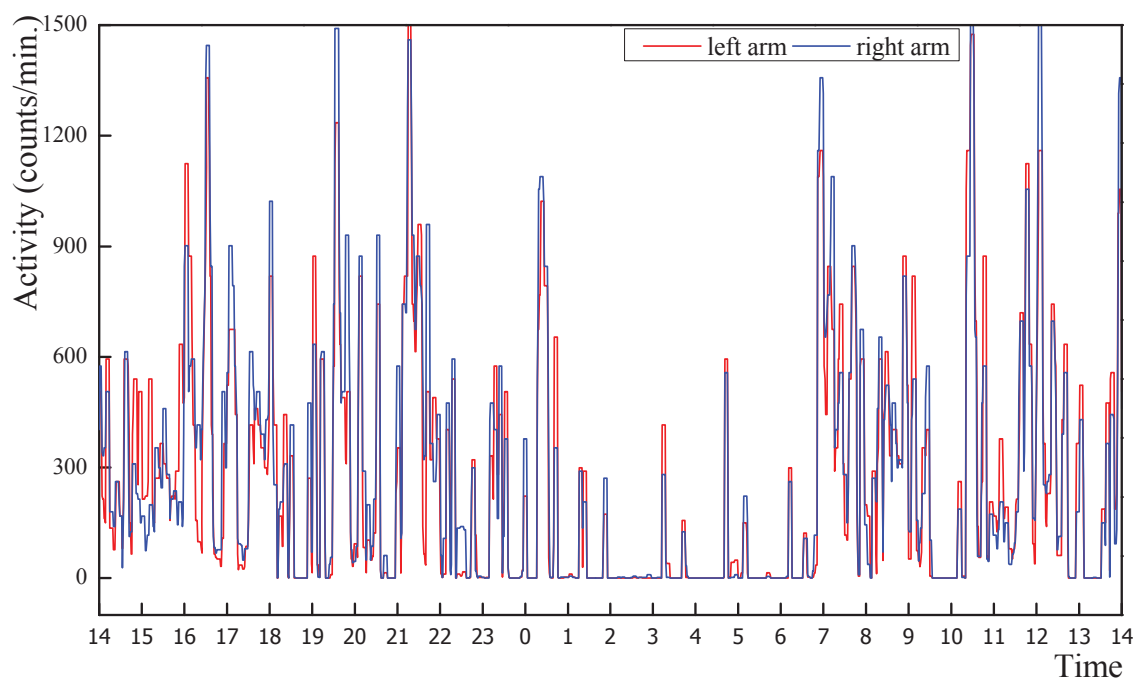
Fig. 2.2.3.1 The movement count–time curve of one patient without abnormal SWA deprived from bimanual synchronous actigraphy recording. With the obtained bimanual movement counts, the spontaneous Spearman's rank correlation coefficient (r_s) for this patient was calculated ($r_s=0.954$). Then, the r_s was used to quantify the bimanual coordination of this patient.

2.3 Statistical evaluation

The total sleep time (TST), the wake after sleep onset (WASO), the proportion of non-rapid eye movement sleep (NREM), and the proportion of rapid eye movement sleep (REM) were assessed from the EEG recordings. The sensitivity of the two actiwatches was calibrated to the same level. The counts per minute of the arm movements were acquired from actiwatchs. The bimanual coordination in the 24 hours, daytime, and sleep time were characterized by the Spearman's rank correlation coefficient (r_s) in the 24 hours (r_{s24h}), daytime (r_{sd}), and sleep time (r_{sn}) of the movement counts of two arms, respectively. In the trial one, the relative arm movement activity (RMA) over 24 hours (RMA_{24h}), in daytime (RMA_d) and during sleep time (RMA_n) were the mean activity of the affected arm in respective time duration divided by that of the unaffected arm in the stroke patients, and the mean activity of the left arm divided by that of the right arm in the control patients. In trial two, the relative movement activity of the left arm compared to right arm over 24 hours (RMA_{24h}), in daytime (RMA_d) and during sleep time (RMA_n) were calculated from the movement counts of two arms.

All data were presented as means ± standard deviation (SD). Group comparisons of the quantified items were based on t-test. The Mann-Whitney test was used to assess group differences in qualitative variables. All tests were 2-sided with $P < 0.05$ considered statistically significant. Statistical analysis was performed using SPSS Statistics 17.0 (SPSS Inc, 2009).

3 Results

3.1 Stroke patients

The demographic and clinical characteristics of the stroke patients and controls are summarized in Table 3.1.1. The sex ratios and ages of the two groups showed no differences. As expected, the sleep time was significantly reduced in the stroke patients than in the controls (P=0.031). There were significant differences in sleep efficiency (P=0.019), percent of non-rapid eye movement (%NREM, P=0.034), wake after sleep onset (WASO, P=0.012) and REM latency (P=0.009) between stroke patients and controls. Moreover, the stroke patients and controls had no differences in sleep architecture parameters except for mean percentage of sleep stage N2 (P=0.003). The stroke patients showed less spontaneous movement activity in their affected arm than control subjects. Compared to controls, the stroke patients showed affected bimanual coordination during daytime (r_s =0.462, P=0.019). And they also presented with lower mean of relative movement activity (RMA) at daytime (P=0.004) and night awake time (P=0.004). Notably, these divergences of r_s and RMA no longer exist during night sleep time (Table 3.1.1).

To further analyze the relation between spontaneous movement activity and EEG pattern, we divided the nine stroke patients into two groups: patients with SWAs (n=4) group and patients without SWAs (n=5) group. The result showed that the two groups were comparable concerning sex ratio, age, interval since stroke onset and NIHSS scores at admission, however, the patients with SWAs had a lower bimanual coordination (assessed by r_s) and a lower relative movement activity of the affected arm at daytime (P=0.050, 0.014 respectively), night wake time (P=0.027, 0.014 respectively), and even of RMA during sleep time (P=0.014) compared to the patients without SWAs. Also, these changes were identical to the NIHSS scores at discharge (P=0.014). The other difference was that the two groups had a difference on the percent of epileptiform discharge activity (P=0.025) .The general sleep parameters and sleep architecture of the two groups, however, did not significantly differ (Table 3.1.2).

The stroke patients were grouped into cortical infarct group and subcortical infarct group according to the area of the lesions. Three of four stroke patients with cortical lesions showed abnormal epileptiform discharge acitivities or SWAs (two patients with

both epileptiform discharge and SWAs). Instead, there was only one patient with SWAs and no patient with epileptiform discharge activity in the subcortical infarct patients. The two groups differed statistically only on NIHSS scores at admission (Table 3.1.3).

Table 3.1.1 Demographics, sleep EEG and actiwatch parameters of the stroke and control group

	Stroke group (n=9)	Control group (n=9)	P
Male : female(ratio)	6:3	7:2	0.730
Age (years, mean±SD)	68.2±7.6	68.2±11.7	0.863
Movement parameters			
r_{s24h} (mean±SD)	0.462±0.249	0.752±0.127	0.019*
r_{sd} (mean±SD)	0.549±0.235	0.802±0.129	0.050*
r_{sn} (mean±SD)	0.405±0.244	0.585±0.215	0.161
RMA_{24h}(%, mean±SD)	38.0±30.5	104.6±45.1	0.004**
RMA_d(%, mean±SD)	40.6±37.5	105.6±36.4	0.004**
RMA_n(%, mean±SD)	52.9±47.5	100.3±42.4	0.077
EEG parameters			
Sleep latency (min, mean±SD)	16.7±7.6	19.0±11.6	0.965
WASO (min, mean±SD)	284.7±126.3	131.9±60.9	0.012*
TST (min, mean±SD)	315.7±125.9	419.2±66.7	0.031*
REM latency (min, mean±SD)	224.2.3±49.8	134.7±66.1	0.009**
Sleep efficiency (%)	55.1±16.9	74.1±9.7	0.019*
Sleep architecture			
R (%, mean±SD)	2.2±1.7	4.6±3.8	0.268
N 1 (%, mean±SD)	16.6±12.0	13.7±4.9	0.847
N 2 (%, mean±SD)	20.9±8.1	36.8±8.5	0.003**
N 3 (%, mean±SD)	15.7±9.5	19.0±11.7	0.700
NREM (%, mean±SD)	53.3±16.3	69.5±16.1	0.034*

Note:** P <0.01,* P <0.05, r_{s24h}= bimanual Spearman's rank correlation coefficient of 24 hours, r_{sd}= bimanual spearman's rank correlation coefficient of daytime (24hours minus the time in bed in the night), r_{sn}= bimanual spearman's rank correlation coefficient of the night (from sleep onset to sleep end) , RMA_{24h}, RMA_d, RMA_n = relative movement activity of the affected arm compared to unaffected arm in stroke patients or the left arm compared to right arm in controls in 24 hours, in daytime and night time, respectively. WASO= wake after sleep onset, TST= total sleep time, NREM= Non-rapid eye movement sleep, REM= rapid eye movement sleep. SD= standard deviation.

Table 3.1.2 Comparison of the stroke patients with SWA and without SWA

	SWA subgroup (n=4)	No SWA subgroup (n=5)	P
Male : female(ratio)	2:2	4:1	0.655
Age (years, mean±SD)	64.7±5.0	68.2±8.1	0.453
Time since stroke (days, mean±SD)	12.0±1.7	8.8±5.1	0.442
Cortical:subcortical stroke (ratio)	3:1	1:4	0.120
NIHSS on admission (mean±SD)	10.3±6.4	6.2±4.4	0.387
NIHSS at discharge (mean±SD)	10.7±2.5	1.8±2.0	0.014*
NIHSS changes(mean±SD)	0.3±4.0	-4.4±4.5	0.080
Patients with epileptic discharges	2	0	0.371
Movement parameters			
r_{s24h} (mean±SD)	0.266±0.152	0.618±0.195	0.050*
r_{sd} (mean±SD)	0.368±0.141	0.693±0.192	0.027*
r_{sn} (mean±SD)	0.251±0.183	0.528±0.228	0.086
RMA_{24h}(%, mean±SD)	8.6±8.2	61.6±16.0	0.014*
RMA_d(%, mean±SD)	6.2±3.9	68.1±26.1	0.014*
RMA_n(%, mean±SD)	8.1±8.3	88.7±28.9	0.014*
General sleep parameters			
Sleep latency (min, mean±SD)	15.9±7.6	17.4±8.4	0.785
WASO(min, mean±SD)	318.5±94.9	257.7±152.0	0.324
Total sleep time (min, mean±SD)	335.9±139.6	299.6±127.9	0.696
REM latency (min, mean±SD)	218.3±71.3	229.0±33.1	0.771
Sleep efficiency (%)	55.7±16.6	54.7±19.2	0.937
Sleep architecture			
R (%, mean±SD)	2.7±2.2	1.7±1.1	0.734
N 1 (%, mean±SD)	14.4±6.4	19.1±16.8	0.867
N 2 (%, mean±SD)	20.9±8.9	20.8±8.4	0.773
N 3 (%, mean±SD)	19.7±11.0	11.6±6.7	0.386
NREM (%, mean±SD)	55.0±16.7	51.6±18.3	0.950

Note: * P <0.05, r_{s24h}= bimanual Spearman's rank correlation coefficient of 24 hours, r_{sd}= bimanual spearman's rank correlation coefficient of daytime (24hours minus the time in bed in the night), r_{sn}= bimanual spearman's rank correlation coefficient of the night (from sleep onset to sleep end) , RMA_{24h}, RMA_d, RMA_n = relative movement activity of the affected arm compared to unaffected arm in stroke patients or the left arm compared to right arm in controls in 24 hours, in daytime and night time, respectively. WASO= wake after sleep onset, TST= total sleep time, NREM= Non-rapid eye movement sleep, REM= rapid eye movement sleep. SD= standard deviation.

Table 3.1.3 Comparison of the patients with cortical and subcortical infarcts

	Cortical infarcts (n=4)	Subcortical infarcts (n=5)	P
Male : female (ratio)	2:2	4:1	0.655
Age (years, mean±SD)	69.3±9.9	65.4±6.1	0.219
Stroke onset time (days, mean±SD)	11.0±3.0	9.4±5.1	0.756
NIHSS on admission (mean±SD)	14.0±1.0	4.0±1.0	0.014*
NIHSS at discharge (mean±SD)	8.7±5.9	3.0±3.5	0.108
NIHSS changes (mean±SD)	-5.3±5.8	-1.0±3.7	0.802
Patients with SWAs	3	1	0.120
Patients with epileptic discharges	3	0	0.025*
Actiwatch parameters			
r_{s24h} (mean±SD)	0.364±0.315	0.540±0.181	0.327
r_{sd} (mean±SD)	0.516±0.279	0.575±0.225	0.462
r_{sn} (mean±SD)	0.387±0.340	0.419±0.179	0.624
RMA_{24h}(%, mean±SD)	23.5±27.5	49.4±30.6	0.221
RMA_{d}(%, mean±SD)	24.2±36.9	53.7±36.2	0.286
RMA_{n}(%, mean±SD)	17.1±25.4	81.5±41.4	0.027*
General sleep parameters			
Sleep latency (min, mean±SD)	13.9±7.6	19.0±7.6	0.327
WASO (min, mean±SD)	271.0±142.7	295.7±127.6	0.806
TST (min, mean±SD)	348.2±128.6	289.8±132.0	0.327
REM latency (min, mean±SD)	224.5±68.4	224.0±38.1	1.000
Sleep efficiency (%)	48.9±15.9	60.1±17.8	0.462
Sleep architecture			
R (%, mean±SD)	2.3±1.9	2.1±1.8	0.773
N 1 (%, mean±SD)	11.7±4.9	21.8±15.6	0.284
N 2 (%, mean±SD)	21.0±9.0	20.8±8.4	0.486
N 3 (%, mean±SD)	16.3±9.9	15.0±7.4	0.691
NREM (%, mean±SD)	48.9±13.1	57.6±20.0	0.386

Note: * P <0.05, r_{s24h}= bimanual Spearman's rank correlation coefficient of 24 hours, r_{sd}= bimanual spearman's rank correlation coefficient of daytime (24hours minus the time in bed in the night), r_{sn}= bimanual spearman's rank correlation coefficient of the night (from sleep onset to sleep end) , RMA_{24h}, RMA_{d}, RMA_{n} = relative movement activity of the affected arm compared to unaffected arm in stroke patients or the left arm compared to right arm in controls in 24 hours, in daytime and night time, respectively. WASO= wake after sleep onset, TST= total sleep time, NREM= Non-rapid eye movement sleep, REM= rapid eye movement sleep. SD= standard deviation.

Three of four cortical infarct patients had similar lesions, but they had different EEG pattern and actiwatch parameters. Patient 1 showed abnormal epileptiform discharges

and no SWA (Fig. 3.1.2). The patient had an ischemic infarct which affected the right peri-insular cortex but spared the subcortical structures such as the basal ganglia and the internal capsule. On admission she was severely affected (NIHSS 14) and subjected to systemic thrombolysis which improved her neurological condition profoundly (NIHSS of 2 at discharge). She showed a high relative movement activity (64.7% within 24 h, 63.7% at daytime and 68.0% at night respectively). Her arm movement activity was highly correlated among the two arms r_s 0.803 at daytime and 0.855 at night, respectively and with a high symmetry across the two arms as evident from the regression coefficient (Fig. 3.1.1).

Patient 2 suffered an ischemic infarct affecting the right pericentral and anterior parietal cortex involving also the hemispheric paraventricular white matter. This subject was severely affected with a NIHSS 13 on admission and 11 at discharge, respectively. The patient showed focal SWA but no epileptiform discharges. The actiwatches showed that he had a low relative movement activity of his affected arm (10.0% within 24 h, 10.0% at daytime and 11.0% at night respectively) and a low correlation of the movement activity of his arms (r_s of, 0.368 at daytime and 0.522 at night, respectively (Fig. 3.1.2).

Patient 3 suffered an ischemic infarct lesion affecting the centre of the territory of the right middle cerebral artery including the insular and temporal cortex as well as the basal ganglia and the entire posterior limb of the internal capsule (Fig. 3.1.3). His NIHSS was 15 at baseline and 13 at discharge, respectively. The patient showed a very low relative movement activity during daytime (2.1%) and even less at night (0.7%) and generated almost no movement activity with his affected left arm but lots of activity with his right arm. His EEG revealed both abnormal epileptiform discharge and focal SWA (Fig. 3.1.3).

It was noted that one patient with a right-sided subcortical infarct showed focal SWA in the EEG. His ischemic infarct lesion involved the basal ganglia and the anterior and posterior limb of his internal capsule. The NIHSS was 3 on admission but he deteriorated despite aspirin treatment leaving him with a NIHSS of 8 at discharge. The patient showed a very low relative movement activity (4.5%) with a low correlation of both arms (Fig. 3.1.4).
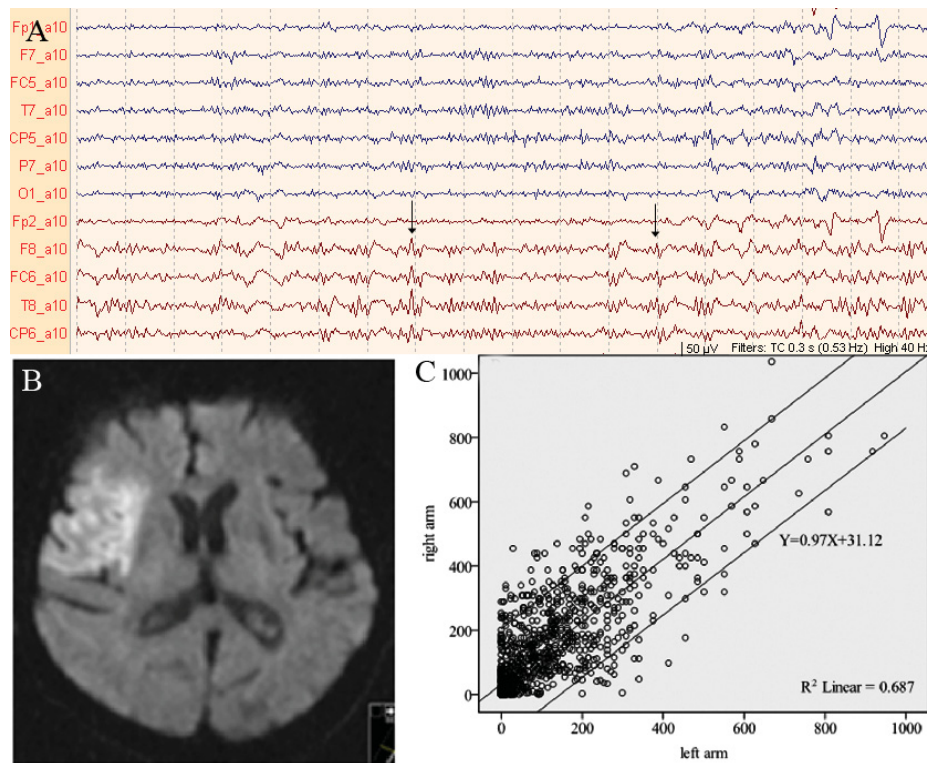
Fig. 3.1.1 A 78 year-old woman with peri-insular infarct and highly correlated arm movement activity and epileptiform discharges in EEG (arrow).
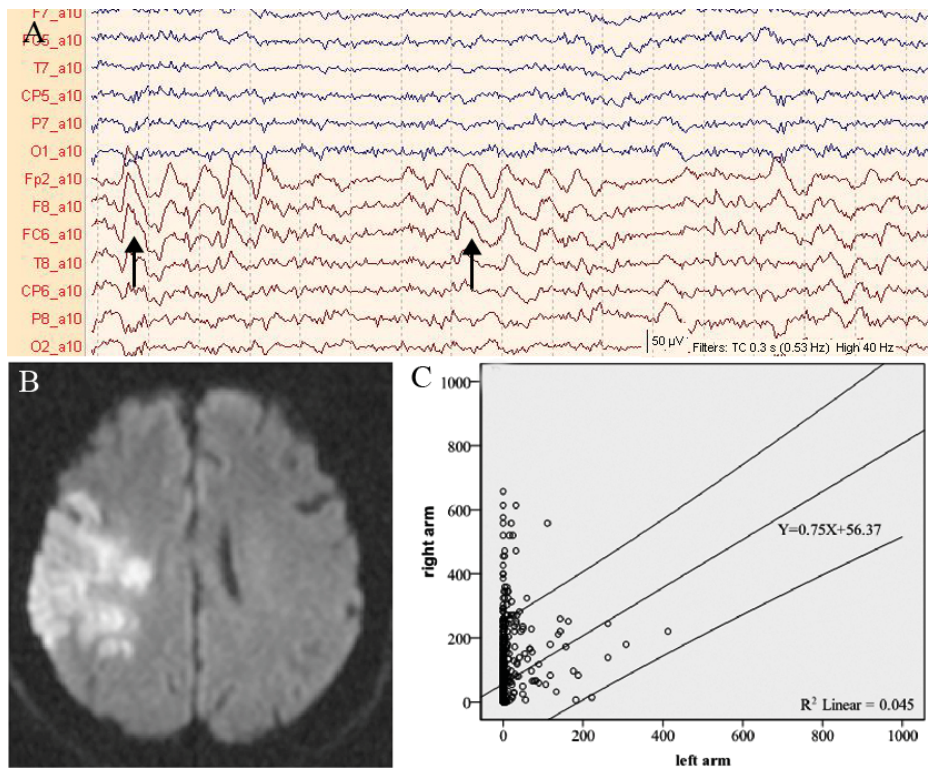
Fig. 3.1.2 A 60 year-old man with an ischemic infarct affecting the pericentral and anterior parietal cortex and a severe clinical involvement. Note the lack of correlation of the activity of his two arms. The EEG revealed focal slow wave activity (thick arrows).
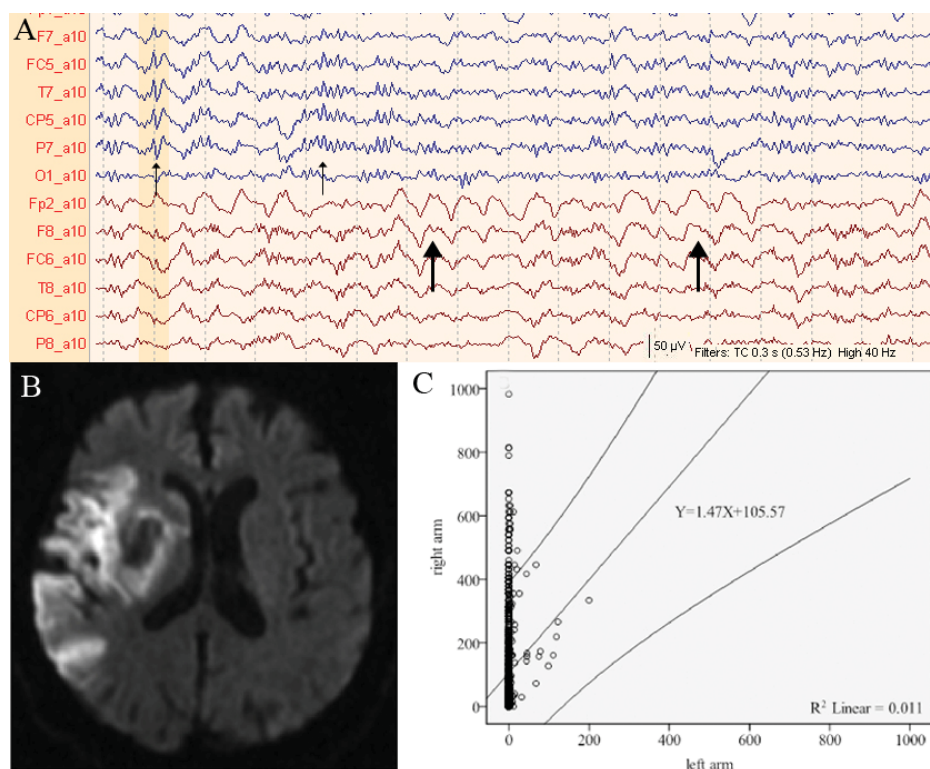
Fig. 3.1.3 A 70 year-old man with an ischaemic infarct of the insular and temporal cortex, basal ganglia and the entire posterior limb of the internal capsule. The EEG showed SWA in right frontal-temporal leads (thick arrows) and epileptiform discharges in left temporal leads (arrows).
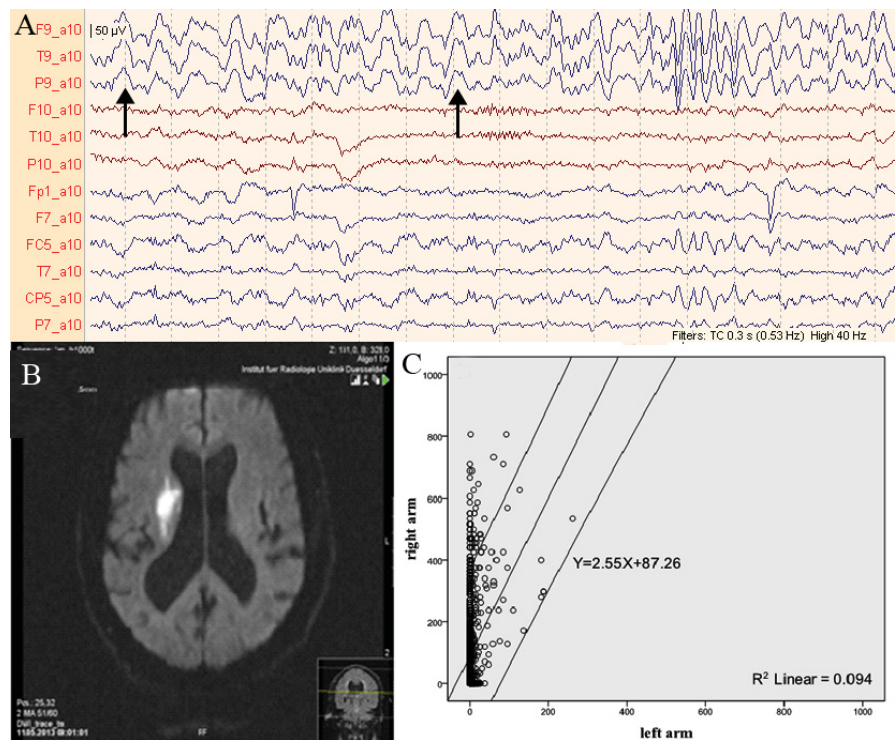
Fig. 3.1.4 A year-old man with an ischemic infarct lesion involving the right basal ganglia and the internal capsule. He had very low relative movement activity of his affected arm (4.5%) and left frontal SWA in the EEG (thick arrows).

3.2 Patients with focal or generalized seizures

153 patients aged 41±17 years were included in the study and completed full data collection. 34 patients aged 44±6 years had SWAs (SWA group), while 119 patients aged 40±17 years showed no SWAs (no SWA group). The sex ratios and ages of the two groups showed no differences (Table 3.2.1). However, all the SWA patients suffered from epileptic seizures including focal, complex-partial and generalized seizures. MRI was abnormal in 23 of 34 patients showing the following abnormalities: cerebrovascular disease (n=11), perinatal hypoxia (n=2), degenerative cerebral atrophy (n=3), postencephalitic lesions (n=3), arachnoidal and choriodal cysts (n=2), and amygdalohippocampectomy (n=2).

The sleep parameters measured with video EEG including sleep latency, wake after sleep onset, total sleep time, and sleep efficiency showed no significance differences among the two groups (Table 3.2.1). Nor were there differences of the non-rapid eye movement sleep (NREM) between the two groups. But the SWA group had a lower proportion of REM sleep ($P<0.05$; Fig. 3.2.1).

The relative movement activity between arms showed no group differences. However, the bimanual coordination of spontaneous movement activity scored by r_s was impaired in the SWA patients (Table 3.2.1). The SWA group showed a lower correlation of movement activity between two arms in the 24 hours, in daytime, and also in sleep time (Table 3.2.1, Fig. 3.2.2). These data showed that the amount of spontaneous arm movement activity was not different across the two groups but they were less coupled in the SWA patients. In an additional analysis it was found that the SWA on the left or right hemisphere had no impact on the amount of spontaneous movement activity ($P>0.05$).

To investigate the influence of interictal epileptiform discharge activity on spontaneous arm movement activity, it was divided the patients into a group with epileptiform discharge activity and another group with no epileptiform discharge activity (Table 3.2.2). Differences between the two groups were found only in sleep architecture. In detail, the patients with epileptiform discharges showed a greater percentage of NREM sleep and a decreased percentage of REM sleep. In contrast, the patients with epileptiform discharge activities showed no differences in sex ratio, age and the parameters of spontaneous movement activity.

A significant difference between SWAs and epileptiform discharge activities was observed: the former patients showed a significant impact on their spontaneous movement activity including the relative movements and coordinate correlation coefficient between two arms, whereas the latter showed a prominent effect on the sleep architectures and no significant on spontaneous movement parameters. In the patients with focal SWAs, there were only 7 (20.6%) patients with interictal epileptiform discharge activities. The distribution of patients with epileptiform discharge activities showed no significant differences between patients with SWAs and patients without SWAs. This might indicate that the focal abnormal SWAs and interictal epileptiform activities had different pathological causes.

Table 3.2.1 Movement activity and sleep characteristics in the SWA patients and no SWA patients

	SWA group (n=34)	No SWA group (n=119)	P
Male : female	17:17	53:66	0.574
Age (years, mean±SD)	44±6	40±17	0.212
Movement parameters			
r_{s24h}(mean±SD)	0.734±0.125	0.803±0.091	0.005**
r_{sd} (mean±SD)	0.675±0.119	0.731±0.115	0.014*
r_{sn} (mean±SD)	0.672±0.179	0.742±0.146	0.041*
RMA_{24h}(mean±SD)	1.193±0.652	0.998±0.309	0.101
RMA_d(mean±SD)	1.193±0.665	0.995±0.323	0.070
RMA_s(mean±SD)	1.198±0.577	1.084±0.449	0.223
Sleep parameters			
Sleep latency (min, mean±SD)	24.6±21.0	21.0±18.9	0.350
WASO (min, mean±SD)	119.9±76.1	100.1±61.5	0.123
TST (min, mean±SD)	412.2±99.6	413.0±95.6	0.978
Sleep efficiency (%,mean±SD)	72.9±14.1	77.0±10.9	0.077
Sleep architecture			
NREM (%,mean±SD)	67.6±12.0	67.7±10.4	0.606
REM (%,mean±SD)	7.1±4.8	9.1±5.6	0.038*
with epileptiform discharge(n)	7	19	0.556

Note:** P <0.01,* P <0.05, r_{s24h}= bimanual Spearman's rank correlation coefficient of 24 hours, r_{sd}= bimanual spearman's rank correlation coefficient of daytime (24hours minus the time in bed in the night), r_{sn}= bimanual spearman's rank correlation coefficient of the night (from sleep onset to sleep end) , RMA_{24h}, RMA_d, RMA_n = relative movement activity of the left arm compared to right arm in 24 hours, in daytime and night time, respectively. WASO= wake after sleep onset, TST= total sleep time, NREM= Non-rapid eye movement sleep, REM= rapid eye movement sleep. SD= standard deviation.

Table 3.2.2 Movement activity and sleep characteristics in the patients with epileptiform discharges compared with patients without epileptiform discharges

	Epileptiform discharge group (n=26)	No epileptiform discharge group (n=127)	P
Male : female (ratio)	8:18	62:65	0.093
Age (years, mean±SD)	41±17	41±17	0.870
Movement parameters			
r_{s24h}(mean±SD)	0.809±0.065	0.784±0.109	0.558
r_{sd} (mean±SD)	0.748±0.090	0.712±0.122	0.230
r_{sn} (mean±SD)	0.746±0.127	0.723±0.161	0.699
RMA_{24h}(mean±SD)	1.034±0.445	1.080±0.229	0.074
RMA_{d}(mean±SD)	1.036±0.460	1.086±0.246	0.074
RMA_{s}(mean±SD)	1.159±0.325	1.090±0.507	0.109
Sleep parameters			
Sleep latency (min, mean±SD)	19.2±13.9	22.4±20.3	0.418
WASO (min, mean±SD)	113.5±58.1	102.6±68.5	0.447
TST (min, mean±SD)	446.1±78.9	405.7±98.5	0.052
Sleep efficiency (%,mean±SD)	76.6±10.1	75.9±12.1	0.729
Sleep architecture			
NREM (%,mean±SD)	71.7±10.2	66.8±10.7	0.002**
REM (%,mean±SD)	5.6±4.3	9.3±5.5	0.035*

Note: ** P <0.01,* P <0.05. r_{s24h}= bimanual Spearman's rank correlation coefficient of 24 hours, r_{sd}= bimanual spearman's rank correlation coefficient of daytime (24hours minus the time in bed in the night), r_{sn}= bimanual spearman's rank correlation coefficient of the night (from sleep onset to sleep end) , RMA_{24h}, RMA_{d}, RMA_{n} = relative movement activity of the left arm compared to right arm in 24 hours, in daytime and night time, respectively. WASO= wake after sleep onset, TST= total sleep time, NREM= Non-rapid eye movement sleep, REM= rapid eye movement sleep. SD= standard deviation.
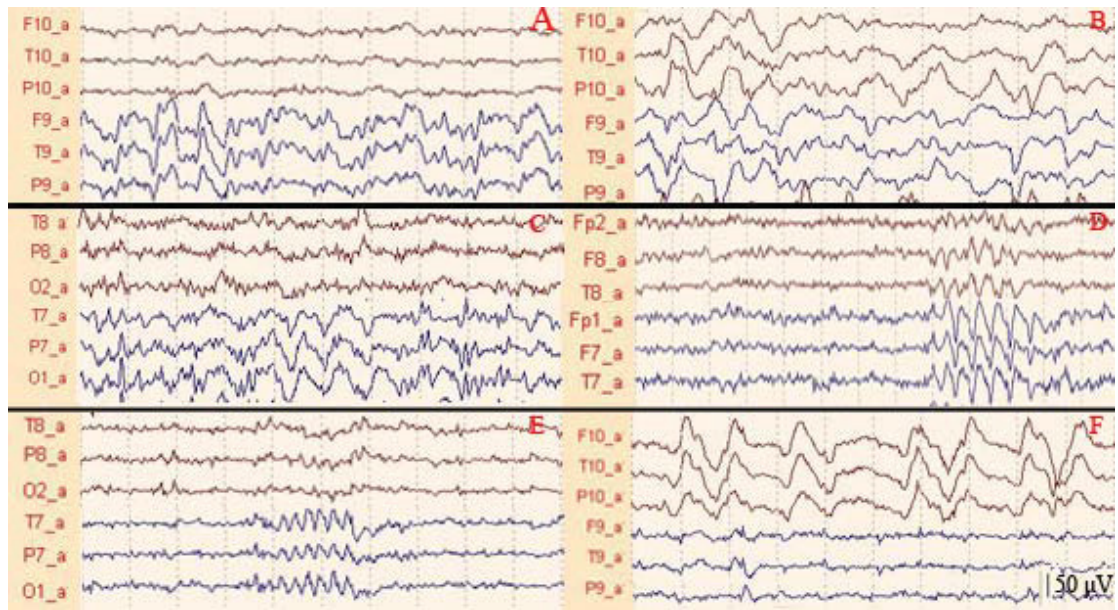
Fig. 3.2.1 Six examples with typical focal abnormal SWAs. A-F the typical focal abnormal SWAs are featured with 1-4Hz frequence, asymmetrical, and repeatedly occurrence in non-deep sleep periods. Filters: 0.3-40Hz.
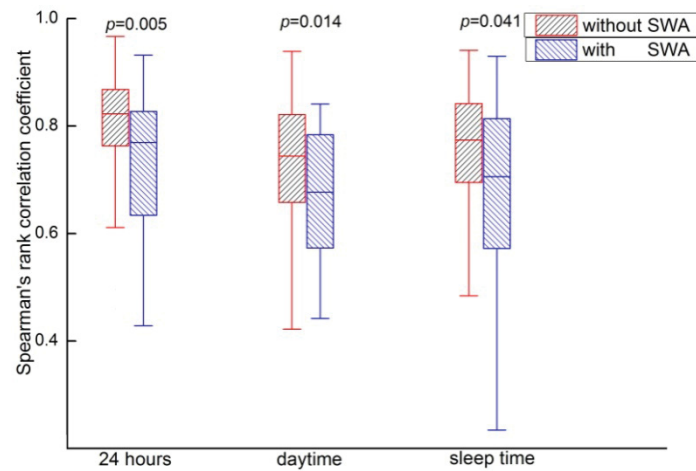
Fig. 3.2.2 Comparison of bimanual movement relation during daytime and night time for the patients grouped by SWA.

4 Discussion

4.1 Reduced sleep and decreased bimanual coordination after stroke

In the trial one of present study, the EEG recordings revealed that the stroke patients had significantly less total sleep time, increased REM latency, less NREM sleep and poor sleep efficiency than the control group. These findings corresponded to the notion that sleep architecture is impaired in stroke patients leading to sleep fragmentation, increased wakefulness and increased REM latency (Terzoudi, et al. 2009). In addition, compared with the control group, the spontaneous movements and bimanual coordination of the affected arm in the patients with stroke were significantly affected. Moreover, the stroke patients with focal abnormal SWAs showed far less spontaneous activity of their affected arm, and poor recover than the patients without abnormal SWAs, even though the two groups had no significant differences in demographics and NIHSS scores at admission. Although the finding of abnormality in bimanual coordination is not surprising, our study first provides the evidences for bimanual synchronization by calculating the Spearman's rank correlation coefficient (r_s) of the both hands.

It was noted that the subgroups of stroke patients with and without focal abnormal SWAs showed no significant differences of the clinical examination on admission (NIHSS). However, the stroke patients with focal abnormal SWAs showed a higher NIHSS at discharge. This finding supported a previous study showing that patients with focal abnormal SWAs would suffer a worse outcome compared with patients without SWAs (Hensel, et al. 2004; Burghaus, et al. 2007). In a more general perspective, focal abnormal SWAs had been reported to be a marker of pathological stages rather than a process of healthy aging (Finnigan, et al. 2004; Finnigan, et al. 2007; Leirer, et al. 2011).

4.2 Abnormal SWA may indicate decreased bimanual coordination

In the trial two of present study, we used actigraphy measurements and video EEG recording to explore the relation of abnormal SWA and spontaneous bimanual coordination in patients suffering from epileptic seizures. The major novel finding was that the patients with focal SWAs showed decreased bimanual coordination scored by r_s

in daily living. However, the decreased coupling of the movement activity in their arms was not related to interictal epileptiform discharges. This finding might indicate that the focal abnormal SWAs and interictal epileptiform discharges had different pathological causes. According to previous studies, it is not unexpected considering that SWA is a marker of a pathological stage rather than healthy aging and it reflects the brain dysfunction despite being non-specific (Leirer, et al. 2011). However, the interictal epileptic discharges are especially important in understanding of patients with known or suspected seizures. Moreover, the relative movement activity between two arms was not significantly different between SWA group and no SWA group, which suggested that the brain pathology in SWA patients affected the interlimb coordination but not the amount of spontaneous arm movement activity. Notably, the patients with SWAs showed decreased bimanual coupling and all the patients enrolled in the study showed no overt or subclinical motor deficit in daily living. This result might indicate that the EEG inspection could be used in more situations to reflect brain function.

4.3 Common pathophysiological changes

The SWA and impaired bimanual coordination can be found in some common pathophysiological diseases. In the first trial, it was found the r_s in the daytime decreased significantly in the stroke patients, compared with control group. This finding supported the notion that due to the disruption of interhemispheric balance, the bimanual coordination was impaired after stroke (Torre, et al. 2012). On the other hand, the increased SWA can also be found after stroke and the slowing and SWAs in the ischemic hemisphere might predict a poor recovery (Burghaus, et al. 2007). Moreover, degenerative brain pathologies like Alzheimer's disease and Parkinson's disease lead to substantial deficits in bimanual motor coordination (Helkala, et al. 1991; Daneault, et al. 2015; Daneault, et al. 2016). An increase in SWA can be also observed in patients with Alzheimer's disease or with Parkinson's disease (Fernandez, et al. 2002; Kamei, et al. 2010). Moreover, the occurrences of SWAs are associated with cortical dysfunctions in patients with AD or PD (Helkala, et al. 1991; Kamei, et al. 2010). Furthermore, previous studies reported that the greater slowing of EEG pattern suggested more severe function deficits in Alzheimer's disease and Parkinson's disease patients (Soikkeli, et al. 1991; Elmstahl, et al. 1994; Strijers, et al. 1997; Locatelli, et al. 1998; Fernandez, et al.

2002; Jeong 2004; Benz, et al. 2014). These studies suggest that the bimanual coordination and focal abnormal SWA may experience substantial common pathophysiological changes.

It was noted that a high proportion of abnormal MRI was found in patients with abnormal SWAs, which might indicate that abnormal SWAs could be caused by various pathogenesis. In fact, the decreased bimanual coordination and increased abnormal SWAs have been found in many common diseases. In previous studies, we have noted that both decreased bimanual coupling and abnormal SWAs could be found in post-stroke patients (Ruan and Seitz 2014). Moreover, the decreased bimanual coordination and increased abnormal SWAs could also be found in neurodegenerative pathologies (Helkala, et al. 1991; Kamei, et al. 2010; Daneault, et al. 2015). These findings are not unexpected considering that extensive cortical networks including premotor cortex, parietal cortex, mesial motor cortices, specifically the supplementary motor area, cingulate motor cortex, primary motor cortex, basal ganglia, and cerebellum were found to contribute to bimanual coupling tasks (Debaere, et al. 2001; Debaere, et al. 2004; Swinnen, et al. 2010). Dysfunctions involving to these areas might cause decreased bimanual coordination and abnormal SWAs, which might be the fundamental reasons to clarify the relation between deficient bimanual coupling and abnormal SWAs.

4.4 The role of mesial frontal motor area in bimanual coordination

Bimanual coordination is involved in most tasks in our daily living which require different actions of two arms simultaneously. A complex neural network contributes to bimanual coordination. These regions comprise areas involved to premotor cortex, the parietal cortex, mesial frontal motor cortex ((pre-SMA and SMA)), the cingulate motor cortex, the primary motor cortex, basal ganglia, and the cerebellum (Debaere, et al. 2001; Debaere, et al. 2004; Swinnen, et al. 2010). The mesial frontal motor area participates in planning and execution of sequential unimanual and bimanual movements (Gerloff, et al. 1997; Toyokura, et al. 1999; Toyokura, et al. 2002). In the cortical network, the mesial frontal area acts a prominent role in promoting or suppressing activity in the cortical motor network driving uni- and bilateral hand movements (Grefkes, et al. 2008; Garbarini and Pia 2013). Moreover, the prominent

corticospinal projection of SMA may subserve the functions of temporal and spatial sequencing for bilateral movements (Seitz, et al. 2000).

There are studies argue that the basal ganglia may mediate temporal and spatial inter-limb coupling as a critical role (Kraft, et al. 2007; Daneault, et al. 2016). It does not absolutely contradict the former notion considering the abundantly connections between basal ganglia and mesial frontal motor cortex (Alexander, et al. 1986; Iansek, et al. 1995). It seems the mesial frontal motor cortex dominated by basal ganglia input considering that the number of cells that project to the mesial frontal motor cortex is ca. 3-4 times greater than the number of dentate neurons that project to these cortical areas (Akkal, et al. 2007). Thus, a safely conclusion could be drew as that the cortico-subcortical circuit between mesial frontal motor cortex and basal ganglia together mediating the execution of bimanual coupling.

4.5 Methodological considerations

Enrolled in the second trial of present study were those patients with epileptic seizures. There were few studies to explore the bimanual coordination in the patients with seizures. Previous studies found that some kind of epilepsy might cause coordination problems in schematic tasks (Hernandez, et al. 2002). Despite that, the result of present study would not be impacted considering that the SWA group and no SWA group showed no differences in demographics. The main finding in the present study emphasized the relation between abnormal SWAs. Moreover, the abnormal SWAs reflected the dysfunction of brains. Even when we found the SWA in a "healthy patient", the patient might showed some abnormalities which were not easy to be found by normal inspection, e.g. deficit in neurotransmitter.

The present study using the counts of spontaneous movement activities, the Spearman's rank correlation coefficient (r_s) was calculated to quantitatively characterize the bimanual coordination of the arms in daily living activity. This was the first time to directly score the bimanual coordination between the two arms in real living. With this approach, the two synchronization modes (in-phase and anti-phase movements) in daily living were included into analysis. Therefore, this kind of method to scoring bimanual coordination using Spearman's rank correlation coefficient is practical and useful. By

nature, the two hands are used mostly together to execute bimanual movements in daily living (Kilbreath and Heard 2005). The actiwatches count the activities of both arms synchronously. Thus, when subjects show dysfunction in bimanual coordination, the r_s will be decreased.

5 Conclusion

The current two experiments combining actigraphy measurements and video-EEG recordings in real daily living revealed that stroke patients showed reduced sleep and had significant deficits in bimanual coordination and spontaneous movement activity particularly during daytime. In both patients with stroke and patients without stroke but with focal or generalized seizures, a decreased function of bimanual coordination in real daily living activity was related to the occurrence of SWAs but not to interictal epileptic discharges. This kind of deficits in bimanual coordination was not become apparent in neurological motor testing of paretic arm impairment. Future studies should explore the mechanism contributing to the association between focal abnormal SWAs and bimanual coordination.

6 Reference

Ahmed, I. (1988). "Predictive value of the electroencephalogram in acute hemispheric lesions." Clin Electroencephalogr 19(4): 205-209.

Akkal, D., R. P. Dum, et al. (2007). "Supplementary motor area and presupplementary motor area: targets of basal ganglia and cerebellar output." J Neurosci 27(40): 10659-10673.

Alexander, G. E., M. R. DeLong, et al. (1986). "Parallel organization of functionally segregated circuits linking basal ganglia and cortex." Annu Rev Neurosci 9: 357-381.

Allan Rechtschaffen, A. K. (1968). A Manual of Standardized Terminology, Techniques and Scoring System for Sleep Stages of Human Subjects. University of California, Brain Information Service/Brain Research Institute.

American Clinical Neurophysiology, S. (2006). "Guideline 5: Guidelines for standard electrode position nomenclature." J Clin Neurophysiol 23(2): 107-110.

Andraus, M. E. and S. V. Alves-Leon (2011). "Non-epileptiform EEG abnormalities: an overview." Arq Neuropsiquiatr 69(5): 829-835.

Arboix, A., E. Comes, et al. (2003). "Prognostic value of very early seizures for in-hospital mortality in atherothrombotic infarction." Eur Neurol 50(2): 78-84.

Baayen, J. C., A. de Jongh, et al. (2003). "Localization of slow wave activity in patients with tumor-associated epilepsy." Brain Topogr 16(2): 85-93.

Babiloni, C., F. Carducci, et al. (2013). "Resting state cortical electroencephalographic rhythms are related to gray matter volume in subjects with mild cognitive impairment and Alzheimer's disease." Hum Brain Mapp 34(6): 1427-1446.

Bassetti, C. L. and M. S. Aldrich (2001). "Sleep electroencephalogram changes in acute hemispheric stroke." Sleep Med 2(3): 185-194.

Benz, N., F. Hatz, et al. (2014). "Slowing of EEG background activity in Parkinson's and Alzheimer's disease with early cognitive dysfunction." Front Aging Neurosci 6: 314.

Briel, R. C., I. G. McKeith, et al. (1999). "EEG findings in dementia with Lewy bodies and Alzheimer's disease." <u>J Neurol Neurosurg Psychiatry</u> 66(3): 401-403.

Brott, T., H. P. Adams, Jr., et al. (1989). "Measurements of acute cerebral infarction: a clinical examination scale." <u>Stroke</u> 20(7): 864-870.

Burghaus, L., R. Hilker, et al. (2007). "Early electroencephalography in acute ischemic stroke: prediction of a malignant course?" <u>Clin Neurol Neurosurg</u> 109(1): 45-49.

Cardoso de Oliveira, S. (2002). "The neuronal basis of bimanual coordination: recent neurophysiological evidence and functional models." <u>Acta Psychologica</u> 110(2–3): 139-159.

Cauraugh, J. H. and S. Kim (2002). "Two coupled motor recovery protocols are better than one: electromyogram-triggered neuromuscular stimulation and bilateral movements." <u>Stroke</u> 33(6): 1589-1594.

Chan, D., R. J. Walters, et al. (2004). "EEG abnormalities in frontotemporal lobar degeneration." <u>Neurology</u> 62(9): 1628-1630.

Chinoy, E. D., D. J. Frey, et al. (2014). "Age-related changes in slow wave activity rise time and NREM sleep EEG with and without zolpidem in healthy young and older adults." <u>Sleep Med</u>.

Chu, R. K., A. R. Braun, et al. (2015). "MEG-based detection and localization of perilesional dysfunction in chronic stroke." <u>Neuroimage Clin</u> 8: 157-169.

Cyril Charlin, M. T., Urbain Calvet,Philippe Martinez,Vincent Larrue, (2000). "The clinical significance of periodic lateralized epileptiform discharges in acute ischemic stroke." <u>Journal of Stroke and Cerebrovascular Diseases</u> 9(6): 298-302.

Daneault, J. F., B. Carignan, et al. (2015). "Inter-limb coupling during diadochokinesis in Parkinson's and Huntington's disease." <u>Neurosci Res</u> 97: 60-68.

Daneault, J. F., B. Carignan, et al. (2016). "Subthalamic deep brain stimulation and dopaminergic medication in Parkinson's disease: Impact on inter-limb coupling." <u>Neuroscience</u> 335: 9-19.

de Jongh, A., J. C. Baayen, et al. (2003). "The influence of brain tumor treatment on pathological delta activity in MEG." <u>Neuroimage</u> 20(4): 2291-2301.

Debaere, F., S. P. Swinnen, et al. (2001). "Brain areas involved in interlimb coordination: a distributed network." Neuroimage 14(5): 947-958.

Debaere, F., N. Wenderoth, et al. (2004). "Cerebellar and premotor function in bimanual coordination: parametric neural responses to spatiotemporal complexity and cycling frequency." Neuroimage 21(4): 1416-1427.

Dringenberg, H. C. (2000). "Alzheimer's disease: more than a 'cholinergic disorder' - evidence that cholinergic-monoaminergic interactions contribute to EEG slowing and dementia." Behav Brain Res 115(2): 235-249.

Elmstahl, S., I. Rosen, et al. (1994). "Quantitative EEG in elderly patients with Alzheimer's disease and healthy controls." Dementia 5(2): 119-124.

Fernandez, A., F. Maestu, et al. (2002). "Focal temporoparietal slow activity in Alzheimer's disease revealed by magnetoencephalography." Biol Psychiatry 52(7): 764-770.

Finnigan, S. P., S. E. Rose, et al. (2004). "Correlation of quantitative EEG in acute ischemic stroke with 30-day NIHSS score: comparison with diffusion and perfusion MRI." Stroke 35(4): 899-903.

Finnigan, S. P., M. Walsh, et al. (2007). "Quantitative EEG indices of sub-acute ischaemic stroke correlate with clinical outcomes." Clin Neurophysiol 118(11): 2525-2532.

Garbarini, F. and L. Pia (2013). "Bimanual coupling paradigm as an effective tool to investigate productive behaviors in motor and body awareness impairments." Front Hum Neurosci 7: 737.

Gerloff, C., B. Corwell, et al. (1997). "Stimulation over the human supplementary motor area interferes with the organization of future elements in complex motor sequences." Brain 120 (Pt 9): 1587-1602.

Glauser, T., E. Ben-Menachem, et al. (2006). "ILAE treatment guidelines: evidence-based analysis of antiepileptic drug efficacy and effectiveness as initial monotherapy for epileptic seizures and syndromes." Epilepsia 47(7): 1094-1120.

Grefkes, C., S. B. Eickhoff, et al. (2008). "Dynamic intra- and interhemispheric interactions during unilateral and bilateral hand movements assessed with fMRI and DCM." Neuroimage 41(4): 1382-1394.

Helkala, E. L., V. Laulumaa, et al. (1991). "Slow-wave activity in the spectral analysis of the electroencephalogram is associated with cortical dysfunctions in patients with Alzheimer's disease." Behav Neurosci 105(3): 409-415.

Hensel, S., B. Rockstroh, et al. (2004). "Left-hemispheric abnormal EEG activity in relation to impairment and recovery in aphasic patients." Psychophysiology 41(3): 394-400.

Hernandez, M. T., H. C. Sauerwein, et al. (2002). "Deficits in executive functions and motor coordination in children with frontal lobe epilepsy." Neuropsychologia 40(4): 384-400.

Hoffmann, R., W. Hendrickse, et al. (2000). "Slow-wave activity during non-REM sleep in men with schizophrenia and major depressive disorders." Psychiatry Res 95(3): 215-225.

Hughes, J. R. and J. J. Fino (2004). "EEG in seizure prognosis: association of slow wave activity and other factors in patients with apparent misleading epileptiform findings." Clin EEG Neurosci 35(4): 181-184.

Iansek, R., J. L. Bradshaw, et al. (1995). Chapter 3 Interaction of the basal ganglia and supplementary motor area in the elaboration of movement. Advances in Psychology. J. G. Denis and P. P. Jan, North-Holland. Volume 111: 37-59.

Iber C, A.-I. S., Chesson AL Jr., Quan SF; (2007). The AASM manual for the scoring of sleep and associated events: rules, terminology and technical specifications. 1st ed. Westchester, IL.

Inui, K., E. Motomura, et al. (2001). "Temporal slow waves and cerebrovascular diseases." Psychiatry and Clinical Neurosciences 55(5): 525-531.

Ishibashi, H., P. G. Simos, et al. (2002). "Detection and significance of focal, interictal, slow-wave activity visualized by magnetoencephalography for localization of a primary epileptogenic region." J Neurosurg 96(4): 724-730.

J Ruan, R. S. (2014). "Impaired Sleep and Reduced Spontaneous Movement Activity in Acute Stroke: An Exploratory Study." J J Neur Neurosci 2014(2): 8.

Jauch, E. C., J. L. Saver, et al. (2013). "Guidelines for the early management of patients with acute ischemic stroke: a guideline for healthcare professionals from the American Heart Association/American Stroke Association." Stroke 44(3): 870-947.

Jeong, J. (2004). "EEG dynamics in patients with Alzheimer's disease." Clinical Neurophysiology 115(7): 1490-1505.

Jordan, K. G. (2004). "Emergency EEG and continuous EEG monitoring in acute ischemic stroke." J Clin Neurophysiol 21(5): 341-352.

Kamei, S., A. Morita, et al. (2010). "Quantitative EEG analysis of executive dysfunction in Parkinson disease." J Clin Neurophysiol 27(3): 193-197.

Kantak, S. S., N. Zahedi, et al. (2016). "Task-Dependent Bimanual Coordination After Stroke: Relationship With Sensorimotor Impairments." Arch Phys Med Rehabil 97(5): 798-806.

Kazennikov, O., S. Perrig, et al. (2002). "Kinematics of a coordinated goal-directed bimanual task." Behav Brain Res 134(1–2): 83-91.

Kilbreath, S. L., J. Crosbie, et al. (2006). "Inter-limb coordination in bimanual reach-to-grasp following stroke." Disabil Rehabil 28(23): 1435-1443.

Kilbreath, S. L. and R. C. Heard (2005). "Frequency of hand use in healthy older persons." Aust J Physiother 51(2): 119-122.

Koeneke, S., K. Lutz, et al. (2004). "Bimanual versus unimanual coordination: what makes the difference?" Neuroimage 22(3): 1336-1350.

Kolassa, I.-T., V. M. Leirer, et al. (2012). "Changes in cortical slow wave activity in healthy aging."

Kraft, E., A. W. Chen, et al. (2007). "The role of the basal ganglia in bimanual coordination." Brain Res 1151: 62-73.

Leirer, V. M., C. Wienbruch, et al. (2011). "Changes in cortical slow wave activity in healthy aging." Brain Imaging Behav 5(3): 222-228.

Lewine, J. D. and W. W. Orrison, Jr. (1995). "Spike and slow wave localization by magnetoencephalography." Neuroimaging Clin N Am 5(4): 575-596.

Lindau, M., V. Jelic, et al. (2003). "Quantitative EEG abnormalities and cognitive dysfunctions in frontotemporal dementia and Alzheimer's disease." Dement Geriatr Cogn Disord 15(2): 106-114.

Locatelli, T., M. Cursi, et al. (1998). "EEG coherence in Alzheimer's disease." Electroencephalogr Clin Neurophysiol 106(3): 229-237.

McCombe Waller, S. and J. Whitall (2008). "Bilateral arm training: why and who benefits?" NeuroRehabilitation 23(1): 29-41.

Meinzer, M., T. Elbert, et al. (2004). "Intensive language training enhances brain plasticity in chronic aphasia." BMC Biol 2: 20.

Muller, K., R. Kleiser, et al. (2011). "Involvement of area MT in bimanual finger movements in left-handers: an fMRI study." Eur J Neurosci 34(8): 1301-1309.

Neufeld, M. Y., M. J. Rabey, et al. (1994). "Effects of a single intravenous dose of scopolamine on the quantitative EEG in Alzheimer's disease patients and age-matched controls." Electroencephalogr Clin Neurophysiol 91(6): 407-412.

Osipova, D., J. Ahveninen, et al. (2003). "Effects of scopolamine on MEG spectral power and coherence in elderly subjects." Clin Neurophysiol 114(10): 1902-1907.

Reith, J., H. S. Jorgensen, et al. (1997). "Seizures in acute stroke: predictors and prognostic significance. The Copenhagen Stroke Study." Stroke 28(8): 1585-1589.

Rockstroh, B. S., C. Wienbruch, et al. (2007). "Abnormal oscillatory brain dynamics in schizophrenia: a sign of deviant communication in neural network?" BMC Psychiatry 7: 44.

Seitz, R. J., T. Hildebold, et al. (2011). "Spontaneous arm movement activity assessed by accelerometry is a marker for early recovery after stroke." J Neurol 258(3): 457-463.

Seitz, R. J., K. M. Stephan, et al. (2000). "Control of action as mediated by the human frontal lobe." Exp Brain Res 133(1): 71-80.

Siekierka-Kleiser, E. M., R. Kleiser, et al. (2006). "Quantitative assessment of recovery from motor hemineglect in acute stroke patients." Cerebrovasc Dis 21(5-6): 307-314.

Sleimen-Malkoun, R., J.-J. Temprado, et al. (2011). "Bimanual training in stroke: How do coupling and symmetry-breaking matter?" BMC Neurology 11: 11-11.

Smith, S. J. M. (2005). "EEG in neurological conditions other than epilepsy: when does it help, what does it add?" Journal of Neurology, Neurosurgery & Psychiatry 76(suppl 2): ii8-ii12.

Soikkeli, R., J. Partanen, et al. (1991). "Slowing of EEG in Parkinson's disease." Electroencephalogr Clin Neurophysiol 79(3): 159-165.

Strijers, R. L., P. Scheltens, et al. (1997). "Diagnosing Alzheimer's disease in community-dwelling elderly: a comparison of EEG and MRI." Dement Geriatr Cogn Disord 8(3): 198-202.

Swinnen, S. P., S. Vangheluwe, et al. (2010). "Shared neural resources between left and right interlimb coordination skills: the neural substrate of abstract motor representations." Neuroimage 49(3): 2570-2580.

Temprado, J. J., R. Salesse, et al. (2007). "Neuromuscular and spatial constraints on bimanual hand-held pendulum oscillations: dissociation or combination?" Hum Mov Sci 26(2): 235-246.

Temprado, J. J., S. P. Swinnen, et al. (2003). "Interaction of directional, neuromuscular and egocentric constraints on the stability of preferred bimanual coordination patterns." Human Movement Science 22(3): 339-363.

Terzoudi, A., T. Vorvolakos, et al. (2009). "Sleep architecture in stroke and relation to outcome." Eur Neurol 61(1): 16-22.

Torre, K., N. Hammami, et al. (2012). "Impairment of bimanual coordination after stroke: The role of afference-based processes."

Torres, F., A. Faoro, et al. (1983). "The electroencephalogram of elderly subjects revisited." Electroencephalogr Clin Neurophysiol 56(5): 391-398.

Toyokura, M., I. Muro, et al. (1999). "Relation of bimanual coordination to activation in the sensorimotor cortex and supplementary motor area: Analysis using functional magnetic resonance imaging." Brain Research Bulletin 48(2): 211-217.

Toyokura, M., I. Muro, et al. (2002). "Activation of pre-supplementary motor area (SMA) and SMA proper during unimanual and bimanual complex sequences: an analysis using functional magnetic resonance imaging." J Neuroimaging 12(2): 172-178.

Visser, S. L., C. Hooijer, et al. (1987). "Anterior temporal focal abnormalities in EEG in normal aged subjects; correlations with psychopathological and CT brain scan findings." Electroencephalogr Clin Neurophysiol 66(1): 1-7.

Vock, J., P. Achermann, et al. (2002). "Evolution of sleep and sleep EEG after hemispheric stroke." J Sleep Res 11(4): 331-338.

Wienbruch, C. (2007). "Abnormal slow wave mapping (ASWAM)--A tool for the investigation of abnormal slow wave activity in the human brain." J Neurosci Methods 163(1): 119-127.

Yener, G. G., A. F. Leuchter, et al. (1996). "Quantitative EEG in frontotemporal dementia." Clin Electroencephalogr 27(2): 61-68.

Part II Cytoarchitecture, probability maps and functions of the human mesial frontal cortex

1 Introduction

1.1 Historical evolution

The human mesial frontal cortex has been extensively explored during the past one hundred years (Walter 1905, Brodmann 1909, Vogt 1910, von Economo and Koskinas 1925, Strasburger 1937, Sarkisov SA 1949, Hopf 1956, Sanides 1962, Braak 1980, Zilles, et al. 1995). The first cortical map of the human brain was drawn by Alfred Walter Campbell. Based on serial sections stained for myelin sheaths and nerve cells, and the cortical macro structures, Campbell roughly subdivided the human cortex into 14 areas and marked the intermediate precentral field, which enclosed the subsequent Brodmann's areas 6 (Walter 1905, Brodmann 1909). After that, based on the comparative cortical cytoarchitectonics, the agranular frontal cortex of humans and non-human primates has been subdivided into areas 4 and 6 by Brodmann (Brodmann 1909). Area 4 is located predominantly in the precentral gyrus and can be easily identified by the giant pyramidal cells or Betz cells organized in layer V. The area 6 lies just anterior to the area 4, in which the Betz cells is absent (Brodmann 1909). In the ventral part, area 6 in Brodmann map located above the cingulated sulcus (Brodmann 1909). Brodmann's map brings us the first insight into cytrocarchitectonic structures (Zilles and Amunts 2010). Vogt and Vogt (1910) published the first detailed myeloarchitectonic map of the human frontal cortex, which contained 66 mainly euradiate areas. The areas V36-V41 may be comparable to Brodmanns' area 6 (Vogt 1910; Zilles 2015). Strasburger (1937), Hopf(1956), and Sanides (1962) adopted the nomenclature from Vogt and Vogt in their maps, although large discrepancies could be found in these maps (Vogt 1910, Strasburger 1937, Hopf 1956, Sanides 1962). Von Economo and Koskinas (1925) published their grand book (Von Economo and Koskinas 1925) which provided a much more detailed verbal and pictorial description of the variations in cellular structure (cytoarchitecture) of cerebral cortical layers, compared to Brodmann's map. In their book, they marked the Brodmann's area 6 as area FB (Von Economo and Koskinas 1925; Triarhou 2007). Later studies performed by Sarkisov

37

(1949) employed Brodmann's nomenclature and marked the mesial frontal area as area 6 (Sarkisov 1949). Braak (1980) identified the similar area as superofrontal magnopyramidal region (sfm) (Braak 1980). Based on a combined myeloarchitectonical and functional study, the frontal motor cortex was subdivided into areas 6aα (the caudal part) and 6aß (the rostral part) (Vogt Cécile 1919). It has to be emphasized that these maps differ regarding the number of subareas, the relative size and extent of areas SMA and pre-SMA. More importantly, these maps do not include interindividual variability of different brains, the definition of cytoarchitectonic areas were made according to observer-depend descriptions and they are only available as two-dimensional schematic drawings and cannot be matched with functional imaging experiments (Fig.1.1.1).

The question how the cortical modules in medial frontal cortex can be defined has been given more solutions in past decade. It has been reported that areas SMA and pre-SMA can be defined by using of diffusion-weighted imaging (DWI) to perform probabilistic tractography, which hypothesises that similar connectivity profiles can be found within an area (Johansen-Berg, et al. 2004; Klein, et al. 2007). More recent hypotheses of mapping emphasize parcellations of functional connectivity. Based on functional connectivity parcellation, one can define the putative areas SMA and pre-SMA by using resting state functional magnetic imaging (Kim, et al. 2010; Joliot, et al. 2015). One other feasible approach which has been used to identify putative areas SMA and pre-SMA is the co-activation based parcellation in a data-driven fashion (Eickhoff, et al. 2011). These clustering solutions for the medial frontal cortex are biologically meaningful considering that the region of interest may show a multi-layered functional hierarchy (Geyer and Turner 2015).

The cytoarchitectonic map of Brodmann's area 4 corresponded to a functional organization: "primary motor cortex" which was seated in the precentral gyrus and famous for the representation of body movements (Penfield's motor homunculus) (Penfield and Boldrey 1937). Based on that, the nomenclature "supplementary motor area" (an additional complete motor representation of the body's periphery; hence the term "supplementary") was introduced by Penfield and Woolsey. This additional "supplementary motor area" corresponded with the mesial surface of Brodmann's area 6 (Penfield and Welch 1951; Woolsey, et al. 1952). The other part of area 6, the part of lateral cortical convexity, was defined as "premotor area" (Fulton 1935). Because of the
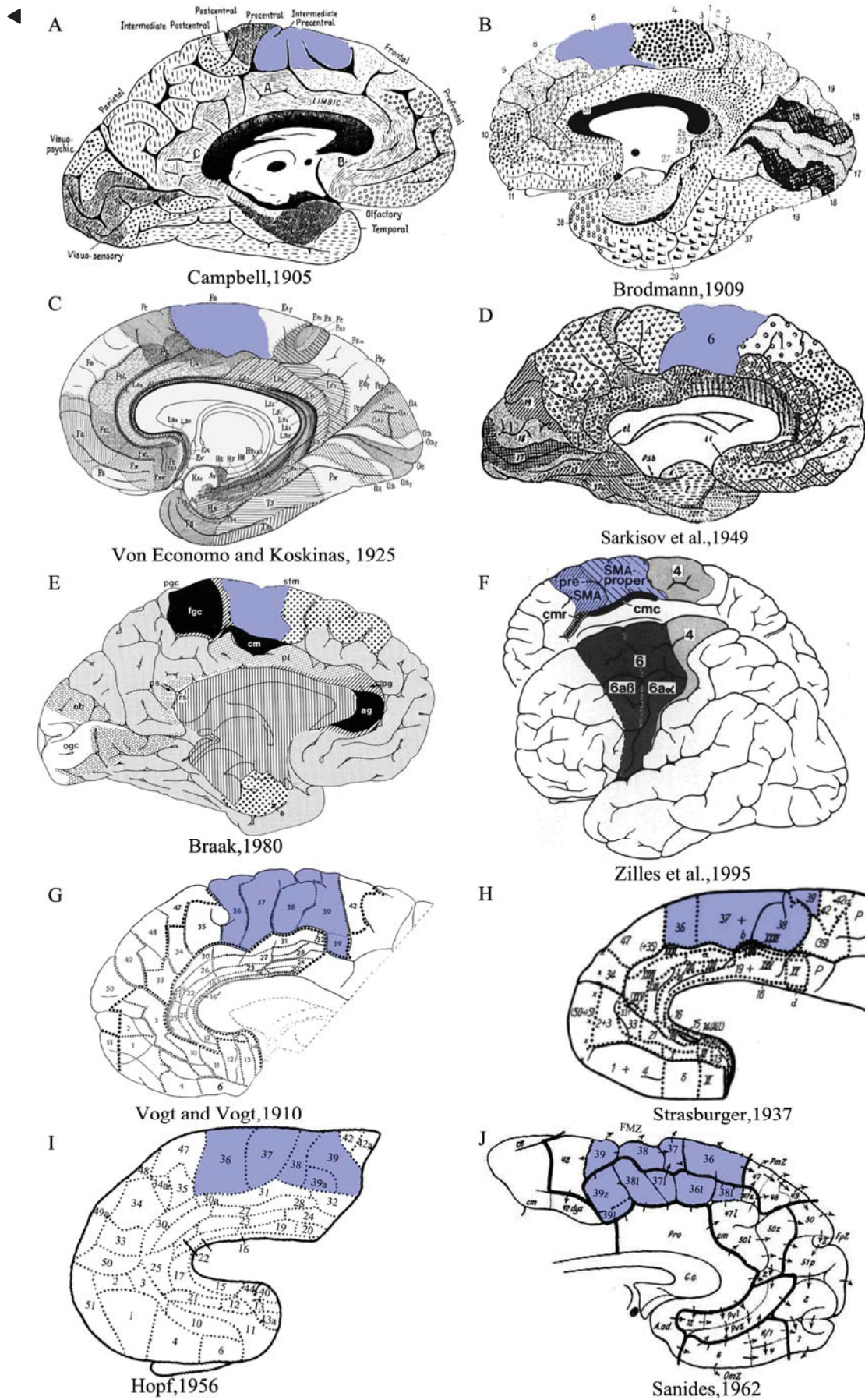
non-objective cytoarchitectonically criterions, the traditionally defined supplementary area has once been thought to constitute a homogeneous entity (Woolsey, et al. 1952; Tanji and Kurata 1982; Mitz and Wise 1987).

With the deepening of understanding, It has been confirmed that the traditional "supplementary motor area" in the medial wall of Brodmann's area 6 has two subregions (Zilles, et al. 1995, Geyer, et al. 2000): the caudal part: supplementary motor area proper (SMA proper or SMA) and the rostral part: presupplementary motor area (pre-SMA), which were roughly corresponding to mesial parts of area 6aα and 6aβ, respectively (Matsuzaka, et al. 1992; Picard and Strick 1996). From a historical view, the map of the mesial frontal cortical surface has been normally divided into two part: the caudal part and the rostral part, which were named differently such as 6aα and 6aβ by Vogt and Vogt (Vogt Cécile 1919), FB and FC by Von Bonin and Bailey (Bailey. 1947), 6DC and MII by Barbas and Pandya (Barbas and Pandya 1987), and F3 and F6 by Matelli (Matelli, Luppino et al. 1985; Matelli, et al. 1991). The rough border between SMA proper and pre-SMA located in the vertical line transversing the anterior commissure (VCA) line (Picard and Strick 1996; Vorobiev, et al. 1998). In principle, the subdivision of caudal-rostral parts in mesial frontal cortex, performed by different researchers, corresponds to the functional entities: SMA proper (or SMA) and Pre-SMA respectively in primate, though the maps of the two parts depicted by different researchers vary in terms of size, territories of the areas and nomenclatures (Tanji and Shima 1994; Zilles, et al. 1995; Rizzolatti, et al. 1996; Rizzolatti, et al. 1998) (Table 1.1.1).

Several recent studies have focused on a new subregion: supplementary eye field (SEF) in the supplementary motor complex. SEF was first described by Schlag J and colleagues in their study (Schlag and Schlag-Rey 1987). Using electrical microstimulation on monkeys, Schlag and colleagues found that the dorsomedial cortical neurons responded to photic stimuli, and stimulation in there could evoke saccades (Schlag and Schlag-Rey 1987). The SEF in humans lie at the border of the SMA and pre-SMA and has a sulcal landmark: the upper part of the paracentral sulcus (Grosbras, et al. 1999; Yamamoto, et al. 2004). The location of SEF in monkeys differs from that in humans. The SEF in monkeys locates on the dorsolateral convexity, not the mesial surface (Schlag and Schlag-Rey 1987; Tehovnik, et al. 2000; Luppino, et al.

2003). The SEF together with the frontal eye fields (FEF), the intraparietal sulcus (IPS), and the superior colliculus (SC) contribute to the generation and control of eye movements (Yamamoto, et al. 2004; Stuphorn, et al. 2010). The SEF does not contribute directly and immediately to the initiation of visually guided saccades, but plays an important role in the condition that when there is conflict between several, ongoing competing saccadic responses (Parton, et al. 2007; Stuphorn, et al. 2010; Stuphorn 2015). Notably, this subarea is defined electrophysiologically in behaving monkeys. And the location of SEF in humans and monkeys varies. It remains to be clarified that whether the SEF, SMA, and pre-SMA have some differences in cytoarchitecture. On the other hand, it is possible that the SEF has nothing special in physical structure, it is similar with the parts of SMA, the representation of legs, the SEF is only the representation of oculomotor and thus SEF may not be treated as a single entity.

Fig. 1.1.1 Published maps of the human mesial frontal motor cortex with the putative homologs with mesial Brodman's area 6 or traditional defined supplementary motor areas (blue color). (References: A: Walter 1905, B: Brodmann 1909, C: Von Economo and Koskinas 1925, D: Sarkisov SA 1949, E: Braak 1980, F: Zilles, Schlaug et al. 1995, G: Vogt 1910, H: Strasburger 1937, I: Hopf 1956, J: Sanides 1962). G-J show only the frontal mesial view of human brain. The maps in B, C, D are based on cytoarchitectonic studies, the maps in A, E, G, H, I, J are based on myeloarchitectonic studies. The map in F is based on combined cyto- and myelo- architectonic studies. The arabic numbers in B, D, F indicate the nomenclature of Brodmann or a nomenclature derived from that.The arabic numbers in G, H, I, J represent the nomenclature of Vogt and Vogt (1910). The letters in C indicate the nomenclature in Von Economo and Koskinas (1925). In F, the Brodman's area 6 in F has been subdivided into SMA proper and pre-SMA.The dark arrows in J indicate the gradation "streams" of structure. sfm in E, superofrontal magnopyramidal region. ▶

A Campbell,1905

B Brodmann,1909

C Von Economo and Koskinas, 1925

D Sarkisov et al.,1949

E Braak,1980

F Zilles et al.,1995

G Vogt and Vogt,1910

H Strasburger,1937

I Hopf,1956

J Sanides,1962

41

Table 1.1.1 The research synopsis of the primate supplementary motor complex on the mesial surface of macaque and human brain hemisphere.

	Generic abbreviation	Brodmann 1909	Vogt Cecile 1919	Von Economo and Koskinas 1925	Bailey. 1947	Barbas and Pandya 1987	Matelli, et al. 1985; Matelli, et al. 1991	Zilles, et al. 1995	Geyer, et al. 1998
Methodology		Cytoarchitecture	Myeloarchitecture	Myeloarchitecture	Cytoarchitecture	Cytoarchitecture myeloarchitecture	Cytoarchitecture	Receptor autoradiography, Functional imaing	Receptor autoradiography
Research subject		Macaque,human	Macaque, human	Human	Macaque	Macaque	Macaque	Macaque, human	Macaque
Generic nomenclature									
Supplementary motor area proper	SMA proper or SMA	6	6aα	FB	FB	6DC	F3	SMA proper, F3	F3
Presupplementary motor area	Pre-SMA		6aβ		FC	MII	F6	Pre-SMA, F6	F6

1.2 Microstructure

In Nissl-stained sections, the SMA proper is poorly laminated and absent of giant pyramidal cells. The most distinguished feature of area SMA proper from the posterior neighbour primary motor area is that there is an increase in cellular density in lower part of layer III and upper layer V. Pre-SMA, standing anterior to SMA, has a better lamination than SMA proper. The prominent characteristic is a dark layer V well demarcated from layers III and VI. It ends rostrally when an incipient layer IV becomes evident. The territories of the area SMA proper and Pre-SMA extend from the middle of the dorsal bank of the cingulate sulcus to the dorsolateral convexity for approximately 2 to 3 mm (Matelli, et al. 1991; Geyer, et al. 1998). However, clear distinctions of cytoarchitectonic features between medial frontal areas and their neighbouring areas have not yet been done with observer-independent analysis.

The areas SMA proper and pre-SMA can be also identified or separated from each other by the density of receptors of classical neurotransmitters. Earlier studies found that there are clear-cut changes in laminar distribution patterns of Alpha-amino-3-hydroxy-5-methyl-4-isoxalone propionic acid ([3H]AMPA), [3H]kainate, and [3H]oxotremorine-M binding sites. Those changes closely match with corresponding cytoarchitectonic borders. In detail, Two prominent step like increases in regional [3H]AMPA binding patterns are clear: the caudal step corresponds to the F1/F3 border in an adjacent cell-stained section, and the rostral one coincides with the F3/F6 border. This is also true for [3H] kainate: there is a caudo-rostral increase in binding densities: primary motor cortex(F1)＜SMA proper(F3)＜pre-SMA(F6). The relevant borders of the areas of SMA proper and pre-SMA towards dorsolatera premotor cortex or cingulated sulcus or prefrontal cortex and can be recognized clearly and match the corresponding cytoarchitectonic borders closely. The [3H]oxotremorine-M binding sites and some other receptor types such as GABAA (GABA-gamma aminobutyric acid) receptor, NMDA (N-methyl-D-aspartate) receptor, 5-HT (5-hydroxytryptamine) receptor, M2 (M2 muscarinic acetylcholine) receptor show similar patterns as [3H]AMPA and [3H]kainite (Zilles, et al. 1995; Geyer, et al. 1998; Zilles and Amunts 2009).

A more recent technique, the immunohistochemical staining on the neurofilament protein triplet with the monoclonal antibody Neurofilament H Non-Phosphorylated

(SMI-32) also provides a morphological basis for defining the pre-SMA and SMA (Sternberger and Sternberger 1983; Lee, et al. 1988). With SMI-32 immunohistochemistry, SMA proper was identified by the absence of Betz cells, a higher density in lower part of III and the overall homogeneous cortex. Area pre-SMA showed a prominent layer V with pyramidal neurons in small to medium size, a better lamination, an absence of Betz cells. The borders here defined by the distribution of SMI-32 immunoreactive neurons corresponded to the borders depicted by cyto-, myelo- and architecture (Baleydier, et al. 1997; Geyer, et al. 2000; Vogt and Vogt 2003). Notably, there are also some other histochemical techniques such as enzyme architecture (Manocha 1970) can be used for brain mapping, but few knowledge about human brains especially the interest areas SMA proper and pre-SMA in this context are known.

1.3 Connectivity

The efferent and afferent connections of SMA and pre-SMA are complicated and these connections suggest that the two entities are responsible for different functions. Notably, most of our knowledge about the anatomical connections of areas SMA and pre-SMA are collected from studies in monkeys. There are three sketches about the connections: SMA and pre-SMA to corticospinal, subcortical to SMA and pre-SMA and corticocortical connections.

SMA and pre-SMA to corticospinal: Anatomical studies on monkeys using retrograde tracing methods revealed that SMA projects directly and substantially to corticospinal tract, which comprises ca.10% of all corticospinal cells (Jurgens 1984; Dum and Strick 1991; He, et al. 1995; Wise 1996). Notably, the cortico-motoneuronal connections originate from both SMA (48% of motoneurons) and primary motor area (48%). Interestingly, the electrical excitatory of the primary motor area is stronger than that of SMA. The morphology of termination of SMA corticospinal cells resembles that of primary motor cortex projections (Dum and Strick 1996; Maier, et al. 2002). Like SMA, area pre-SMA also has direct access to the spinal cord, but sparser than that of SMA (Dum and Strick 1991; Luppino, et al. 1994). Meanwhile the SMA projects to corticospinal sparser than that of primary motor area (Maier, et al. 2002). This may give a good interpretation of the fact that the electrical excitability of the primary motor

cortex is stronger than that of the SMA. And the electrical excitability of area SMA is stronger than that of area pre-SMA (Luppino, et al. 1991; Luppino and Rizzolatti 2000; Maier, et al. 2002).

Subcortical to SMA and pre-SMA: The subcortical structure: basal ganglia provide internal motor cues that enable the release of submovements from SMA and contribute to maintain the movement sequences in readiness for running and execution, which may be owed to the connections between basal ganglia and SMA (Iansek, et al. 1995). In detail, pre-SMA receives its input from the caudate, while SMA accepts the projections from the putamen and pallidum (Alexander, et al. 1986). Moreover, a study using retrograde transneuronal transport of neurotropic viruses on cebus monkeys verified that both of SMA and pre-SMA are connected by the projections from the internal segment of the globus pallidus (GPi) and the dentate nucleus of the cerebellum as well. In addition, it seems that the two cortical areas are dominated by basal ganglia input considering the number of cells that project to SMA and pre-SMA is ca. 3-4 times greater than the number of dentate neurons that project to these cortical areas (Akkal, et al. 2007). Areas SMA and pre-SMA input to different parts of striatum, and further orients to the GPi directly and indirectly (Inase, et al. 1996; Inase, et al. 1999). Some findings from monkey studies have been confirmed in study on human. Using diffusion weighted imaging probabilistic tractography on healthy volunteers, Draganski and co-workers confirmed the notion of coexistence of parallel and integrative pathways in anatomically and functionally specific cortico-subcortical circuit (Draganski, et al. 2008). The functional meta-analysis also demonstrated indirectly the connections between cerebellum and area SMA: significant co-activations among dentate nucleus, thalamus, and SMA were observed, whereas limited co-activations were presented between interposed nucleus and SMA (Tellmann, et al. 2015).

It has been well known that thalamic inputs to the SMA (Rouiller, Tanne et al. 1999). Studies performed on monkeys revealed that SMA proper receives its predominant thalamic input from the nucleus ventralis lateralis parsoralis (VLo), while the input to pre-SMA originates often from the nuleus ventralis anterior pars parvocellularis (VApc), area X (according to the nomenclature of Olszewski) (Olszewski 1952; Schell and Strick 1984; Wiesendanger and Wiesendanger 1985). Moreover, there is a certain extent overlap on the origins of the thalamocortical projections directed to SMA and primary

motor cortex (Rouiller, et al. 1999). Interesting, both SMA and pre-SMA have 'hyperdirect' cortical inputs to the subthalamic nucleus (STN) (Nambu, et al. 1996; Nambu, et al. 2002). Notably, the connections between SMA and basal ganglia function via the thalamus. These different projections comprise different circuits and the circuits function together (Schell and Strick 1984; Wiesendanger and Wiesendanger 1985; Alexander, et al. 1986). The dysfunction of the basal ganglia-thalamo-SMA loop results in gait disturbance in Parkinson disease and vascular Parkinsonism (Iseki and Hanakawa 2010).

Corticocortical connections: SMA and pre-SMA differ in the corticocortical connections. SMA is more related with primary motor cortex and the posterior premotor cortex and cingulate area 24d, whereas pre-SMA receives a rich connection from the anterior premotor areas and cingulate area 24c (Luppino, et al. 1993). Using postmortem dissection and diffusion imaging tractography on humans, a recent study has found that area SMA sent U-fibres to precentral gyrus and cingulate gyrus, medial fibres to striatum, 'aslant' fibres to inferior frontal gyrus (Vergani, et al. 2014). Moreover, the microstructures of pipelines in the white matter per se could also impact the function of the cortex (Scholz, et al. 2009; Sampaio-Baptista, et al. 2013).

The connection of supplementary eye field: The supplementary eye field (SEF) has extensive connections. Studies in monkey have found that SEF is connected with frontal eye field, thalamic nuclei, prefrontal cortex, claustrum, ventral anterior nucleus, pars magnocellularis, nucleus X, posterior subdivision of the ventral lateral nucleus, multiform, parvocellular and magnocellular. In addition, area SEF projects to pre- and paraoculomotor structure of the brainstem such as superior colliculus, pretectal olivary nucleus, nucleus of the optic tract and nucleus raphe interpositus (Huerta and Kaas 1990; Shook, et al. 1990; Shook, et al. 1991; Stanton, et al. 1993). Unfortunately, the connections of SEF in human remain to be clarified. There are few studies about SEF connection in human available.

1.4 Function

The areas SMA and pre-SMA are involved to a variety of functions related with motor sequence processing, planning and executing (Hoshi and Tanji 2004; Cona, et al.

2016; Hupfeld, et al. 2016), temporal and spatial processing of movements (Mita, et al. 2009; Kotz and Schwartze 2011). Besides that, the area pre-SMA and area SMA also contribute to motor learning, speech and language processing (Kim and Shin 2014; Hertrich, Dietrich et al. 2016).

With the renovation of concepts about the functions of SMA, pre-SMA, the foci of researchers evaluated from detection the representations of body, the possible single function of each area in early stage to the exploration of the temporal sequential organization, the co-activations among cortex or subcortical areas. Along this line, it can be untied preliminarily the function outline of areas SMA and pre-SMA.

1.4.1 Classical parcellation

According to Tanji (Tanji 1996), there are two classical notions: one is that the SMA is involved in a high degree of complex voluntary movements. The other one is that SMA is primarily related to controlling proximal limb. These notions have been updated according to recent studies.

One study using fMRI on healthy volunteers revealed that both complex motor task and simple motor task (here means flexing and extending the right thumb repeatedly and as quickly as possible without moving the wrist) activated the SMA, with different degree of activation (Chung, et al. 2000). Using high resolution EEG on healthy subjects, Cui and co-workers found that area SMA participated in both simple and complex movements (Cui, et al. 2000). In fact, the earlier studies performed by Tanji and colleagues found that even simple motor tasks such as pushing buttons need the neuronal activities in both SMA and pre-SMA (Tanji and Shima 1996). Infact, we cannot simply use "simple" task or "complex" task to descript the functions of SMA. Firstly, it is difficult to characterize whether the task is "simple" or "complex". According to Tanji, "simple" task means conducting a "kind of motor task that does not include a temporal or spatial structure imposing a great deal of specific requirements for the subject" (Tanji 1994). Another condition, easy to be neglected is that some tasks for one subject are "simple" tasks, but are "complex" tasks for other subjects. One study using fMRI on piano players and control subjects for the same movements reveals that the professional piano players recruit lesser neurons and the volume of the activated

cortical area in the professional piano players is smaller than that in the non-professional players (Krings, et al. 2000). Based on these findings, it could be concluded that the SMA participates in both "simple" and "complex" tasks.

One other classic notion is that SMA primarily related in proximal limb. This issue has been discussed in detail by Tanji in his articles, in which he suggested that SMA was involved in controlling both proximal and distal limbs (Tanji 1994; Tanji 1996). Later studies (Nirkko, et al. 2001) using fMRI found that SMA was activated despite proximal or distal movements in the ipsilateral or contralateral hand. This study also confirmed the effects of hemispheric dominance, which attributed exclusively to secondary areas (Nirkko, et al. 2001). In fact, the human handedness is related to the interconnections in primary motor cortex of the dominant hemisphere which forms a neural substrate favouring the formation of experience-dependent excitatory and inhibitory interactions (Hammond 2002).

1.4.2 Motor representations.

Area SMA in monkeys is somatotopicallly organized and has a complete motor representation with hindlimb movements located caudally, forelimb movements located centrally. Area pre-SMA, however, includes poor representations of limbs (Mitz and Wise 1987; Luppino, et al. 1991). Experiments with intracotical microstimulation (ICMS) showed that electrical excitability thresholds and characteristics of the areas: primary motor area, SMA and pre-SMA differ. Movements were more difficult to elicit from pre-SMA than from SMA or from primary motor cortex. Eliciting in pre-SMA could evoke larger percentage of complex movements, which was lack of segregation between proximal and distal movements. Slow movements were more frequently evoked in area pre-SMA, whereas fast movements were easier to be elicited in primary motor cortex and SMA (Luppino, et al. 1991). The somatotopic organization in area SMA is not as precise as that of primary motor cortex (Fried, et al. 1991). Studies on monkeys confirmed this somatotopic organization in SMA, where the neurons contacted with the distal and proximal forelimb movements were arranged in a rostro-caudal direction with some overlap (Tanji and Kurata 1979; Wise and Tanji 1981; Tanji and Kurata 1982). In human, the electrical stimulations in different regions of the SMA can elicit synergistic and complex movements of face, vocalization, speech (Fried, et al.

1991). There are many studies on human brains put us into a dilemma on the issue of SMA somatotopy: One study using a gamma camera detecting regional cerebral blood flow (CBF) invalidates the somatotopic organization of the SMA (Orgogozo and Larsen 1979). One other study with positron emission tomography (PET) also found no somatotopy in SMA of humans (Matelli, et al. 1993). Thus, it seems that controversy still exists about whether area SMA in human is somatotopically organized.

Fontaine and co-workers using partial resection of the SMA on the patients with tumor found that there was a good correlation between clinical patterns of deficit and the extent of SMA resection, confirmed the somatotopic organization of the SMA (Fontaine, et al. 2002). One study using fMRI in healthy volunteers located the face, hand, foot representations in SMA successfully (Chainay, et al. 2004). Thus, it can be drew a conclusion that the SMA in monkeys and humans is somatotopic organized in principal but the somatotopy in human is not apparent as that in monkeys.

1.4.3 Internal task vs. external task.

The "internal" means there is no change in the environment but a change in the subject itself while the "external" means there is a change in the environment including visual signals, tactile signals or auditory signals (Tanji and Kurata 1982; Geyer, et al. 2000). Scalp electroencephalography (EEG) recordings found cerebral potential, known as Bereitschaftpotential (BP, or readiness potential), preceding voluntary finger movements (Kornhuber and Deecke 1965; Deecke, et al. 1969; Deecke and Kornhuber 1978). The maximal Bereitschaftspotential emerges at the vertex leads, marked negativity also over parietal areas, but there is virtually no potential in contra- or ipsilateral precentral leads at the hand representation of the primary motor cortex. So probably it could attribute the Bereitschaftspotential to the mesial SMA and pre-SMA (Deecke and Kornhuber 1978). One recent study using fMRI confirmed the role of SMA on Bereitschaftpotential (Cunnington, et al. 2003). Interestingly, the lesions of SMA can reduce the BP amplitudes preceding simple movement (Deecke, et al. 1987; Jahanshahi, et al. 1995). Moreover, the BP also depresses in other disease such as schizophrenia (Dreher, et al. 1999) and catatonic (Northoff, et al. 2000). These findings provide evidence that the SMA has an important role in the early stage premovement activity and the readiness for voluntary movements (self-initiated movements)

(Cunnington, et al. 2003). Notably, humans can still exert a "veto" even after onset of BP of self-initiated movements. However, the veto must occur before a point of no return is reached (Schultze-Kraft, et al. 2016). This cannot-avoid moving "point" still needs to be clarified.

There is no simple dichotomy that can be drawn to summarize the involvement of the SMA, pre-SMA and lateral premotor cortex in internal and external task (Tanji 1994; Tanji 1996). Recent studies reveal that the SMA has an important role in the execution of both externally triggered task (Thaler, et al. 1988; Thickbroom, et al. 2000; Hoshi and Tanji 2004; Ariani, et al. 2015; Cunnington, et al. 2002) and internally initiated task (Thaler, et al. 1988; Jenkins, et al. 2000; Cunnington, et al. 2002), the pre-SMA also acts as an important component in the performing of both external movements (Ariani, et al. 2015; Cunnington, et al. 2002; Nachev, et al. 2005) and internal movements (Cunnington, et al. 2002). In detail, the hemodynamic response time of pre-SMA is significantly earlier for self-initiated tasks than that for externally triggered tasks (Cunnington, et al. 2002). The pre-SMA is more extensive activated in self-initiated movements than in externally triggered movements (Deiber, et al. 1999). Moreover, studies using PET on human volunteers revealed that pre-SMA is more activated when the subjects confront choices of actions instructed by external signals (Jenkins, et al. 2000). This is consistent with the fact that patients with pre-SMA injury have a selective deficit in the ability to inhibit a response in the context of competition between actions (Nachev, et al. 2007). Furthermore, premovement potentials in areas SMA and pre-SMA are more likely seen in slow rate of repetitive finger movements and seldom seen in rapid rate finger movements (Kunieda, et al. 2000). Areas pre-SMA and SMA cooperate with each other to complete the task regardless of self-initiated or externally triggered, but they have functional specificities with respect the mode of movement initiation (internal movement or external movement) and movement type (fast or slow).

1.4.4 Temporal and spatial coding.

Wealth of studies on monkeys or humans demonstrated that the pre-SMA is more involved in movement preparation, whereas the SMA is more related with execution of task (Tanji 1985; Tanji and Kurata 1985; Luppino, et al. 1993; Matelli, et al. 1993; Yazawa, et al. 1998; Jenkins, et al. 2000; Hoshi and Tanji 2004). The generation and

control of a sequence of movements is of crucial interest to complete a movement successfully. And multiple single movements must request a variety of spatial and temporal configurations for purposeful motor behaviour (Tanji 2001). Thus from a higher perspective, these two entities pre-SMA and SMA code the motor or task on temporal and spatial scales. This process includes many functions such as preparation, execution, alteration, inhibition, updating etc. One meta-analysis of functional neuroimaging studies has found that the activations associated with sensory, non-sequential and suprasecond temporal processing tend to locate to the rostral pre-SMA, while the opposite is true for the caudal SMA, which indicates that there was a functional dissociation of pre-SMA and SMA in temporal processing (Schwartze, et al. 2012).

Temporal coding: Kotz and colleagues pointed out that area pre-SMA was involved in explicit encoding of temporal structure in perception and production, while area SMA used this information to execute a sequential action. They have classified the differential input of SMA to a temporal processing network (Kotz and Schwartze 2011). It is by no means only the pre-SMA and SMA to undertake the temporal processing. The temporal processing network comprise of subcortico-thalamo-cortical. The pre-SMA is involved in the cognitive control of interval timing by decoding time information as a categorical signal and generating an appropriate interval, whereas the SMA appears to be modest effect to this aspect of behavioural control (Mita, et al. 2009). One study focusing on how area pre-SMA operates, showed that the neurons in area pre-SMA appear to monitor the performance of the behavioural trials in a binary-coded manner, resembling the operation of binary counting elements (artificial computing devices) (Shima and Tanji 2006).

What happens in the condition when subjects need to update the movement plans (switching task)? One study performed on monkeys found that when the monkeys are required to change directions of forthcoming arm movements, many neurons (31%) in area pre-SMA recorded show the shift-related activity, whereas, only 7% of recorded neurons in the SMA show such an activity (Matsuzaka and Tanji 1996). Another study also found the pre-SMA is more active during a process when monkeys were required to update motor sequences (Shima, et al. 1996). In switching tasks of human, fMRI studies have confirmed the limited importance of pre-SMA for sensory attentional switching

(Rushworth, et al. 2002; Kennerley, et al. 2004). Another important aspect of movement execution is inhibitory control. This issue is often explored according to Go/No-go task. The fMRI studies on healthy volunteers showed successful inhibitions or less STOP signal reaction time were associated with greater activation in the pre-SMA (Li, et al. 2006; Chao, et al. 2009). Notably, the preceding context can affect this process of inhibition (Durston, et al. 2002). By integrating fMRI and Go/No-go tasks, Durston and colleagues found that the medial wall is more active during Go trials, which is not in accordance with the former study. The reason may lie in different context paradigm setting (Liddle, et al. 2001). Some patients with a lesion of the caudal pre-SMA have no impairment for STOP task, but with a deficit for switching task (Roberts and Husain 2015). This suggests that the different parts of area pre-SMA may be responsible for different tasks such as switching task or No-go task.

Evidences from the electrophysiology also deepen our knowledge about the function of temporal coding of area pre-SMA and SMA. The peri-movement beta band event-related desynchronization (ERD) activities are quite sensitive to cue-related temporal factors (Heinrichs-Graham, et al. 2016) and give a good spatiotemporal discrimination (Defebvre, et al. 1994). This may reflect the function of temporal coding in SMA. By simultaneous recording from areas in human brain, Ohara and colleagues investigated the movement-related change in cortical EEG signal. It was revealed that area SMA had earlier onset of event-related desynchronization (Ohara, et al. 2000. After movement, a transient increase in activity (event-related synchronization, ERS), which may reflect the inhibition of networks, can be observed in SMA. This indicates that the background cortical activity in the SMA proper has a specific temporal pattern with respect to self-paced movement (Ohara, et al. 2000; Pfurtscheller, et al. 2003). This kind of oscillation could be connected with the function of temporal coding considering the fact that patterns of ERD during planning could be differentiated by the category of action sequences (Park, et al. 2013).

In addition, the activation of pre-SMA also related to the temporal discrimination task. One study using fMRI on healthy volunteers suffering inter-stimulus intervals electrical pulses revealed that activation of pre-SMA and anterior cingulate cortex is involved in the temporal discrimination task (Coull, et al. 2004; Pastor, et al. 2004). Notably, it remains to be clarified whether this function relates to temporal coding. It is

possible that the result of a voluntary movement will be conversely a new stimulation in the cortex. The subjects need to pay attention to time in both the voluntary movements and inter-stimulus intervals, which may be attributed to special function of the pre-SMA.

Spatial coding: Not only the sequence organization is critical, but also the spatial coding is important for completing movements. The spatial scale means what extent and trajectory the arm or other effectors should reach. Studies in monkeys and humans suggest that there is a role for supplementary areas in spatial and temporal coordination of bilateral movements (Uhl, et al. 1996; Obhi, et al. 2002). Using visual signal cues to lead target-reaching movements in monkeys, found that pre-SMA neurons are associated with the location of the target, and SMA neurons are correlated with which arm to use (Hoshi and Tanji 2004). The function of SMA proper participating in the control of kinematic parameters of endeffector motion has been supported by other studies (Tankus, et al. 2009).

1.4.5 Abstract mental computations

In the mirror-image judgement task or dynamic visuo-spatial imagery task or mental rotation task, the pre-SMA (along with other brain areas like the ventrolateral prefrontal and parietal cortex) is more active (Richter, et al. 2000; Lamm, et al. 2001; Windischberger, et al. 2003; Johnston, et al. 2004). This function has been sustained by the fact that some patients with Parkinson's disease showed deficits of visuo-spatial orientation in tasks like mental rotation (Lee, et al. 1998; Crucian, et al. 2003; Amick, et al. 2006). Of interest is that the dopamine does show no significant influence on rotation abilities of patients with Parkinson's disease (Crucian, et al. 2014). On the other hand, short time motor imagery (playing soccer or tennis) can boost the motor imagery patterns in motor related areas including premotor cortex, SMA and so forth. This may be a promising additional tool in future rehabilitation programs (Wriessnegger, et al. 2014). In sum, this special feature proposes a relatively abstract spatial computational role within the SMC beyond the traditional notions and it defines and predicts a predominant function involving the SMC in a diverse range of cognitive control (Leek and Johnston 2009).

1.4.6 Learning

When monkeys performed a sequential button-press task after pre-SMA inactivation (locally injected muscimol), the number of errors increased for performing novel sequences, but not for performing learned sequences. This result suggested that mesial frontal cortex, especially pre-SMA, is involved to the sequence acquisition rather than execution (Hikosaka, et al. 1996; Nakamura, et al. 1998; Nakamura, et al. 1999). Moreover, a study on monkeys has noted that the pre-SMA is related to visuo-motor association components, in which the pre-SMA activation decreases during learning of sequences, indicating that the process of individual visuo-motor associations were replaced by the formation of sequential procedural memory, which happens outside the pre-SMA (Sakai, et al. 1999). Using positron emission tomography on healthy volunteers, Garraux and colleagues observed a higher increase of dopamine levels in pre-SMA and a lower dopamine release in sensorimotor part of globus pallidus pars interna (GPi) during learning (Garraux, et al. 2007). This may clarify a mechanism of motor learning related collaborating between dopamine release in GPi and pre-SMA, which is corresponding to the connectivity discussed previous.

Some studies showed that SMA is not related to learning, but is associated with the execution of sequential movements (Hikosaka, et al. 1996). Other studies argue that the SMA is also related to learning (Aizawa, et al. 1991; Lee and Quessy 2003). Studies on monkeys found that about a third of SMA neurons revealing gradual changes in neural activity are related to experience with a movement sequence across trials. Moreover, about a quarter of SMA neurons show similar changes within individual trials. Moreover, when an overlearned movement sequence is performed repeatedly, the learning-related changes in neural activity will decrease. This indicates that a part of SMA neurons are related to learning, some other parts of SMA neurons are related to performance (Lee and Quessy 2003). Interestingly, lesions of the primary motor cortex can lead to an increased premovement activation of neurons in SMA, indicating the use-dependent reorganization of the neurons in SMA (Aizawa, et al. 1991). Notably, the process of learning may be involved to working memory, which may be also attributed to the supplementary motor complex (Smith, et al. 1998; Pollmann and von Cramon 2000; Linden, et al. 2003).

1.4.7 Language generation.

The activation of SMA was observed during the word generation task (Gyung Ho Chung 2004). Indeed in clinical practice SMA resection can result in language deficits or mutism (Fontaine, et al. 2002; Potgieser, et al. 2014). fMRI studies on humans during sentence generation task revealed that the language SMA is located anterior to motor SMA (Chin-shoou lin 2007).

1.4.8 The function of supplementary eye field

The supplementary eye field (SEF) does not contribute directly and immediately to the initiation of visually guided saccades but plays an important role in monitoring search performance (Stuphorn, et al. 2010; Purcell, et al. 2012). Moreover, the SEF and frontal eye field (FEF) collaborate dynamically to execute ocular decisions: to decode the timing, amplitude and direction of saccades (Ohmae, et al. 2015). Compared to FEF, readiness potential from SEF and pre-SMA precede readiness potential from FEF (Yamamoto, et al. 2004). In addition, the SEF is more related to interpret the task but is less involved to execute the motor (Yang and Heinen 2014). The activity of SEF conveys the error-related and conflict-related signals and plays an important part in discerning the generator of the error-related negativity (Emeric, et al. 2010). Studies on monkeys revealed that the SEF encodes confidence in decision. During the process of decision-making, the neural signals in the SEF appeared after the choice and diminished before the choice outcome (So and Stuphorn 2016). During the value-based decisions, the SEF encodes first the desired economic good and later the saccade of the chosen action (Chen and Stuphorn 2015). In detail, the SEF executes the function of decision-making by increasing activity to signal their preferred (agonist) rule-state and decreasing activity to signal their non-preferred (antagonist) rule-state. This process is a winner-take-all like model, in which the activities of SEF neurons decrease rapidly in anticipation of the antagonist rule-state or easier to predict rule-state (Ray and Heinen 2015). Notably, to emphasize the role of SEF in oculomotor saccade, it is by no means that area pre-SMA is not responsible for the eye movements. In fact, both the SEF and

pre-SMA are activated during the process of horizontal saccade (earlier than the FEF) (Yamamoto, et al. 2004).

1.4.9 Other functions

Area SMA has been found to be related to sensory task using functional MR imaging (fMRI) in humans during sensory task (Chung, et al. 2005). Moreover, areas SMA and pre-SMA play an important role in supporting interactions between motor and sensory processes and area part of the network supporting the spontaneous motor programs related to sounds (Lima, et al. 2016). Using fMRI in humans, Lau and co-workers (Lau, et al. 2004) found an enhancement of activity in pre-SMA was associated with attention to intention rather than attention to the actual movement. This may suggest that activity in the pre-SMA reflects the representation of intention. These non-traditionally functions of supplementary motor complex remain to be clarified in further work.

1.5 Action with abnormal mesial frontal cortex

It is well known that patients who underwent complete resection of SMA exhibit a decrease of spontaneous movements and difficulty in performing voluntary motor task in the contralateral limbs (Laplane, et al. 1977; Bannur and Rajshekhar 2000; Krainik, et al. 2001; Kasasbeh, et al. 2012). Moreover, following surgery in the SMA, the patients will experience a global reduction in spontaneous speech, known as akinetic mutism (Laplane, et al. 1977; Pai 1999; Krainik, et al. 2003; Mendez 2004). This syndrome, following unilateral resection of the SMA, is featured by a global akinesia on the contralateral side, which is known as SMA syndrome. The study in humans revealed that the patients will experience a typical characteristic of SMA syndrome immediately after the resection of SMA. Moreover, the degree of deficits is corresponding with the extent of the SMA resection (Ulu, et al. 2008). Interestingly, a remarkable characteristic of SMA syndrome is that the deficits almost completely recover within weeks to months (Potgieser, et al. 2014). Long after the operation, some squeal such as disorder of alternating movements of the hands or a deficit in bimanual coordination may be observed (Laplane, et al. 1977; Brinkman 1981). The abnormal lateral of the resected SMA may be partially compensated by a recruitment of the contralesional SMA

(Krainik, et al. 2004). After a lesion, the contralateral SMA in healthy hemisphere shows an increased activation, which indicates a plastic change of SMA function (Krainik, et al. 2003).

Following a lesion of caudal pre-SMA, The patient showed no impairment in distracting stimuli or STOP task. However, a deficit can be observed during rapidly switching task (Roberts and Husain 2015).

The lesions of supplementary motor complex are not necessarily to cause merely deficits of movements. Several lesions in SMA have been reported in patients with alien hand syndrome, characterizing by semi-purposeful movements (for example, grasping objects in vicinity) (Feinberg, et al. 1992; Scepkowski and Cronin-Golomb 2003; Hassan and Josephs 2016). The unwanted movements in alien hand syndrome are related to the dysfunctional neural network, involving brain regions known to be related to movement execution and planning (Schaefer, et al. 2010). One study using fMRI on a patient with alien hand movements found that the unwanted movement is corresponding with a selective activation of contralateral primary motor cortex, whereas voluntary movements in the unaffected hand activate extensive brain regions including the primary motor area, the SMA, the premotor cortex, et al (Assal, et al. 2007). The patients with SEF and SMA lesions showed a dysfunction of inhibitory effect (ocular or manual), indicating that the SEF and SMA regulate automatic effector-specific suppression of motor task (Sumner, et al. 2007). Moreover, behavioural testing on the patient with lesions in the SEF revealed that the patients showed abnormalities in switching between anti- and pro-saccades or in conflicting stimulus-response rules for saccades (Parton, et al. 2007). Some other movement abnormalities (for example gait apraxia) have also been reported in the patients with SMA lesions (Sala, et al. 2002).

1.5.1 Temporal and spatial coding in lesions of mesial frontal cortex

There is less studies focus on the issue of temporal and spatial coding after lesion of supplementary motor complex. Tan and colleagues injected bilaterally a GABA receptor agonist-muscimol into either the SMA or pre-SMA in monkeys, and then they trained the monkeys to execute three different sequence movements in memorized order (without visual signals). They found that the monkeys were severe impaired in

performing the sequence of movements from memory, although they could perform the sequence movement correctly from visual signal cues (Shima and Tanji 1998). Another study using the same methods revealed that the number of errors increase for learning new sequences, but not for learned sequences, after pre-SMA inactivation. The trend is similar after SMA injections, but not significant (Nakamura, et al. 1999). These results suggest that the pre-SMA plays an important role in learning new sequences.

1.5.2 Internal task vs. external task.

There are several evidences supporting the notion that the lesions in SMA could disturb the internal task and lead to an intact external task, regardless in humans or in monkeys. Studies on monkeys showed that bilateral lesions of SMA resulted in a transient and almost complete dysfunction in movement initiation when all external cues were absent (Kazennikov, et al. 1998). In humans, the patients with lesions involving the SMA showed severe impairment in performing rhythms from memory, but producing the rhythms well under external signal cues (Halsband, et al. 1993). This trend is still true in the memory-guided saccade sequence, of which the chronology was disturbed in the patients with SMA lesions (Gaymard, et al. 1993). Notably, the studies on humans have some limitations. E.g. the territory of lesions may be not confined to the supplementary motor complex accurately. One study reported a patient with a rare highly selective lesion of the SEF impaired in control in switching the direction of his eye movement, but the subject could find the errors and adjust the errors immediately (Husain, et al. 2003). This may indicate that SEF is involved to implementing oculomotor task during conflict condition, but not responsible for error monitoring (Husain, et al. 2003). However, this patient with lesions in SEF could perform the order of memory-guided saccades correctly without significant difficulties, but with difficulties in response for conflicting rules governing stimulus (Parton, et al. 2007). This manifestation (disorder in novel movements, normal in learned movements) is same with the tasks executed by patients with Parkinson's disease (Hodgson, et al. 1999).

1.5.3 Parkinson's disease.

One of the main symptoms in patients with Parkinson's disease (PD) is akinesia, which is similar to that seen in lesions of SMA in humans (Marsden 1989; Jenkins, et al. 1992). Study using PET in humans with Parkinson's disease revealed that activation of the SMA and putamen is impaired during voluntary movement when the patients are off treatment (Playford, et al. 1992; Jahanshahi, et al. 1995). Also, in these Parkinson's disease patients the BP is also abnormal during performing self-paced voluntary movements (Dick, et al. 1989). All these evidences suggest that there is a closely relationship between SMA and readiness potential. Thus it might provide an insight into the treatment of Parkinson's disease. A randomized controlled study showed that using 1-Hz repetitive transcranial magnetic stimulation (rTMS) over the SMA in patients with PD can improve the motor symptoms (Shirota, et al. 2013). Moreover, the treatment with dopamine replacement therapy (for example levodopa or apomorphine) significantly improves the functional activities of SMA in Parkinson's disease patients and improves the akinesia symptom (Jenkins, et al. 1992; Rascol, et al. 1994), which suggests that dopaminergic medication seems to function by enhanced connectivity within cortical–subcortical loop (Michely, et al. 2015).

1.6 The aim of the present study

The aim of the present study was therefore to analyze the cytoarchitecture of the human mesial frontal motor area in serial histological sections of 10 human postmortem brains using a statistical approach for an observer-independent detection of borders between cortical areas (Schleicher, et al. 2005; Schleicher, et al. 2009). The individual maps of areas SMA and pre-SMA will be produced. Using the individual maps of areas SMA and pre-SMA, we aim to calculate probabilistic maps of areas SMA and pre-SMA which will be transferred to a sterotaxic reference space. Thus, the definite locations of areas SMA and pre-SMA will be identified by cytoarchitectonic analysis. One other aim of the present study was to detect the function of areas SMA and pre-SMA based on a coordinate-based meta-analysis. The functional co-activation patterns of areas SMA and pre-SMA will be investigated. In sum, this study was oriented to provide a new style to understand the map and function of areas SMA and pre-SMA. Together with previous studies, the current study provides a multi-layered hierarchy to understand the structure and function of areas SMA and pre-SMA.

2 Methods and Material

2.1 Histological processing of postmortem brains

Ten brains of subjects without a clinical history of neurological or psychiatric diseases (5 females and 5 males; Table 2.1.1), were obtained for the present study via the body donor program of the Department of Anatomy at the University of Düsseldorf governed by the local ethics committee. The brains were extracted from the skull within 24 h after death and fixed in either in 4% buffered formalin (pH=7.4) or a mixture of formalin, glacial acetic acid, and ethanol (Bodian mixture, (100ml including 90ml 80% ethanol+5ml glacial acetic acid+5ml of glutaraldehyde)) at least 6 months. Histological processing was consistent with previous studies in our laboratory (Amunts, et al. 1999). Nine whole paraffin-embedded brains were serially sectioned in the coronal plane on a microtome (Polycut E, Reichert-Jung, Germany; thickness=20 μm). Approximately 6500 to 7500 sections, depending on the individual brain size, were obtained. One brain in the same setting was serially cut in the horizontal plane (case 17, 4996 sections). Each 15th section was mounted on a glass slide and stained for cell bodies using a modified silver staining (Merker 1983) (Fig. 2.1.1).

Table 2.1.1 sample of postmortem brains obtained for cytoarchitectonic analysis

| Brain code	Gender	Age (year)	Cause of death	Cutting	Fresh weigh(g)
1	Female	79	Bladder cancer	Coronal	1350
2	Male	56	Rectal cancer	Coronal	1270
4	Male	75	Necrotizing glomerulonephritis	Coronal	1349
6	Male	54	Myocardial infarction	Coronal	1622
9	Female	79	Generalized atherosclerosis, ventricular failure	Coronal	1216
10	Female	95	Small bowel obstruction	Coronal	1046
12	Female	43	Pulmonary heart disease	Coronal	1198
17	Female	50	Acute myocardial infarction	Horzizontal	1328
20	Male	65	Congestive heart failure, respiratory failure,	Coronal	1392
21	Male	30	Bronchopneumonia, Hodgkin's disease, deep vein thrombosis	Coronal	1409
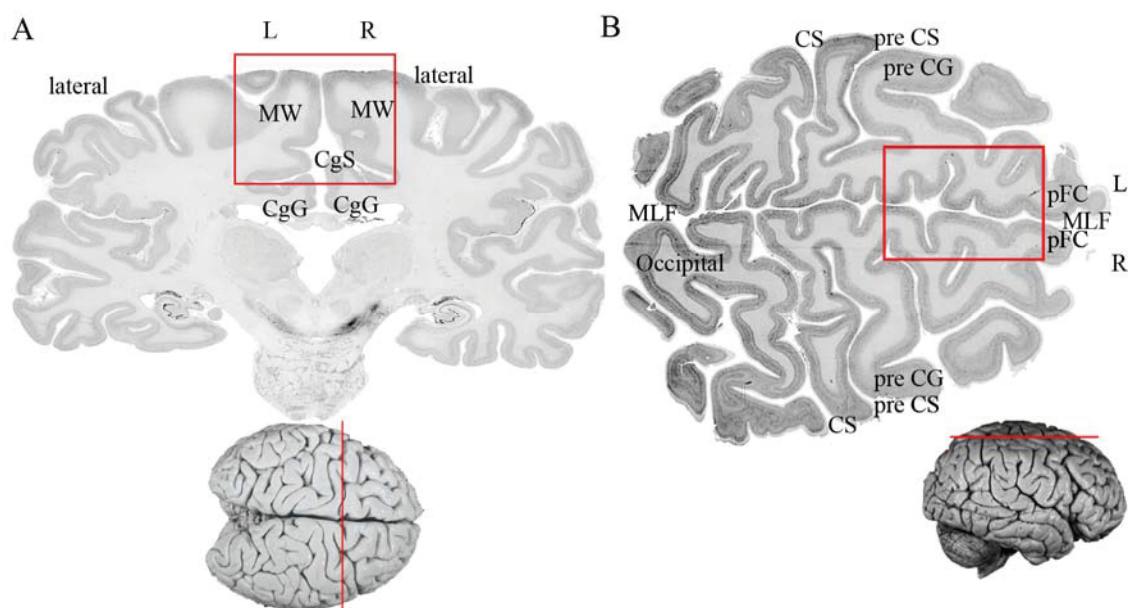
Fig. 2.1.1 Histological sections of human brains stained for cell bodies. A One brain (case 12) cut in coronal plane. B One other brain (case 17) used in the study in the horizontal plane. The red frame indicates the region of interest including SMA and pre-SMA in the medial wall. pFC= prefrontal cortex, MLF=Medial longitudinal fissure, CS=central sulcus, pre CG= precentral gyrus, pre CS=precentral sulcus, CgG=cingulate gyrus, CgS=cingulated sulcus, MW= medial wall. L=left hemisphere of the brain, R=right hemisphere of the brain. The red frames in A and B are roughly the regions of interest. The red lines are the cutting directions (A coronal cutting and B horizontal cutting).

2.2 Observer-independent detection of cytoarchitectonic borders based on the analysis of the grey level index

An observer-independent mapping approach (Axel Schleicher 1998; Schleicher, et al. 1999; Amunts and Zilles 2001; Schleicher, et al. 2005) was employed to delineate different areas. In this approach, the author made the imagination that the laminar pattern of the grey level index (GLI) is similar within a cytoarchitectonic area, but varied abruptly at the border between two areas. In this approach, rectangular regions of interest (ROIs) were defined in the histological sections and obtained with a high resolution CCD-Camera (Axiocam MRM, ZEISS, Germany), which worked with an optical light microscope (Axio Observer Z1, ZEISS, Germany). The control of the microscope and process of the images were performed using the Zeiss image software Axiovision (version 4.6).

The GLI, evaluating the area fraction of cell bodies, was measured by adaptive thresholding in continuously adjoining cortical tiles (17×17 pixel) (Schleicher and Zilles

61

1990; Wree, et al. 1982). The GLI images of the ROIs were calculated with in-house software written in MatLab (The MathWorks, Inc., Natick, MA). The cytoarchitectonic analysis was carried out by measuring the GLI in ROIs. The size of ROIs varied in dependence on sulcal properties (ca. 1.5-2cm). The ROIs were digitized with an in-plane resolution of 1.02 μm per pixel. Then, the laminar change was defined in cortical cell density as GLI profile which was from the outer contour line (the border between layers I and II) to the inner contour line (the border between layer VI and the white matter). The curvilinear traverses between the two contour lines, oriented parallel along the cell columns, were calculated using a physical model based on electric field lines (Jones, et al. 2000). The traverses in the ROIs were arranged at equidistant intervals of ca. 96 μm. Profiles, covered in the cortex in the ROIs, were extracted from the GLI values of those traverses. A set of ten features (including the mean GLI value, the center of gravity in axis of the cortical depth, the standard deviation, the skewness, the kurtosis, and the analogous parameters for the first derivative of each profile) were used to characterize the laminar pattern of every GLI profile (Dixon 1988; Amunts, et al. 1997; Amunts, et al. 2000; Schleicher, et al. 2005; Schleicher, et al. 2009). Each profiles was normalized to a standard length corresponding to a cortical thickness of 100 % (from 0% to 100%= from the border between layers I and II to the border with white matter). Thus the profiles with different lengths could be compared (Fig.2.2.1, 2.2.2).

The extracted features were combined into a ten-element feature vector which was used to calculate the Mahalanobis distance (MD) (P. C. Mahalanobis 1949) between two neighboring groups of profiles for quantifying laminar differences. In order to detect the border, a specified number of profiles (block size from 10 to 30 profiles) were grouped into a block of profiles (Schleicher, et al. 2000). Then, a statistical analysis between two neighboring blocks of profiles in the laminar pattern was carried out using feature vectors. The blocks were moving simultaneously in steps over the entire cortical ROI. This objective, quantitative mapping procedure is not by means of a purely visual, microscopical examination of histological specimens, which is thought as an observer independent measurement for cytoarchitectonic differences (Schleicher and Zilles 1990; Schleicher, et al. 1999; Schleicher, et al. 2000; Schleicher, et al. 2005). A following Hotelling's t^2 test with Bonferroni correction was selected for testing the significance of D^2 (a =0.001). Higher D^2 value was corresponding to greater difference of laminar patterns. The cortical borders were registered, if the borders were consistently identified

at the same position across several block sizes, and if the positions were found at comparable locations in neighboring sections (Fig. 2.2.2).
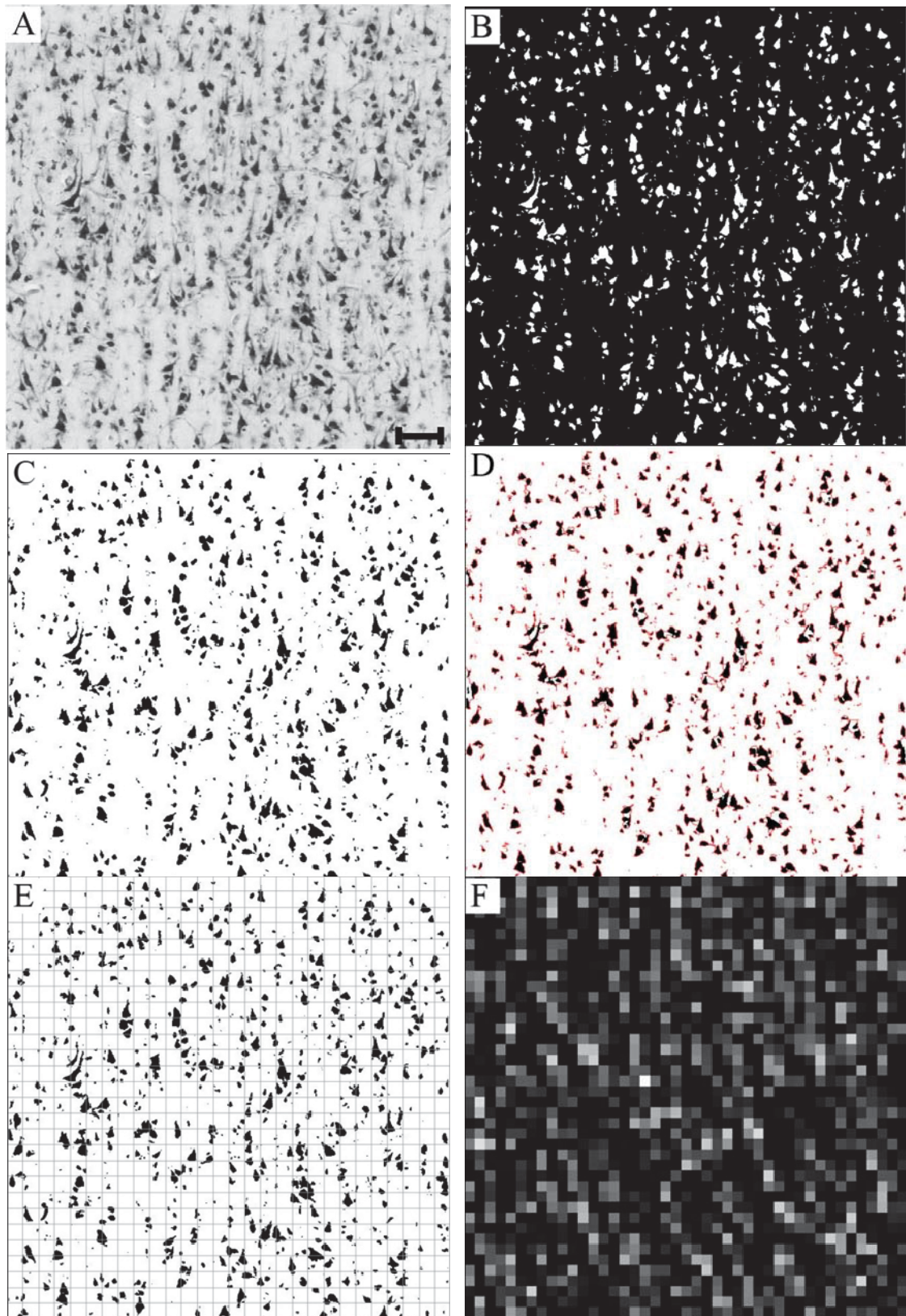
Fig. 2.2.1 Process of cell body detection using in-house software. The legend in next page. ▶

◄Fig. 2.2.1 Process of cell body detection using in-house software. Illustration of the different steps of image post-processing from A: the original digitized region of interest (ROI) to D: the cell body detection. A: The original digitized photomicrograph of isocortcal with an in-plane resolution of 1.02 μm per pixel. Scale bars = 0.5mm. B: Binary image of A, generated by adaptive thresholding filter to eliminate small particles. The areal density of white cellular transects is 0.19 and the GLI-estimate 19%. C and D: Binary overlay of the original image to visualize cell body detection. E: Binarized ROI superimposed by a 17×17 grid used for the generation of GLI images. The related GLI image recalculated to the same size. F: Resulting GLI-image. Each pixel in the GLI image indicates an appraisement for the volume fraction of the cell bodies in a related measuring area of size (17×17 pixel) in the original digitized image coded by 8 bit grey values.

Fig. 2.2.2 Observer-independent border detection. A: Digitized ROI with contour lines and superimposed numbered curvilinear traverses indicating where the GLI profiles were extracted. The bars at profile positions 87 and 238 corresponds to the significant maxima of the MD function in D and E caused by the cytoarchitectonic border between CgG and SMA, SMA and M1 which has been confirmed by visual examination under the microscope. This section was selected from the left hemisphere of the brain showed in Fig. 2.1.1A. B: "maximal distance function". The positons of significant maxima of the MD function (black dots) showed in different block size. The result has been corrected with Bonferroni correction (P=0.001). Most dots are aligned at profile positions 87 and 238. B: "raw frequencies", "frequencies thresholded". The corresponding frequency of significant maxima at different maxima at different profile positions across block size 12-30. The highest frequency occurred at profile positions 87 and 238, which were selected as putative cytoarchitectonic borders. C: The borders detected by the MD function and marked by the analysis system corresponding to the significant maxima of the MD function in B. D: Single MD function at block size 24 with a significant maximum at profile positions 87 and 238. SMA= supplementary motor area. CgG= cingulate gyrus, M1=primary motor cortex (Brodmann area 4).►
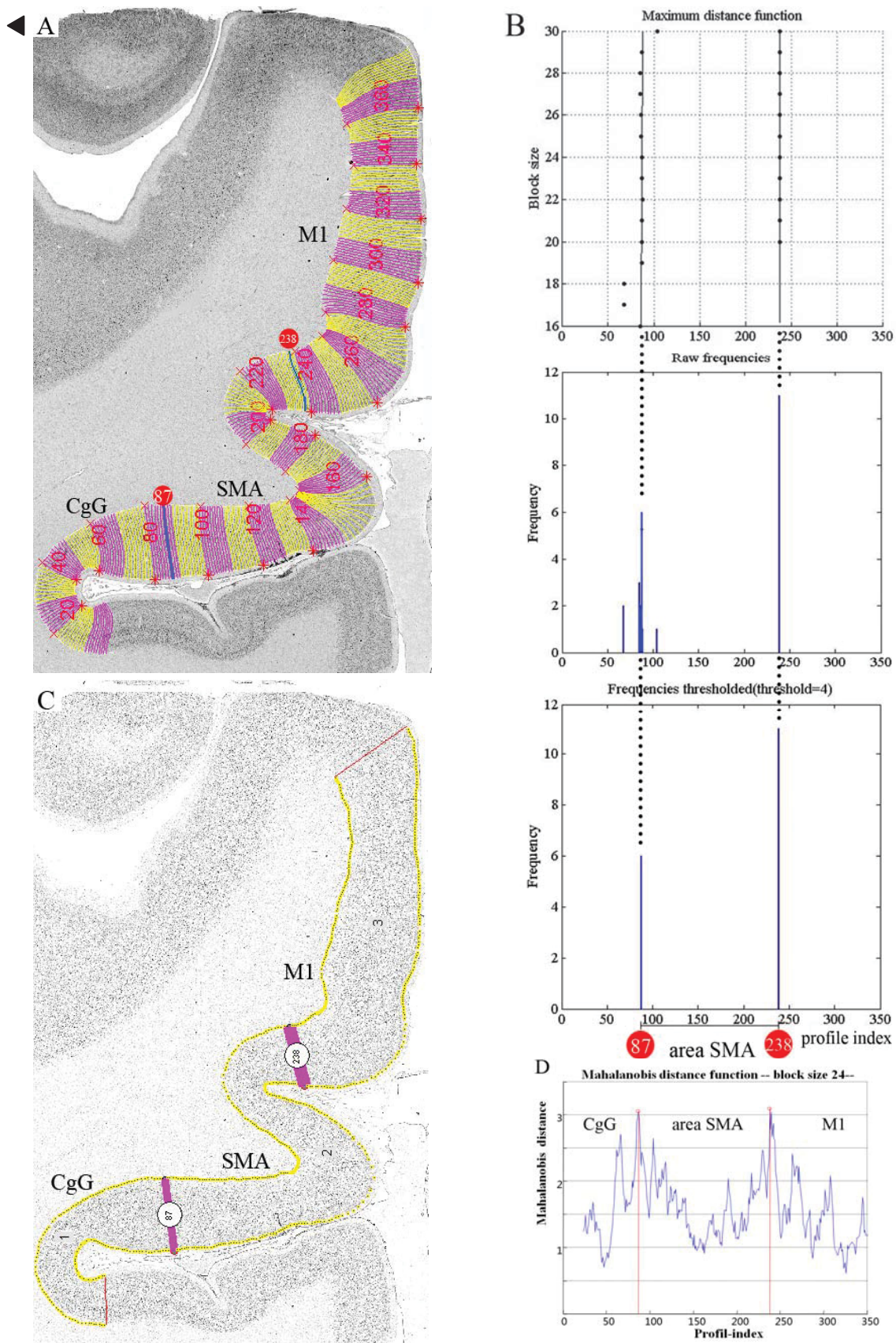
Fig. 2.2.2 Observer-independent border detection. The legend in last page.

2.3 Interareal, interhemispheric, and gender comparisons of cytoarchitectonic parameters and volumes

After delineated the borders of areas SMA and pre-SMA, the differences of interareas, interhemispheres, and genders was investigated. This process has been described as previous study (Amunts, et al. 1999). In each brain, three typical ROIs of each area were sampled per area and hemisphere. The mean GLI of a cortical area in each brain and hemisphere was calculated. The hemisphere and gender divergences were compared by analysis of variance (ANOVA). The level of significance was adjusted with Bonferroni correction.

To test the left-right hemisphere divergences in overall cell density, the asymmetry coefficient (AC, %) (Galaburda, et al. 1987; Amunts, et al. 1999) was employed. AC was calculated according to the following formula:

$$AC = 100\% \times (GLI_L\text{-}GLI_R)/[(\ GLI_L\text{-}GLI_R)/2]$$

The GLI_L and GLI_R are the mean cell densities of the left and right sides, respectively. The volume analysis (AC_{vol}) was performed with this same equation.

To quantitatively detect cytoarchitectonic differences between areas SMA and pre-SMA, the GLI profile of each area between outer (between layers I and II) and inner (between layer VI and the white matter) cortical contours were divided into ten bins with a 10%-interval: bin 1 (0%-10%), bin 2 (10%-20%), ……，bin 10 (90%-100%). In each area, representative blocks of 15 GLI-profiles were extracted from three sections. Thus, a sum of 1800 profiles (15 profiles × 3 sections ×2 areas×2 hemispheres ×10 brains) were employed for calculating mean GLI profiles of ten bins in the two areas. Mean profiles of ten bins for area SMA were then compared with those of bins for area pre-SMA (P<0.05, Pairwise comparison). To reduce data artificial interference, ROIs were collected at sites where the cortex appeared to be cut vertical to the surface without any visible artefacts of the cytoarchitectonic structure.

2.4 Hierarchical clustering analysis between cytoarchitectonical similarities

Hierarchical clustering was performed to detect the cytoarchitecture similarities or dissimilarities between area SMA and area pre-SMA. In this process, the cytoarchitecture features of areas were extracted from the GLI-profiles. The hierarchical clustering cohered the cortical areas in a sequence of similarity. The Ward method

(Ward 1963) and the Euclidean distance were adopted in the crucial setting of this explorative analysis to quantify the degree of dissimilarity between areas SMA and pre-SMA. In each brain, three typical ROIs of each area were sampled per area and hemisphere. The selected sections were same with the sections used in the process of detecting areal cytoarchitectonic differences. It means that each area representative blocks of 15 GLI-profiles were extracted from three sections. Thus, a sum of 1800 profiles (15 profiles × 3 sections ×2 areas×2 hemispheres ×10 brains) were employed for hierarchical clustering.

2.5 3D reconstruction and probabilistic maps

To minimize distortions, compression damage and other artefacts, the brains were suspended during fixing process in a plastic container in the fixation solution. Following fixation and removal of the meniges, each brain experienced a MRI (1.5 Tesla, Siemens, Germany)) inspection in the T1-weighted phase. MR imaging was performed as previously described and validated (Roland and Zilles 1994; Zilles, et al. 1995; Amunts, et al. 2000). The follow 3D-FLASH sequence parameters were used in current study: 40°flip angle, 40ms repetition, 5ms/image echo time, 128 single-section images in the sagittal plane with a respective spatial resolution of 1x1x1.17mm (resolution in the layer plane x thickness). To identify the orientation of macroscopic and microscopic images, photographs of all brains from ventral, dorsal, and lateral views were created (Amunts, et al. 2000). The MRI sequences of fixed brain and the digitized histological sections were used for producing 3D reconstructed histological volumes of each brain, excluded for distortions. Matching between MRI sequences and histological sections was carried out according to both linear and nonlinear fluid transformations (Henn S 1997; Hömke 2006; Schormann, et al. 1996; Schormann and Zilles 1997; Schormann and Zilles 1998). Then, the different areas were superimposed and continuous probabilistic map was generated for each area in MNI space. Each voxel in the probabilistic map of a given area represents how many individual brains overlapped with the respective cytoarchitectonic area in that voxel. The probabilistic cortical map was rendered by color-coded and values from 0% to 100%. Thus, these maps quantitatively describe the intersubject variability of a cortical area in stereotaxic space (Evans, et al. 1992; Evans, et al. 2012; Roland and Zilles 1998).

Finally, a maximum probability map (MPM) was calculated (Eickhoff, et al. 2005; Eickhoff, et al. 2006). Each voxel was assigned to the cytoarchitectonic area with the most likely anatomical area. The surface based on the MPM in the reference space of the T1-weighted single-subject template of the Montreal Neurological Institute (MNI) brain was calculated (Evans, et al. 1992; Evans, et al. 2012). These MPMs of areas SMA and pre-SMA were employed to define the regions of interest in the coordinate-based meta-analysis.

2.6 Volumetric analysis of areas SMA and pre-SMA

The fresh weight of the analyzed brain has been weighed (Table 2.1.1) (Hans, et al. 1971). Due to the shrinkage of histological processing, a shrinkage factor for correction was defined for each postmortem brain as the ratio between the fresh volume and the histological volume (Amunts, et al. 2007). To estimate the fresh volumes of the delineated regions in hemispheres, the high-resolution flatbed scan delineations and Cavalieri's principle (Gundersen, et al. 1988) was employed.

The proportion of area volume in total brain volume was calculated. The differences of volume proportion in aspect of hemisphere and gender was tested with pair-wise permutation test using in-house software written in Matlab (Eickhoff, et al. 2007). The null distribution was evaluated by Monte-Carlo simulation with a repetition of 1,000,000 iterations. The P value in each test is less than 0.05 will be considered as significant result (Eickhoff, et al. 2007; Bludau, et al. 2014)). In Addition, the correlations between volume and age by computing the spearman correlation coefficient was explored.

2.7 Meta-analytic connectivity modeling (MACM)

Meta-analytic connectivity modeling (MACM) (see details in website BrainMap: http://brainmap.org) is a simple, easily adaptable, data driven method and is mainly oriented to identify functional connections within brains (Robinson, et al. 2010; Eickhoff, et al. 2011; Robinson, et al. 2012; Fox, et al. 2014; Langner, et al. 2014). It was performed using a revised activation likelihood estimation (ALE) technique based on the database BrainMap (Laird, et al. 2005; Laird, et al. 2011; Eickhoff, et al. 2012).

The delineated regions (MPMs of areas SMA and pre-SMA) were defined from our cytoarchitectonic study in present approach. The co-activation areas were found from different experiments that activate the delineated regions could be found. The location query was performed within the database BrainMap (http://brainmap.org). The BrainMap Project was developed at the Research Imaging Institute of the University of Texas Health Science Center San Antonio orienting to share neuroimaging data and allow meta-analysis on different human brain functions (Laird, et al. 2009). This process was carried out by the special software GingerALE (version2.3.6, http://brainmap.org/ale) (Fox and Lancaster 2002). From the BrainMap database, only those experiments were included, that reported stereotaxic coordinates from normal individual mapping studies in healthy humans using fMRI or PET. According to the inclusion criteria, functional neuroimaging experiments (1398 Experiments on pre-SMA (18574 subjects, 21552 foci), 597 Experiments on SMA (7947 subjects, 9112 foci)) were included. The main principle of the activation likelihood estimation (ALE) method is to treat the reported foci as centers for 3D Gaussian probability distributions to capture the spatial uncertainty related with each focus. The protocol presents statistical convergence of reported activations across different experiments detected via the database of BrainMap. To recognize random and non-random foci convergence, the obtained ALE values were compared with a null-distribution reflecting a random spatial correlation between the considered experiments (Eickhoff, et al. 2012). The analysis set a threshold at a cluster-level family-wise error (FWE) corrected p<0.05 (cluster-forming threshold at voxel-level p < 0.001).

3 Results

In the present study of areas SMA and pre-SMA, the observer independent cytoarchitectonic technique was applied for detecting areal borders in 10 brains (nine brains in coronal cutting, one brain in horizontal cutting). And the maximum probability maps (MPMs) of cytoarchitectonically defined areas SMA and pre-SMA were produced. Using the MPMs of areas SMA and pre-SMA, a coordinate-based meta-analysis was performed to detect the functional connectivity of areas SMA and pre-SMA.

3.1 Identification of areas SMA and pre-SMA

Two agranular areas, SMA and pre-SMA were identified on the mesial frontal motor surface (Brodmann's area 6). Area SMA, an agranular cortex, was found on the basis of poor lamination, prominent large size pyramidal cells in the lower part of layer III, and absence of Betz cells in layer V. area pre-SMA differed essentially from area SMA by the pronounced layer V well demarcated from layers III and VI (Fig. 3.1.1). Due to the dark layer V, the distributions of layers in area pre-SMA were more visible than those in SMA. However, the layering of layer II and layer III showed differently: Layer II and layer III in pre-SMA normally fused, but the layer II and layer III in area SMA showed a more distinct border. The columnar pattern in the deep layers of area SMA was conspicuous, which was not obvious in pre-SMA. The main criterions for identification of areas SMA and pre-SMA were summarized in Table 3.1.1. These qualitative findings allowed us to identify and distinguish regions with the observer independent quantitative procedure.

The observer-independent approach showed maximal values exactly when the profiles were located at the point of an areal border (Fig. 3.1.2, Fig.3.1.4). As an example, figure 3.1.3 showed mean cell density profiles of neighbouring areas from the border between area SMA and area pre-SMA in the right hemisphere of case 17, which were obtained from the section shown in Figure 3.1.1 and Figure 3.1.2 (Fig. 3.1.3). In the profiles of area SMA, the conspicuous high percentage of GLI in the lower part of layer III was observed. The boundary between layer III and V in SMA was not clearly visible, the same boundary in pre-SMA, however, was distinct to be found (Fig. 3.1.1, Fig. 3.1.2). Figure 3.1.4 as another example showed the border between area SMA and

pre-SMA in a coronal cutting brain (case 6). The divergences of areas SMA and pre-SMA could be observed obviously. Area SMA had a poor lamination and large size pyramidal cells in the lower part of layer III. Area pre-SMA, however, had a better lamination, and a relative dark layer V. The border between layer II and layer III in SMA was more visible than that in pre-SMA. This border has been demonstrated by the distance function (Fig. 3.1.4).

Table 3.1.1 Criterions for identification of areas SMA and pre-SMA under microscopical inspection.

| Area	Criterions
SMA	1. Prominent large size pyramidal cells in the lower part of layer III.
	2. Poor lamination, especially in the part of layer IIIc and layer Va fuses
	3. Columnar pattern present mainly in the deep layers.
	4. Occasional presence of big pyramidal cells in layer V, absent of Betz cells.
	5. Layer II has a clear border with layer III.
PreSMA	1. Dark layer V well demarcated from layers III and VI.
	2. Better lamination.
	3. Layer II and layer III fuse normally.
	4. Normally, the size of pyramidal cells standing in the lower part of layer III is smaller than those in SMA.
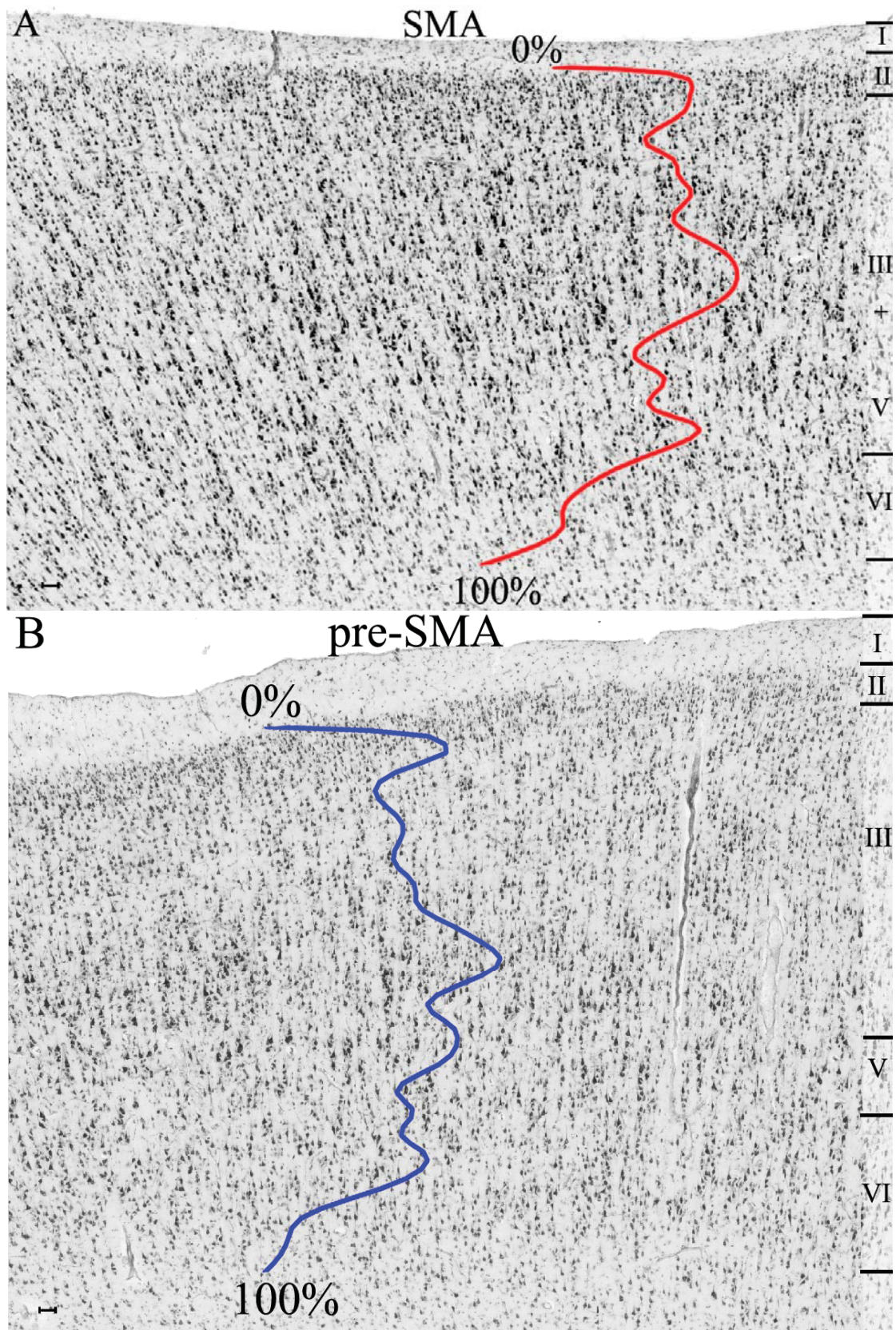
Fig. 3.1.1 Photomicrographs of cytoarchitecture of area SMA(A) and pre-SMA(B) in horizontal, cell body-stained sections. Brain code 17, right hemisphere. The color lines mark the mean profiles of area SMA and pre-SMA. Roman numerals indicate the different cortical layers. Scale bars = 0.5mm.
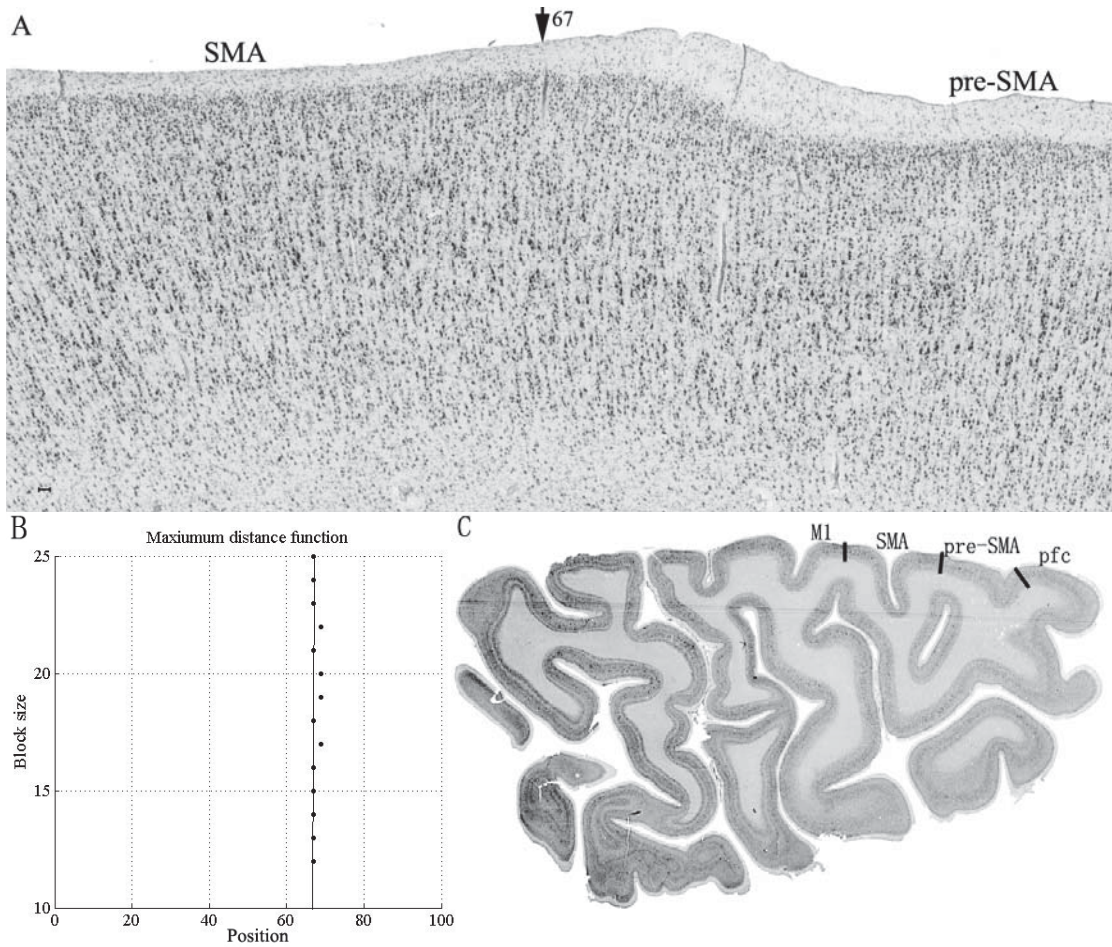
Fig. 3.1.2 Border between areas SMA and pre-SMA in a section of case 17 at position 67 (arrowhead) of the distance function. A: Photomicrograph of a horizontal, cell body stained section (the same place with Fig. 3.1.1). B: The maxiumum distance function D^2 at position 67(*P<0.01) exactly matches the border. C: Location of the region of interest in the right hemisphere. The dark lines between areas mean the rough borders. The dark line between SMA and pre-SMA indicates the borders between the two areas. M1= primary motor area, pfc = prefrontal cortex.
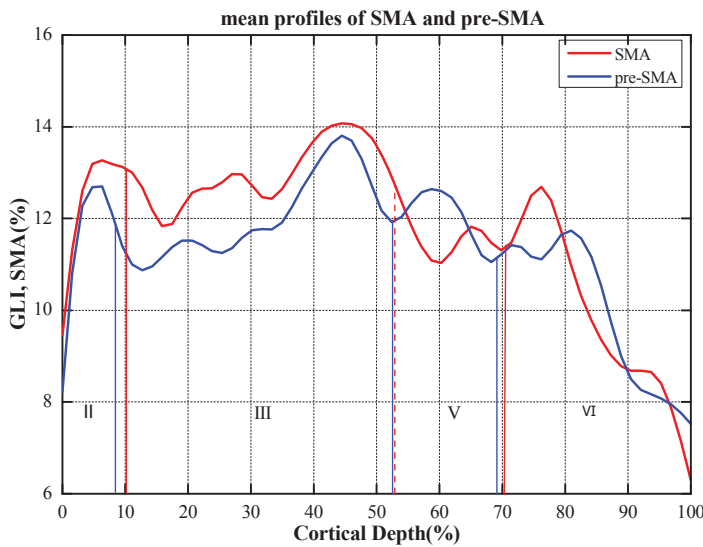

Fig. 3.1.3 Mean cell density profiles (ordinate, gray level index; GLI, in %) for areas SMA (red line) and pre-SMA (blue line) of brain case 17 showing laminar changes from the layer I/II border (abscisa, 0%) to the white matter (abscisa,100%). Profiles were obtained from the section shown in Figure 3.1.1 and Figure 3.1.2. The vertical lines indicate the border between layers. The dash line for SMA means the layer III and layer V somewhat fused. Roman numerals indicate different cortical layers of each area.

Figure 3.1.5 - 3.1.8 showed the caudal-rostral sequences of eight histologic sections containing area SMA and pre-SMA. It could be clearly seen that the borders between regions of interest (SMA or pre-SMA) and the lateral convexity (lateral area 6) were almost always in the upper angular corner except the transition parts in the caudal and rostra. In the ventral, however, the cytoarchitectonic borders were not corresponding with reliably identifiable macroscopic features. This may be caused by the large variability in the cingulated sulcus of each brain (Fig. 3.1.9). Thus, macroscopic anatomy and areal borders (particular in the ventral bench) differ independently.
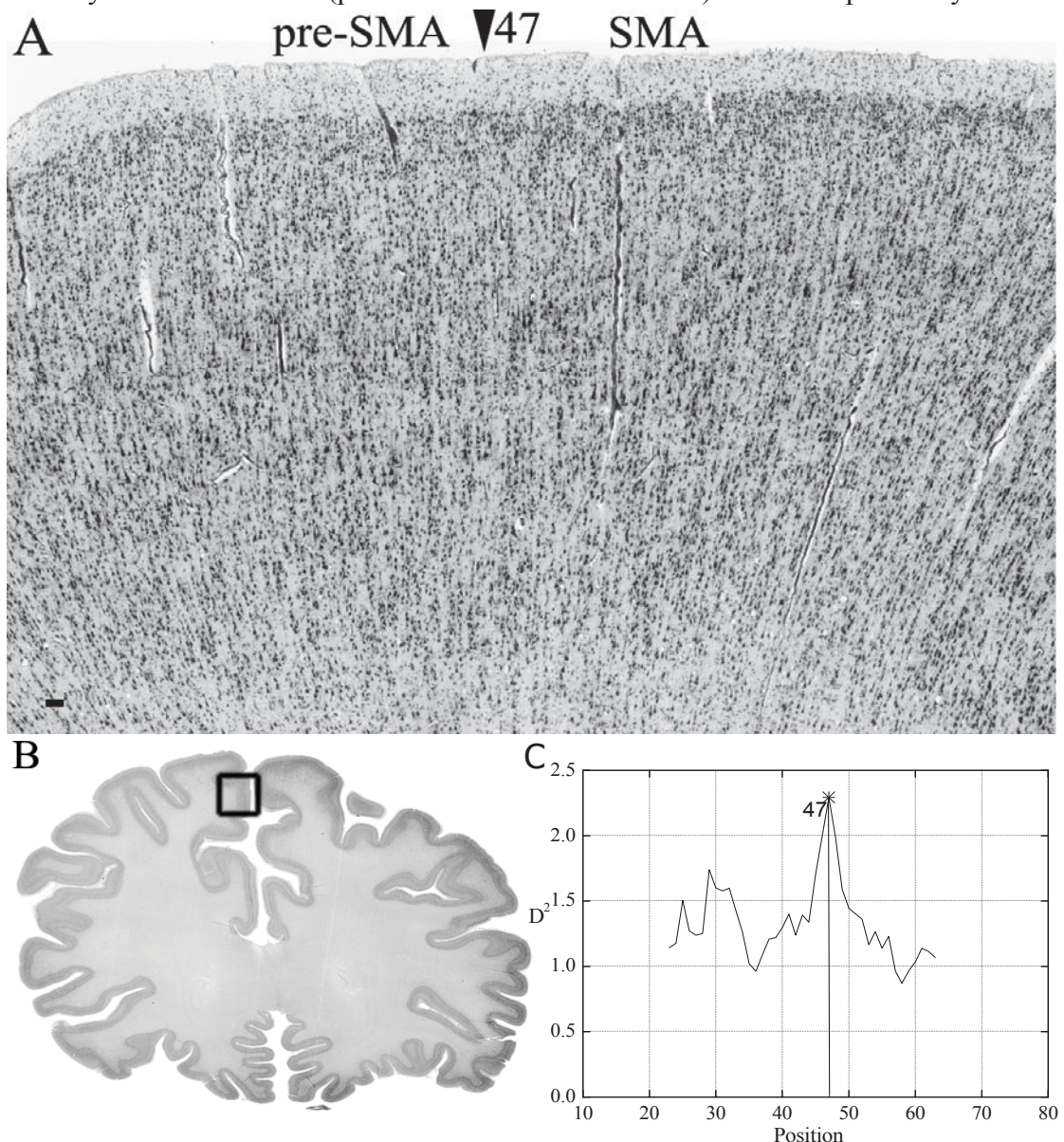

Fig.3.1.4 Typical border between area SMA and area pre-SMA in a section of case 6 at position 47 (arrowhead) of the distance function. A: Photomicrograph of a coronal, cell body stained section. Note the large size pyramidal cells in the lower part of layer III and the relatively more visible border between layers II and III in SMA. In pre-SMA, dark layer V well demarcated from layers III and VI can be observed and the Layer II and layer III fuse. B: Location of the region of interest in the left hemisphere. C Significant maximum at position 47(*P<0.01). Scale bar = 0.5mm.
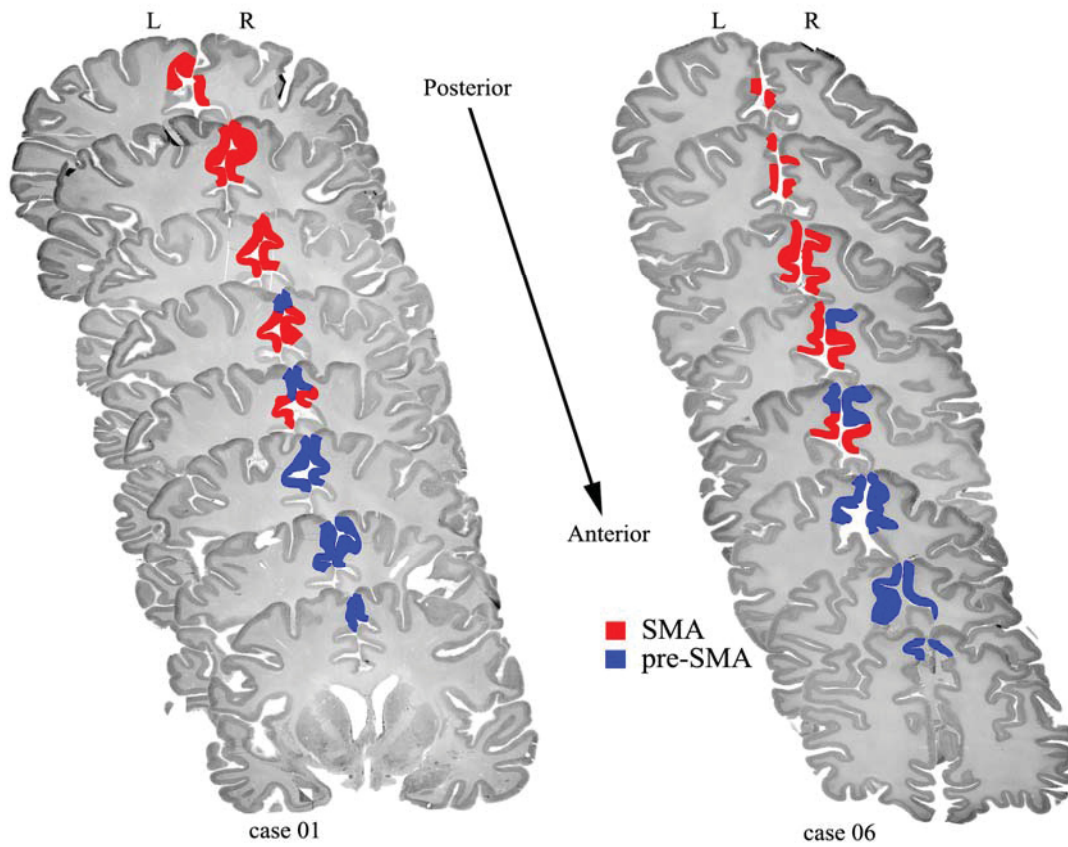
Fig. 3.1.5 Posterior-anterior sequences of eight coronal histological sections through the left and right hemispheres of case 01 and 06. Areas SMA and pre-SMA are shown by red and blue color. The cingulated sulcus varied in inter-brains.
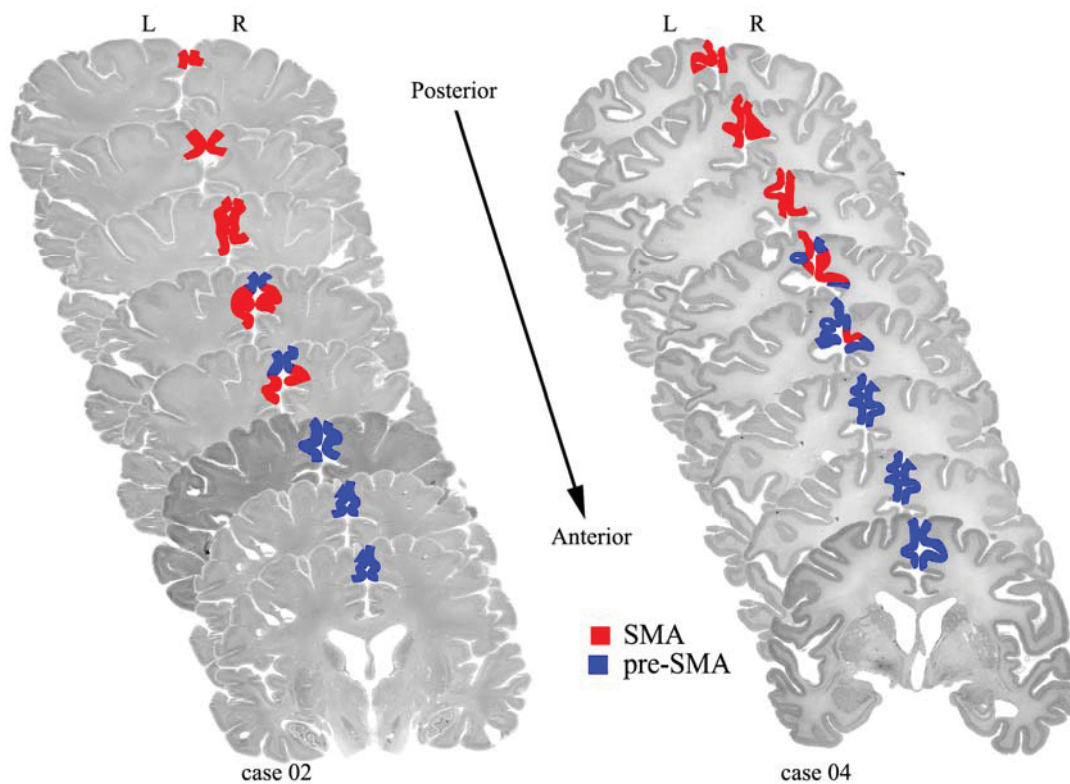
Fig. 3.1.6 Posterior-anterior sequences of eight coronal histological sections through the left and right hemispheres of case 02 and 04.

Fig. 3.1.7 Posterior-anterior sequences of eight coronal histological sections through the left and right hemispheres of case 09 and 20.The cingulated sulcus varied in inter-brains.
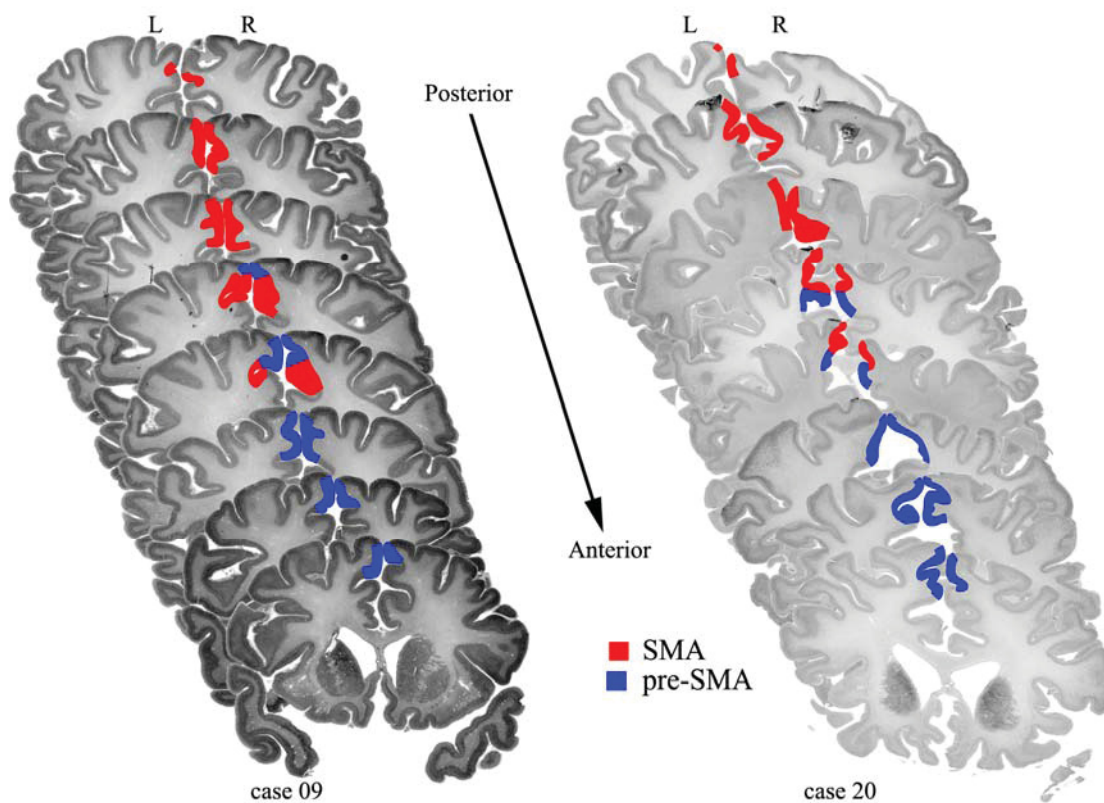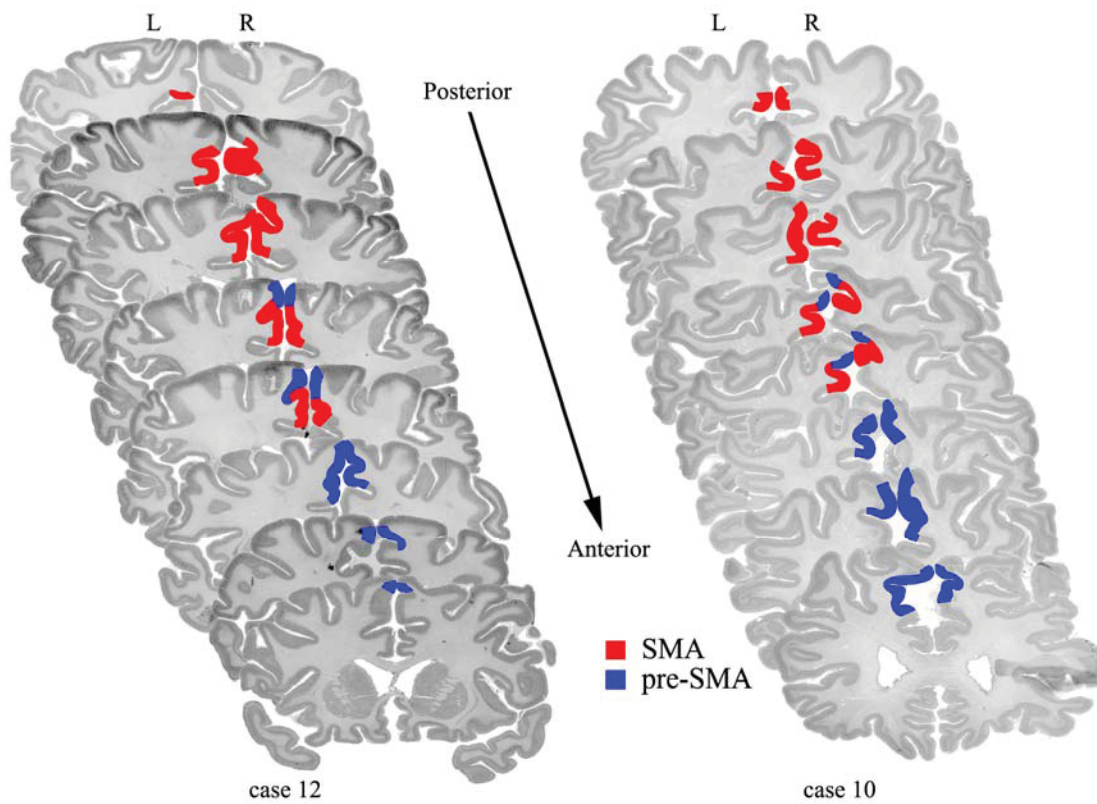
Fig. 3.1.8 Posterior-anterior sequences of eight coronal histological sections through the left and right hemispheres of case 10 and 12.The cingulated sulcus varied in inter-brains.
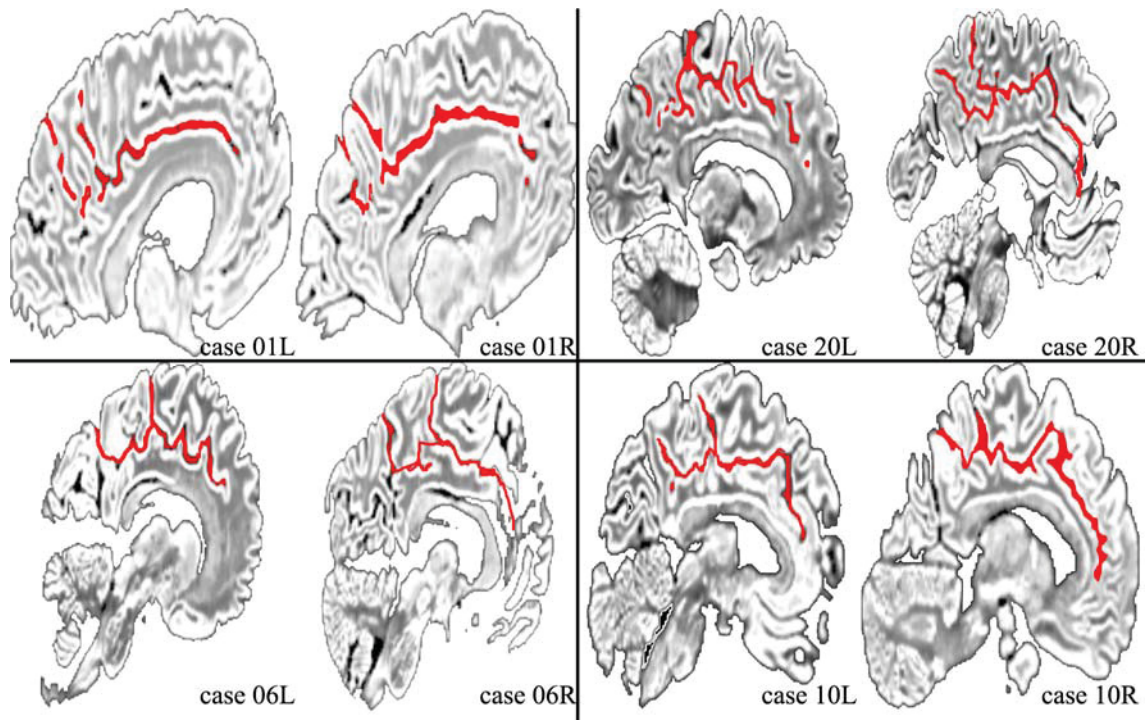

Fig. 3.1.9 The mesial view of the brains (case 01, 06, 10, 20). The cingulated sulcus was shown by marked red color indicating the large variability across individualities.

3.2 Cytoarchitectonic borders of areas SMA and pre-SMA with neighboring cortical areas

According to the observer-independent procedure, the outer borders of area SMA and pre-SMA were also defined. It was found that areas SMA and pre-SMA were located in the mesial surface of Brodmann's area 6, anterior to precentral gyrus (Brodmann's area 4), posterior to a granular prefrontal cortex (Brodmann's area 8). And they bordered with the dorsal lateral cortical convexity (premotor cortex, lateral Brodmann's area 6) at the dorsal direction, and with Brodmann's area 24 (area 24d in caudal and area 24c in rostral) at the ventral parts. The transition between area 4 (M1) and area SMA located roughly coincide with the transition between area 23 and area 24. In the dorsal lateral direction, the onset of SMA in caudal and the end of pre-SMA in rostral were roughly corresponding with the onset of PMdc (premotor dorsal rostral) and end of PMdr (premotor dorsal rostral).Area SMA might have a common border with area 23 in the extremely caudal part of SMA (case 1, 10, 21), which was acceptable considering the large individual divergences of the 10 brains. All these borders have been confirmed by the observer-independent approach.

SMA and primary motor cortex. SMA located just anterior to primary motor cortex (area 4, M1) in the medial surface. Both areas SMA and the primary motor cortex were absence of layer IV and poorly laminated. The primary motor cortex was characterized by the giant pyramidal cells (Betz cells) in layer Vb. Unlike primary motor cortex, the SMA showed no giant pyramidal cells in layer Vb. Most importantly, area SMA showed an increased cellular density in the lower part of layer III (Fig. 3.1.1, 3.2.1, 3.2.6).

SMA and dorsal caudal premotor. The SMA bordered with dorsal caudal premotor (PMdc) (dorsal part of Brodmann's area 6) in the dorsal lateral direction. Figure 3.2.2 (upper) showed a high-power photomicrograph of area PMdc. Figure 3.2.6 showed a typical border between areas SMA and PMdc. Both PMdc and SMA were poorly laminated. Both areas SMA and PMdc showed poor laminations and had a conspicuous layer IIIc, but the PMdc had a higher cellular densitiy in the layer IIIc in comparison of that in area SMA. Moreover, the cell size of layer IIIc in PMdc were large than those of layer IIIc in area SMA. Layer VI in area PMdc was more recognizable than that in area SMA (Fig. 3.1.1, 3.2.2, 3.2.7).

SMA and 24d. The SMA bordered with area 24d in the ventral part. Figure 3.2.3 (upper) showed a high-power photomicrograph of area 24d. Figure 3.2.8 showed a typical border between areas SMA and 24d. Both areas were agranular and poorly laminated. In area SMA, a prominent layer IIIc with medium size pyramidals could be recognized, in area 24d, however, the cells in the lower part of layer III showed a smaller size. Moreover, a dark layer V with big or even giant pyramidal cells and well demarcated layer VI were easily identified in area 24d (Fig. 3.2.3, 3.2.9). Due to the Betz cells could be found in area 24d, the area 24d also called gigantopyramidal field. Compared with the Betz cells of the primary motor area (Brodmann area 4), those of the cingulate area displayed numerous primitive traits (Braak and Braak 1976).
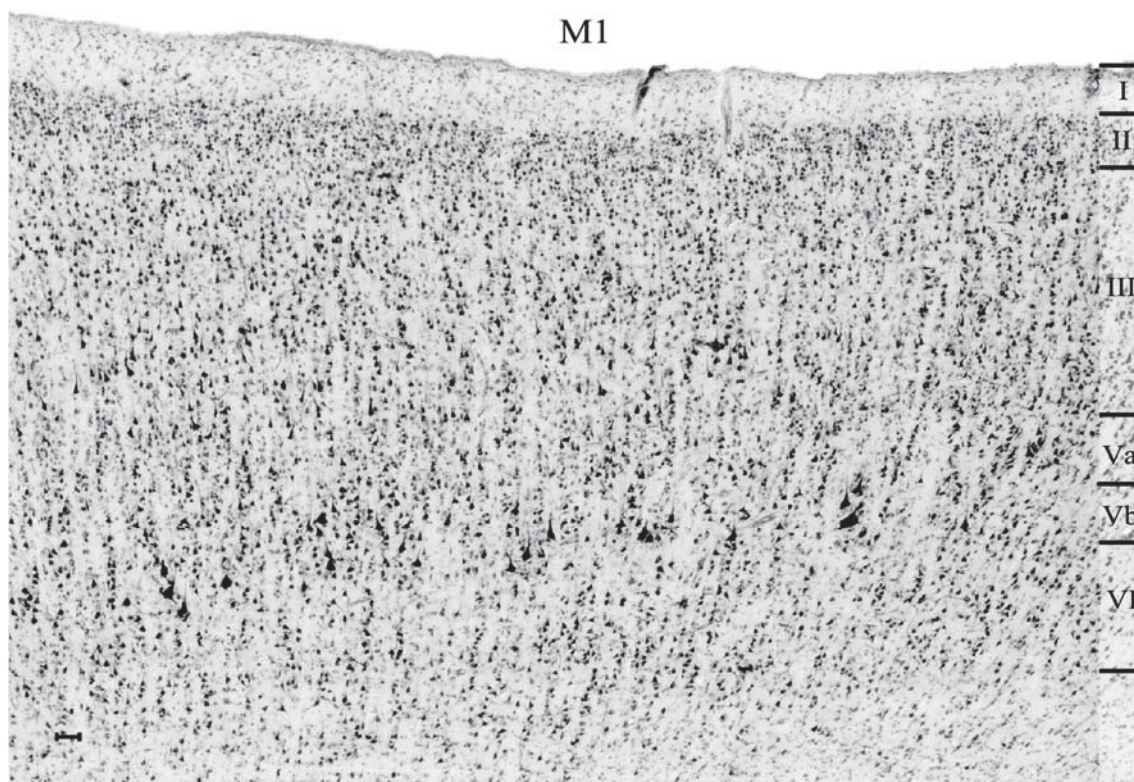
Fig. 3.2.1 Photomicrographs of cytoarchitecture of area M1. Note the betz cells in layer Vb. M1, primary motor cortex, Brodmann's area 4.

Pre-SMA and dorsal rostral premotor. Figure 3.2.7 showed the dorsal border between pre-SMA and dorsal rostral premotor (PMdr). A high-power photomicrograph of area PMdr was shown in Figure 3.2.2 (lower). Both area pre-SMA and area PMdr showed better laminations and darker layer V compared with the caudal part of each area: area SMA and area PMdc, respectively. The border between layer II and layer III in areas pre-SMA and PMdr were both somewhat fused. However, the area PMdr

showed a more demarcated layer VI, and the cell size of layer V in PMdr was larger than that in area pre-SMA (Fig. 3.2.2, Fig. 3.2.8).

Fig. 3.2.2 Photomicrographs of cytoarchitecture of area PMdc (upper, case 4, left hemisphere) and PMdr (lower, case 12, left hemisphere) in coronal. cell body-stained sections. Roman numerals indicate the different cortical layers. PMdc, premotor dorsal caudal; PMdr, premotor dorsal rostral. Scale bars = 0.5mm.
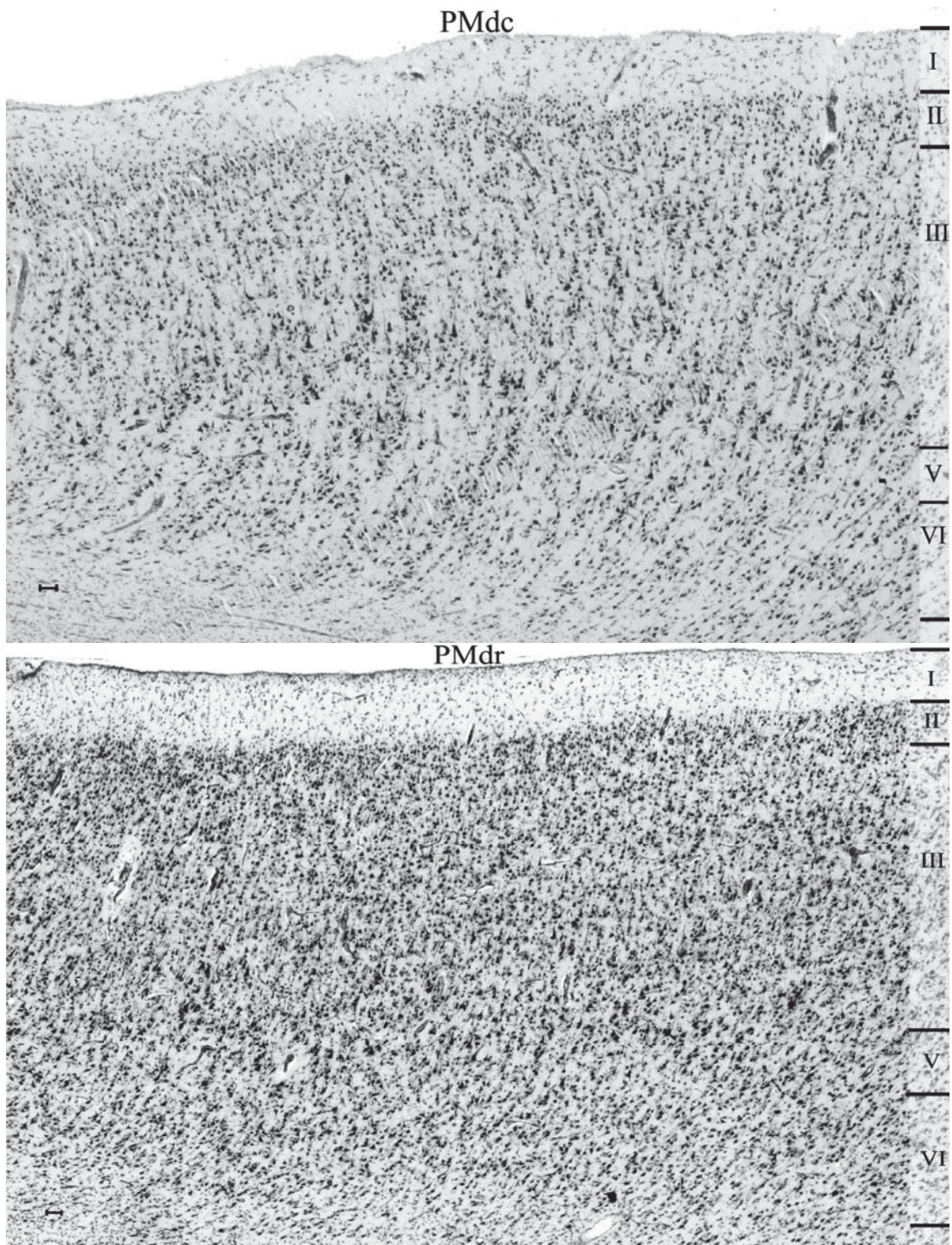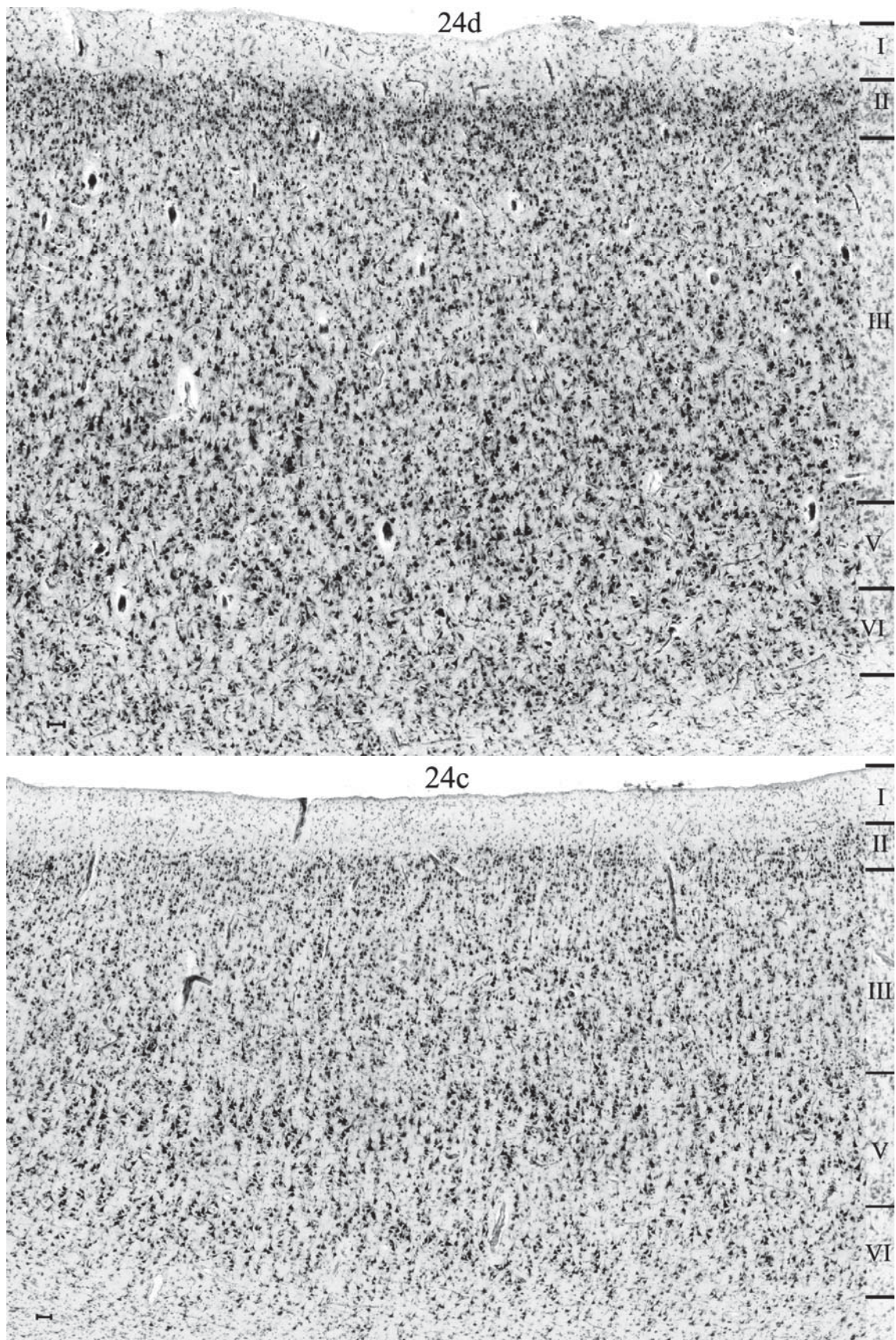
Fig. 3.2.3 Photomicrographs of cytoarchitecture of area 24d (upper, case 12, right hemisphere) and 24c (lower, case 10, right hemisphere) in coronal, cell body-stained sections.Roman numerals indicate the different cortical layers.Scale bars = 0.5mm.
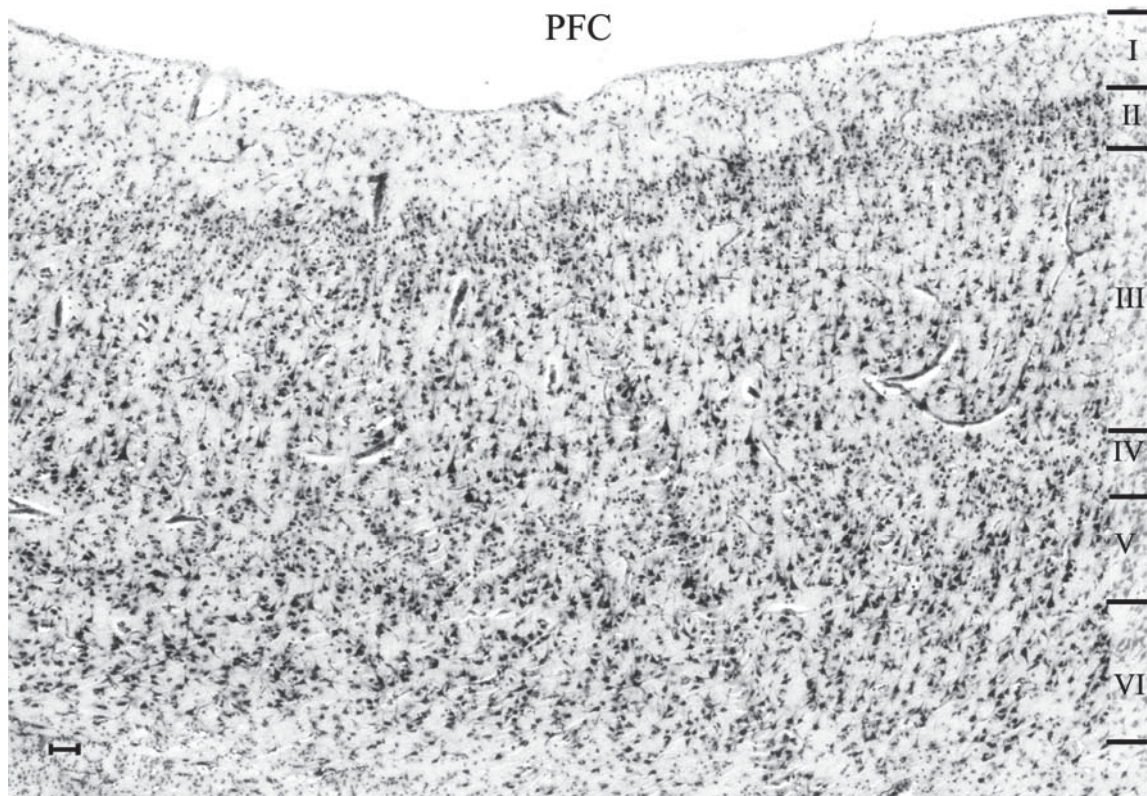
Fig. 3.2.4 Photomicrographs of cytoarchitecture of area PFC in coronal (case 20). Note the incipient layer IV. Cell body-stained sections. Roman numerals indicate the different cortical layers.PFC, prefrontal cortex (Brodmann area 8), Scale bars = 0.5mm.

Pre-SMA and 24c. Both area pre-SMA and area 24c showed better laminations and darker layer V. However, the layers V and VI in area 24c demarcated better than that in area pre-SMA.and the cell size of layer V in PMdr was larger than that in area pre-SMA (Fig. 3.1.1, Fig. 3.2.3, Fig. 3.2.10).

Pre-SMA and PFC. In the rostral part, the pre-SMA bordered with area PFC (prefrontal cortex, Brodmann area 8). Pre-SMA was the most rostral agranular frontal area. The border between area pre-SMA and area PFC could be identified when an incipient layer IV became recognizable. The border could be detected by the observer-independent procedure (Fig. 3.2.11). A high-power photomicrograph of cytoarchitecture of area PFC was shown in Figure 3.2.4.

Due to the transition between area M1 and area SMA was roughly coincide with the transition between area 23 and area 24d, and the large individual anatomical differences of the 10 brains, the most caudal part of area SMA in three of 10 brains (case 1, 10, 21) have a common border with area 23. Figure 3.2.5 and 3.2.12 showed the high-power photomicrograph of area 23 in coronal and the border of area SMA with area 23,

respectively. The area 23 was characterized by the demarcated layer IV, which could be distinguished from area SMA easily (Fig. 3.2.5, 3.2.12).
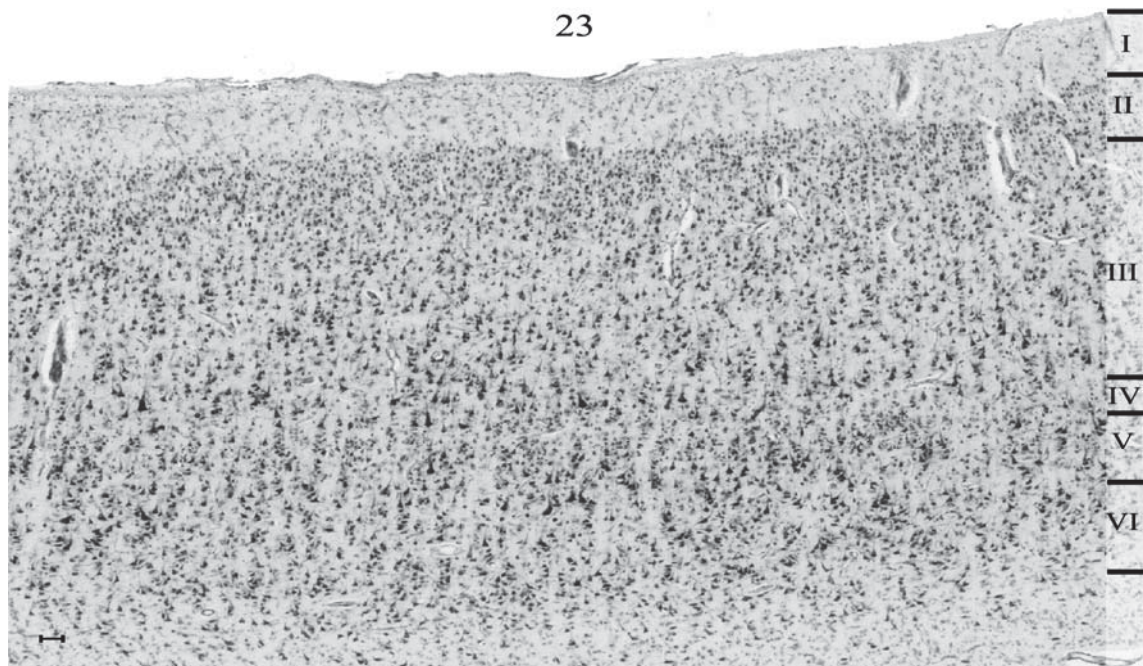
Fig. 3.2.5 Photomicrographs of cytoarchitecture of area 23 in coronal (case 21). Area 23 is granular. Note the demarcated layer IV. Cell body-stained sections.Roman numerals indicate the different cortical layers.

Fig. 3.2.6 Caudal border of area SMA with M1. A: photomicrograph of a section from case 17 showing the border between areas SMA and M1 (arrowhead). Due to the transition between areas, the scatter betz cells could be found in the area M1. The arrowhead indicates position of profiles 59. B: location of the region of interest. C: significant maximum at position 59 corresponding with figure A indicates the border between areas SMA and M1. M1, primary motor area, Brodmann area 4. Scale bar = 0.5 mm.

Fig. 3.2.7 Dorsal caudal border of area SMA with PMdc. A: photomicrograph of a section from case 4 showing the border between areas SMA and PMdc (arrowhead). The arrowhead indicates position of profiles 41. Note the darker layer III and layer V and well demarcated layer VI in PMdc. A higher magnification of the cytoarchitectonic features of area PMdc was shown in figure 15. B: location of the region of interest. C: significant maximum at position 41 corresponding with figure A indicates the border between areas SMA and PMdc. PMdc, premotor dorsal caudal. Scale bar = 0.5 mm.

Fig. 3.2.8 Dorsal rostral border of area pre-SMA with PMdr. A: photomicrograph of a section from case 12 showing the border between areas pre-SMA and PMdr (arrowhead). The arrowhead indicates position of profiles 51. Note the darker layer V and higher overall cell density in PMdr. A higher magnification of the cytoarchitectonic features of area PMdr was shown in figure 15. B: location of the region of interest. C: significant maximum at position 51 corresponding with figure A indicates the border between areas pre-SMA and PMdr. PMdr, premotor dorsal rostral. Scale bar = 0.5 mm.
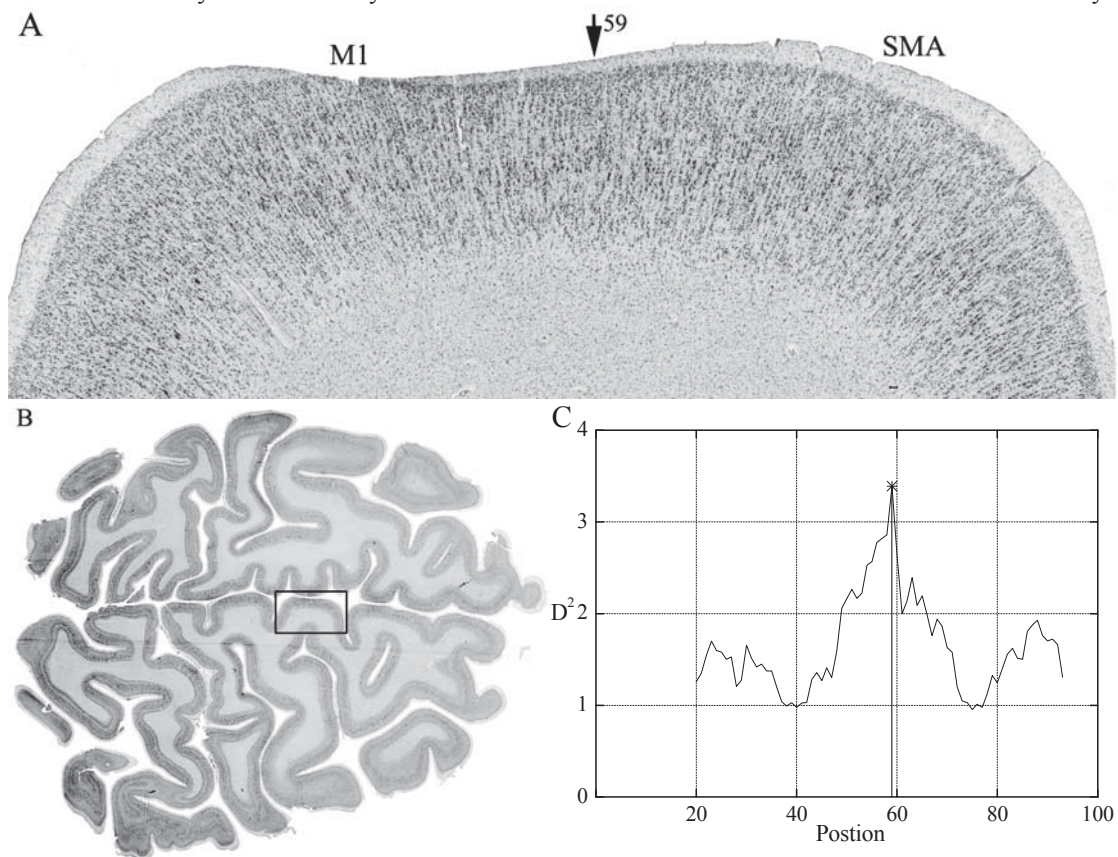
Fig. 3.2.9 Ventral border of area SMA with area 24d. A: Photomicrograph of a section from case 10 showing the border between areas SMA and 24d (arrowhead). The arrow indicated positions of profiles 73. B: Location of the region of interest. C: Significant maximum at position 73 (*P*<0.01) indicates the border between areas SMA and 24d. Scale bar = 0.5 mm.
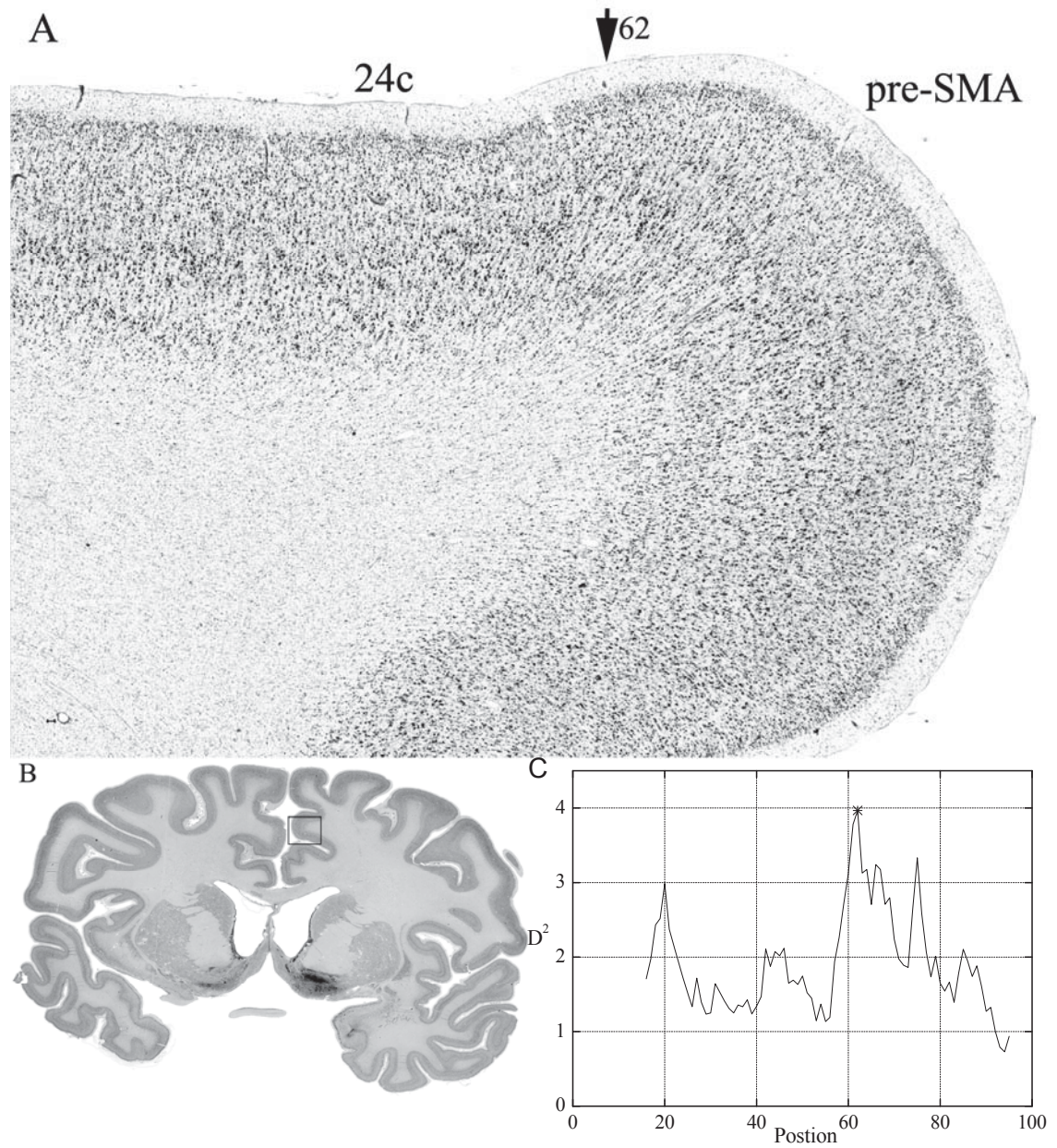
Fig. 3.2.10 Ventral border of area pre-SMA with area 24c. A: Photomicrograph of a section from case 12 showing the border between areas SMA and 24c (arrowhead). The arrow indicated positions of profiles 62. B: Location of the region of interest. C: Significant maximum at position 62(P<0.01) indicates the border between areas pre-SMA and 24c. Scale bar = 0.5 mm.
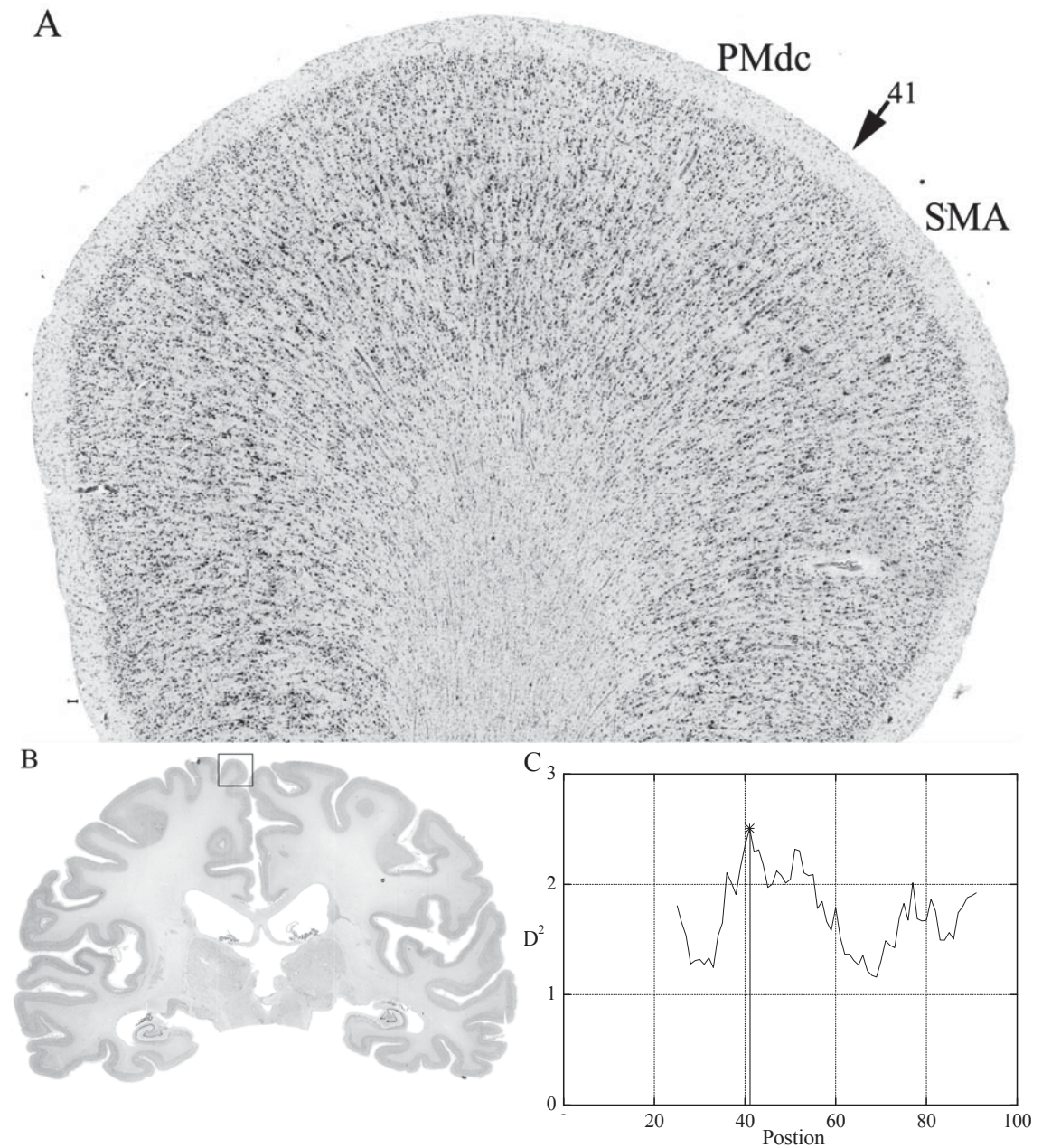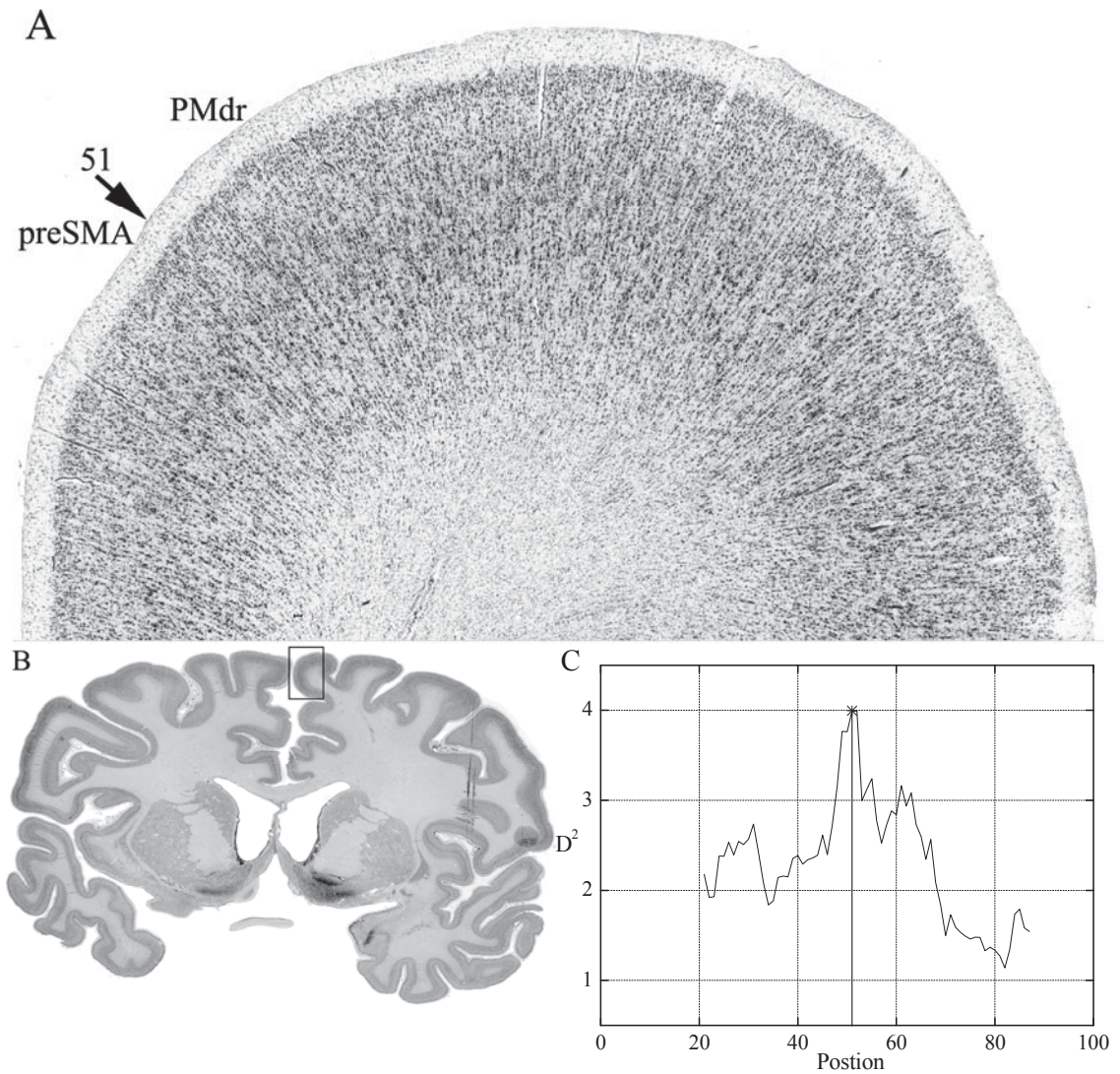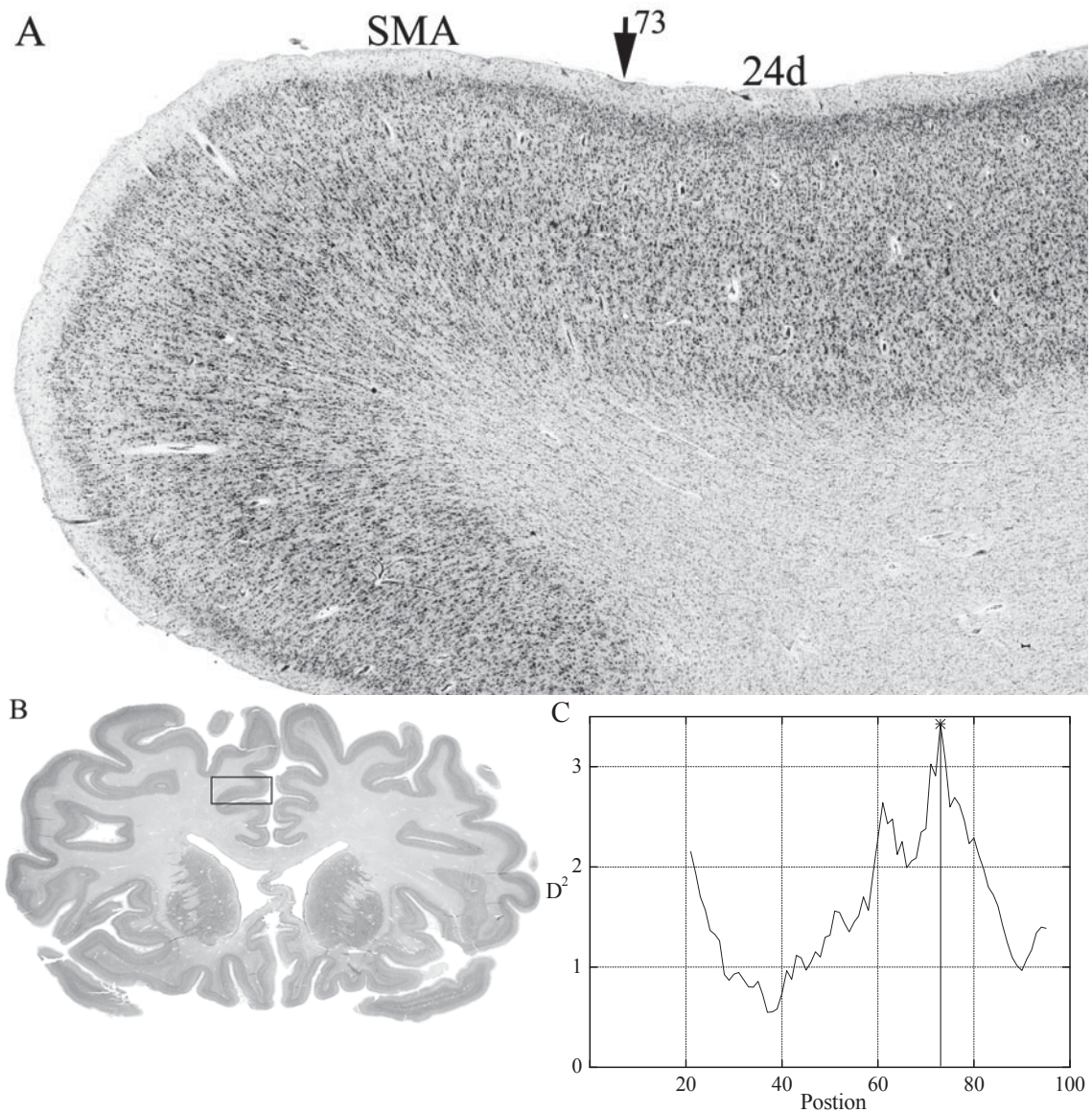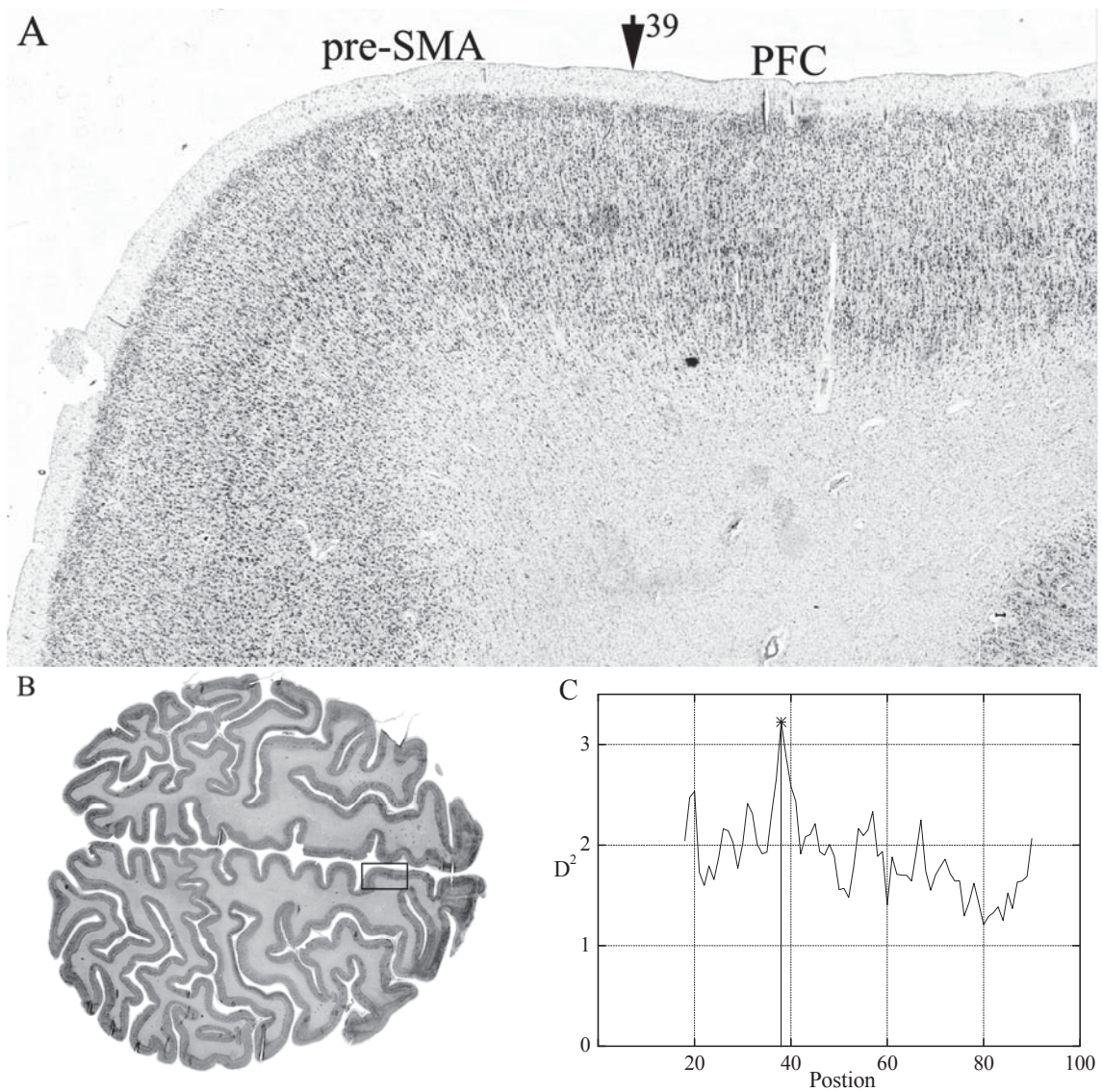
Fig. 3.2.11 Rostral border of area pre-SMA with area PFC. A: Photomicrograph of a section from case 17 showing the border between areas pre-SMA and PFC (arrowhead). The arrow indicated positions of profiles 39. B: Location of the region of interest. C: Significant maximum at position 39(P<0.01) indicates the border between areas pre-SMA and PFC. PFC, prefrontal cortex. Scale bar = 0.5 mm.
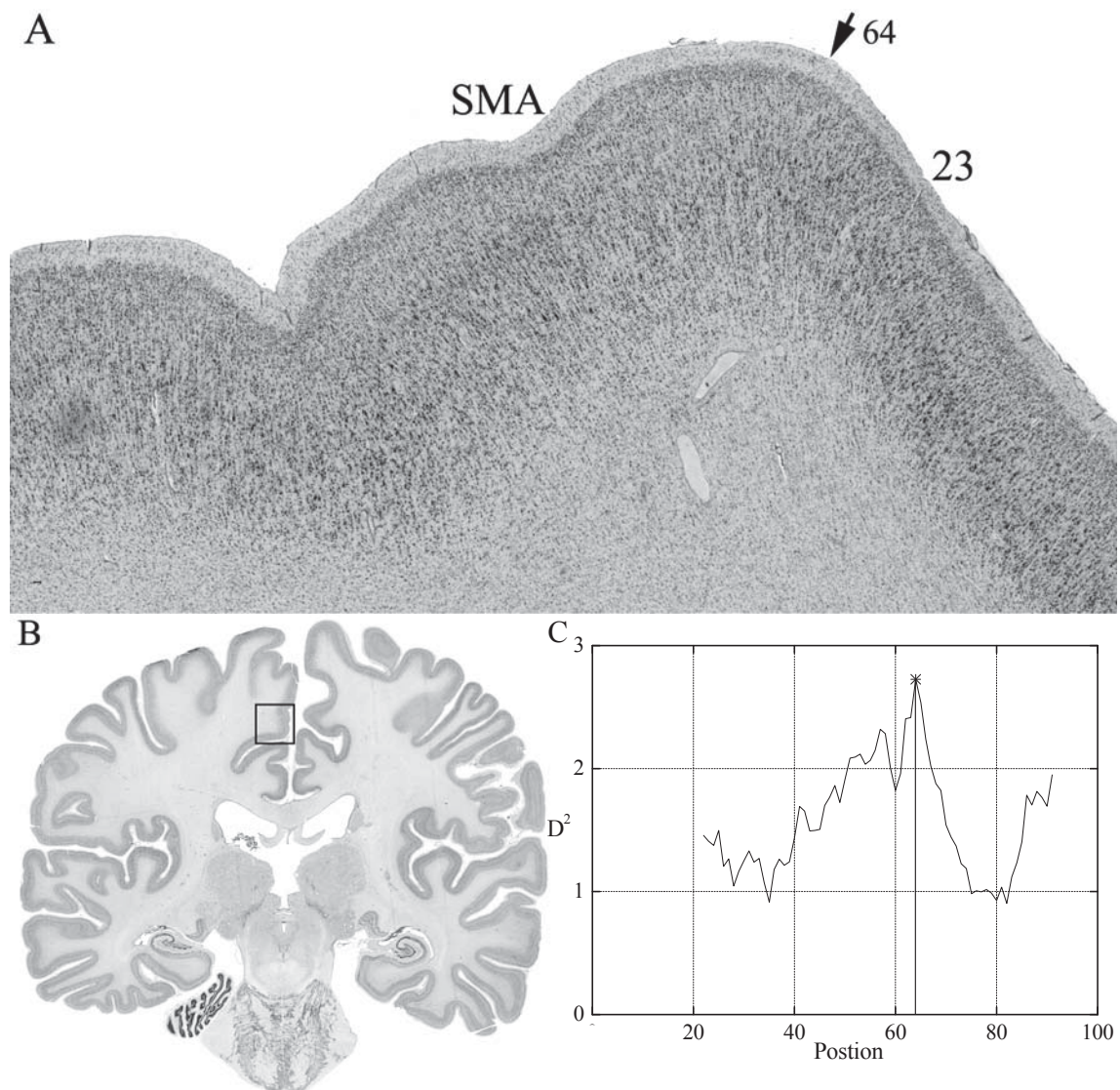
Fig. 3.2.12 Border of area SMA with area 23. This border could be found in three of 10 brains (case 1, 10, 21). It is easily to be understood considering that the transition between area M1 and area SMA was roughly coincide with the transition between area 23 and area 24. A: Photomicrograph of a section from case 21 left hemisphere showing the border between areas SMA and Brodmanns area 23 (arrowhead). B: Location of the region of interest. C: Significant maximum at position 64 (P<0.01) indicates the border between areas SMA and 23. Scale bar = 0.5 mm.

3.3 Hierarchical clustering analysis

To quantitatively describe the inter-areal similarities and dissimilarities in cytoarchitecture as compared to interhemispheric differences, the hierarchical cluster analysis of the cytoarchitectonical profiles was executed (Fig. 3.3.1). The representative cortical areas with few artefacts were included in the process of analysis. The inter-areal divergences (SMA and pre-SMA) in cytoarchitecture of the selected areas were stronger

92

than the inter-hemispheric divergences (left SMA and right SMA, left pre-SMA and right pre-SMA) (Fig. 3.3.1). This result supports the principal segregations of mesial frontal cortex in the present study.
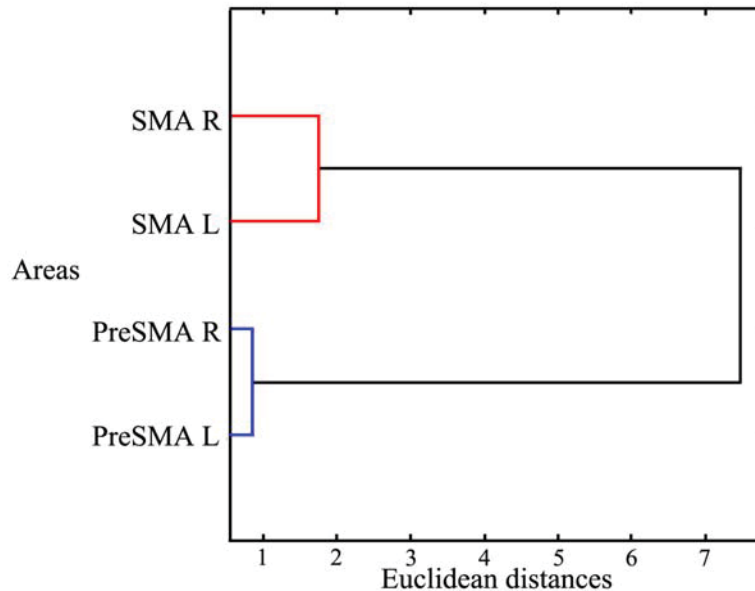
Fig. 3.3.1 Hierarchical cluster analysis (Ward linkage, Euclidean distances) of cytoarchitectonically defined areas of areas SMA and pre-SMA. Based on the result of hierarchical cluster analysis, it was found that the higher cytoarchitectonic similarity within SMA or pre-SMA between the left and right hemisphere. It supports the principal segregation on the mesial motor surfaces.

3.4 Comparison of interareal cell density

As clarified in the part of methods and material, the GLI characterized the cell density of areas. Although significant differences were found between the cell density profiles of areas SMA and pre-SMA in individuality, it was found that the overall cell densities of areas SMA and pre-SMA in the entire subjects showed no significant differences. This finding may be caused by the large intersubject variability in the cytoarchitecture of each cortical area. The gender- and hemispheric- dependent differences in cell densities also could not be detected ($P > 0.05$, two-way ANOVA).

However, the cell distributions of areas SMA and pre-SMA differed significantly. In detail, the area cortex was divided into 10 bins with 10%-intervals: bin 1(0%-10%), bin 2(10%-20%), ……, bin 10 (90%-100%). Areas SMA and pre-SMA showed significant differences in bin 4 and bin 5 ($P < 0.05$, Pairwise comparison). The position in bins 4 and

5 was roughly the location of low part of layer III. This supported our definitions of areas SMA and pre-SMA in the present study under microscope checking, that prominent large size pyramidal cells in the lower layer III could be found in SMA, the pyramidal cells of layer IIIc, however in pre-SMA was smaller and less densely (Fig. 3.4.1).
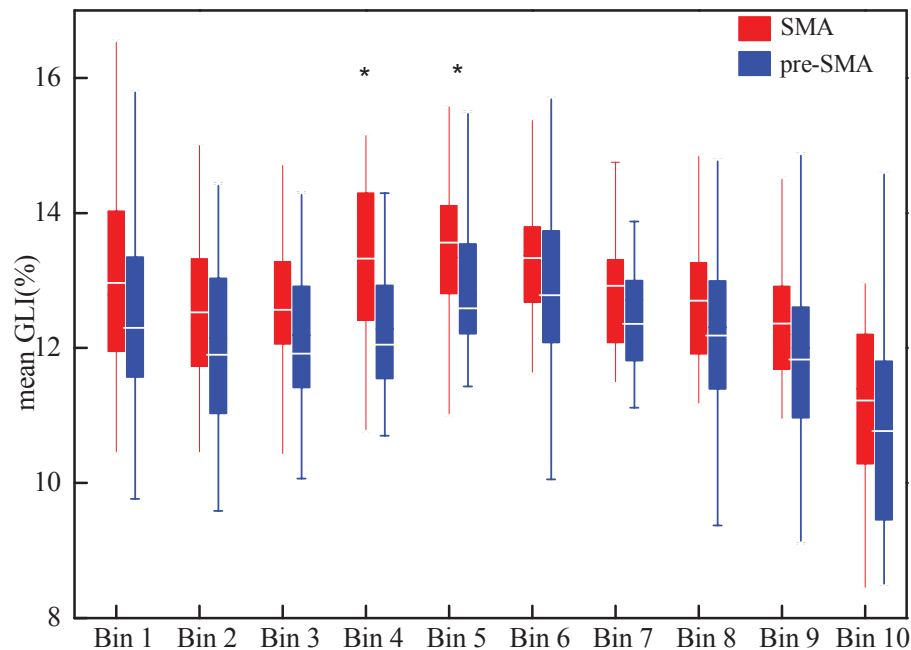
Fig. 3.4.1 Mean profiles of all subjects (gray level index, GLI, %) in areas SMA and pre-SMA showing in 10%-interval bins. Bin 1, Bin2,……Bin 10 indicated the mean profiles from outer border between layers I and II to position 10%, positions 10% to 20%,…… and positions 90% to 100% (white matter), respectively. Center horizontal indicated the mean values of the areas. *The bins 4 and bins 5 in the two groups showed significant differences ($P<0.05$, Pairwise comparison).

The overall cell densities in areas SMA and pre-SMA did not show significant asymmetry or gender differences. Three of five females showed a left-over-right asymmetry (AC>0) in both area SMA and area pre-SMA, the left two showed a right-over-left asymmetry (AC<0). For the males, there were two of five showing a left-over-right asymmetry (AC>0) in area SMA, and three of five showed a left-over-right asymmetry (AC>0) in area pre-SMA (Fig. 3.4.2).
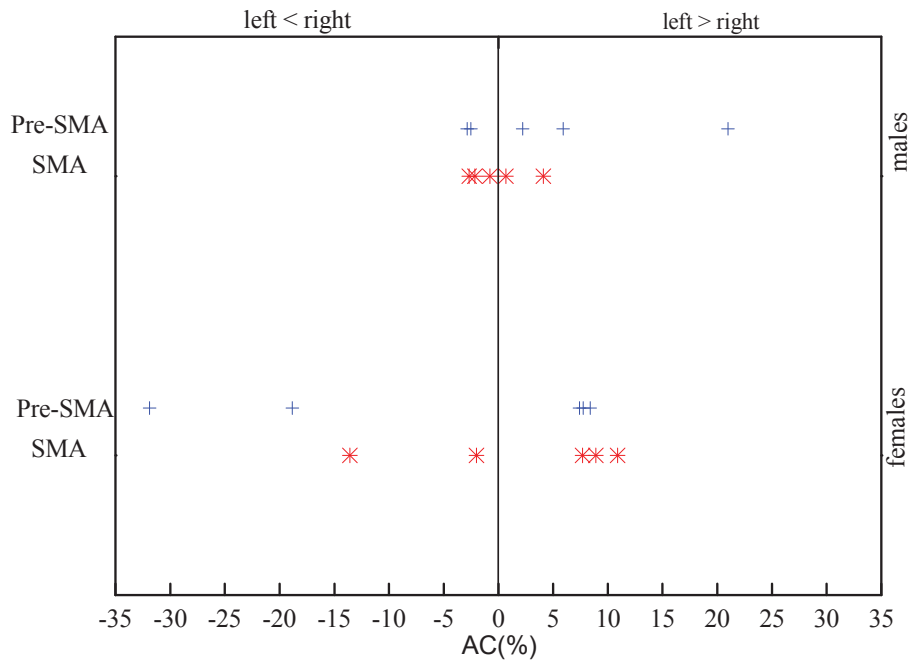
Fig. 3.4.2 Asymmetry coefficient (AC,%) of overall density of cell bodies (gray level index) collapsed over all cortical layers in areas SMA and pre-SMA of female(lower part) and male (upper part) brains. The distributions of areas SMA and pre-SMA showed no differences, but they had a high correlation (Pearson Correlation = 0.699, *P*<0.05).

3.5 Volumetric analysis of areas SMA and pre-SMA

The volumes of the area SMA and area pre-SMA were corrected by shrinkage factor. The volume of each area after adjusted was shown in figure 3.5.1. To better compare the volumes of areas, the volume proportion of each area was calculated. The average total volume proportions of left SMA (n=10), right SMA (n=10), left pre-SMA, and right pre-SMA were 1.3%, 1.27%, 1.51%, and 1.47%, respectively. The combined volume proportions of areas SMA and pre-SMA of one hemisphere in each brain were left 2.80%, right 2.73% respectively. To analyze the gender differences, the author calculated the volume proportions of area SMA (both hemisphere) and area pre-SMA (both hemisphere). The volume proportions of area SMA, area pre-SMA, and total area in the male and were 2.58% vs. 2.55%, 3.02% vs. 2.92%, 5.60% vs. 5.47%, respectively. The values of the hemispheric gender changes were also calculated: -0.01%, and 0.06% for hemispheric changes of areas SMA and pre-SMA in female. These numbers were 0.06%, and 0.01% in male. However, the permutation test showed no significant differences of the volume proportions between genders, hemispheres, gender hemispheric interactions (Table 3.5.1). In both areas SMA and pre-SMA, interactions

between age and volume were not found in the correlation test (area SMA: $r_s = 0.036$, P = 0.920; area pre-SMA: $r_s = -0.067$, P = 0.854).

Table 3.5.1 Volume proportion analyses of area SMA and pre-SMA grouped by hemisphere and gender. The data was represented as mean ± SD. (Volume proportion of area SMA and pre-SMA = volume area/brainvolume*100%; SD = standard deviation; p = contrast estimate of the pair wise permutation tests (significant differences if p< 0.05, L = left hemisphere, R = right hemisphere)).

Areas	Hemispheric differences			Gender differences			Hemispheric gender Interaction		
	L	R	p	Female	Male	p	Female: L-R	Male: L-R	p
SMA(mean±SD)	1.30±0.14	1.27±0.10	0.52	2.58±0.18	2.55±0.24	0.86	-0.01±0.16	0.06±0.12	0.45
pre-SMA(mean±SD)	1.51±0.15	1.47±0.14	0.49	3.02±0.57	2.92±0.58	0.74	0.06±0.52	0.01±0.36	0.68
Total (mean±SD)	2.80±0.46	2.73±0.28	0.42	5.60±0.75	5.47±0.79	0.73	0.06±0.67	0.08±0.41	0.90
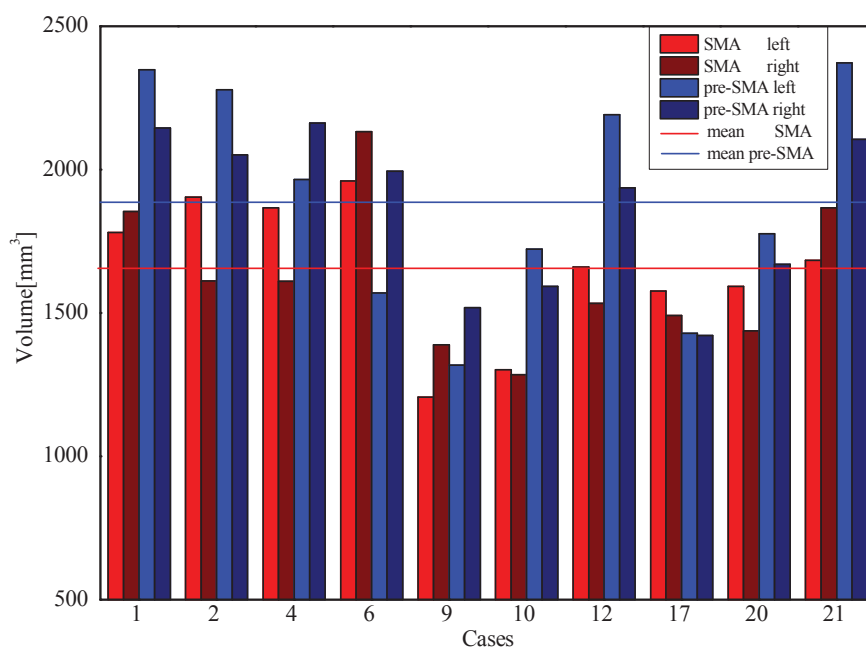
Fig. 3.5.1 Comparison of single hemisphere volumens of areas SMA and pre-SMA. The numerals in abscissa indicate the cases used in the present study.

3.6 3D probability maps and maximum probability maps

Probabilistic cytoarchitectonic maps of areas SMA and pre-SMA were computed in the anatomical MNI reference space (Holmes, et al. 1998; Amunts, et al. 2005) (Fig. 3.6.1, 3.6.2). The superimposition core of all ten brains showed that areas SMA and pre-SMA located above the cingulate sulcus in the mesial view. Because of large interindividual anatomical variability of the areas, the voxels in the periphery of the

maps with low overlap (blue) were more frequent than central voxels with high overlap (red). Therefore, the parcellations of area SMA and pre-SMA overlapped at lower frequencies, and they could be distinguished dramatically.
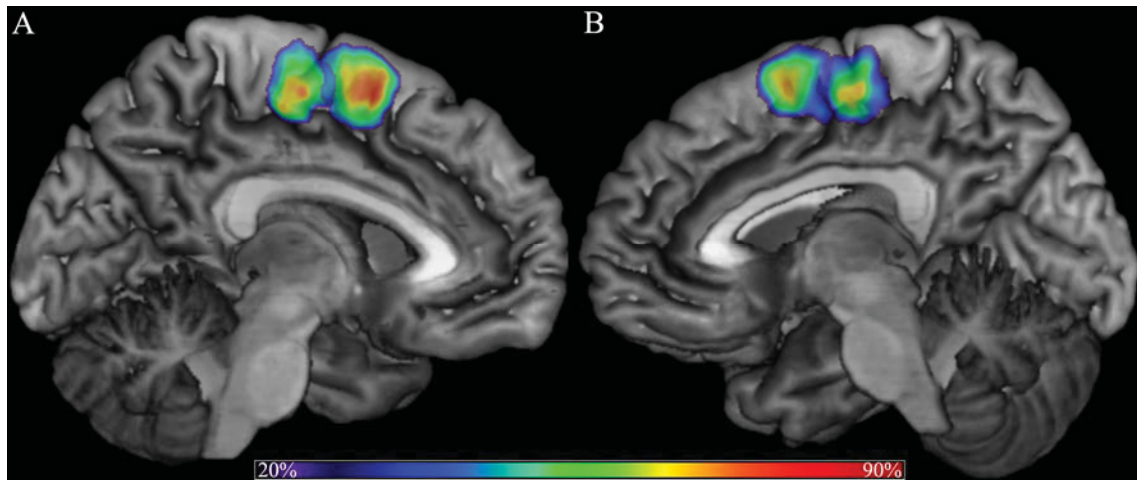
Fig. 3.6.1 The present probability maps of areas SMA and pre-SMA registered to MNI reference brain. Left (A) and Right (B) hemisphere medial view onto the probabilistic maps of the delineated areas SMA (caudal part) and pre-SMA(rostral part).the number of overlapping brains for each voxel is color coded(E.g., green means approximately 6 of 10 brains overlapped in this voxel).

Due to the continuous probability maps of different adjoining areas overlap, the maximum probability maps (MPMs) of areas SMA and pre-SMA were computed. This non-overlapping parcellation of areas SMA and pre-SMA, from a sample of ten human post mortem brains, reflected the most likely areas (Fig. 3.6.3). The caudal boundary of area SMA was located anterior to vertical posterior commissure (y = -28); the border between areas SMA and pre-SMA was close located in the vertical anterior commissure (y = 0). The MPMs were used as seed regions for the subsequently MACM analysis (Fig. 7). And the MPMs were used for the subsequently MACM analysis. Moreover, the mean gravity centers of areas SMA and pre-SMA in the MNI template brain were calculated using the ten-brain-sample (Table 3.6.1).

Table 3.6.1 The gravity center in the MNI template of each area.

Area	Center of Gravity					
	x	y	z	dx	dy	dz
Left SMA	-5.3	-10.4	54.1	0.7	4.2	5.5
Right SMA	4.1	-10.6	52.9	0.9	4.8	3.6
Left pre-SMA	-5.2	6.4	53.1	1.1	3.9	3.1
Right pre-SMA	4.2	6.1	52.9	0.6	4.5	2.8
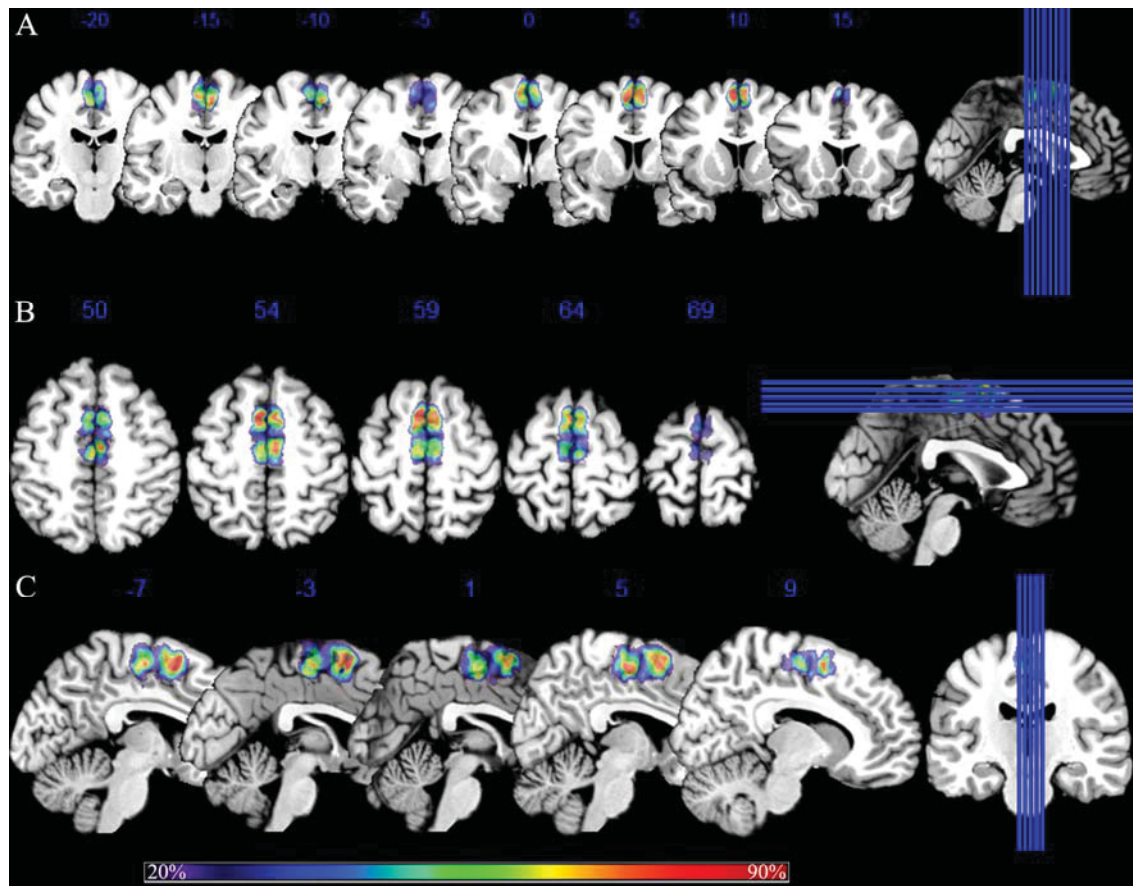
Fig. 3.6.2 Continuous probability maps of areas SMA and pre-SMA. Cytoarchitectonic probability map in anatomical MNI space in coronal (A), horizontal (B) and sagittal (C) directions, respectively. The number of overlapping brains for each voxel is color coded. The left and right side of each section in A and B indicate the left and right hemisphere, respectively. The area SMA located in the caudal parts of the maps. The blue numbers in A, B, and C indicate the y-, z-, x-coordinates, respectively. The extreme right images in A, B, and C indicate the rough locations of corresponding sections.
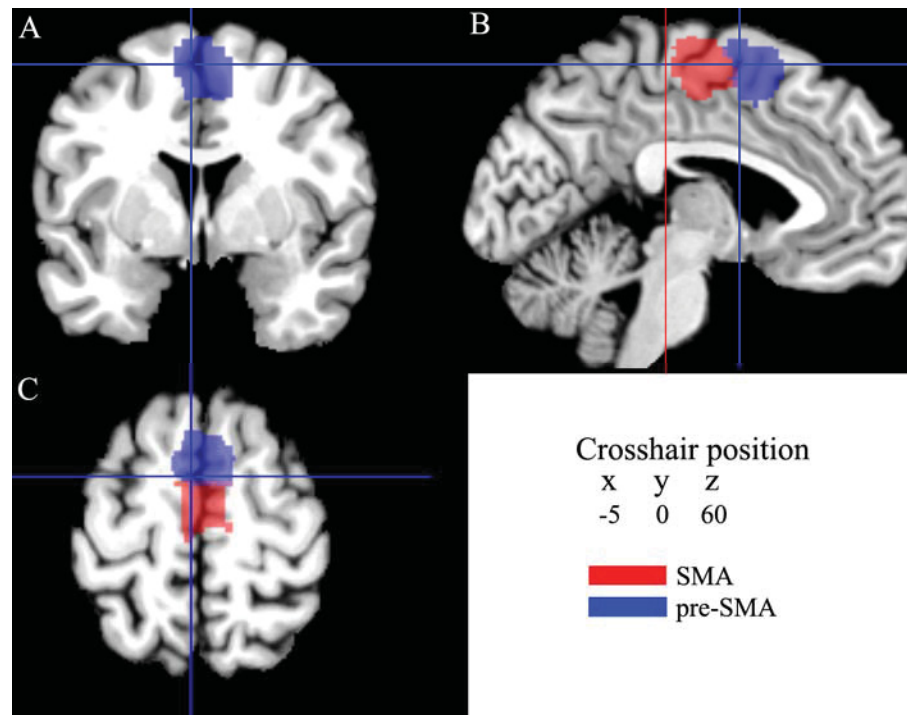
Fig. 3.6.3. sections through the MNI single subject template showing the maximum probability maps of areas SMA and pre-SMA in the coronal (A), sagittal (B), and horizontal (C) planes of sectioning. The vertical axis of the crosshair in B crossed the anterior commissure (y = 0). The red line in B crossed the posterior commisure (y = -28).The current version of the maximum probability maps were used for the analysis or structural magnetic resonance imaging data by means of the anatomy Tool box (Eickhoff, Stephan et al. 2005), can be downloaded at www.fz-juelich.de/inm/inm-1/spm_anatomy _toolbox.

3.7 MACM analysis of functional studies reporting areas SMA and pre-SMA

3.7.1 Functional connectivity of areas SMA and pre-SMA

To explore the function of the areas SMA and pre-SMA, a coordinate based meta-analysis of areas SMA and pre-SMA co-activations within functional imaging studies was carried out. Using the BrainMap database, task-based co-activations of area SMA and pre-SMA were quantitatively mapped. 1398 Experiments on area pre-SMA (18574 subjects, 21552 foci), and 597 Experiments on area SMA (7947 subjects, 9112 foci)) were included in the procedure of analysis. Significant patterns of co-activation clusters for each of areas were identified.

According to the conjunction analysis of area SMA and pre-SMA, it was found that the two areas shared some common co-activation clusters: precentral gyrus, thalamus, supra marginal gyrus, putamen, superior frontal gyrus, rolandic operculum, cerebellum (Table 3.7.1, Fig. 3.7.1). In detail, 13 co-activation clusters for area SMA (both hemispheres) could be found according to Statistical Parametric Mapping (SPM,

SPM12) tool. The largest co-activation clusters for area SMA were located on precentral gyrus, supramarginal gyrus, putamen, superior frontal gyrus, BA 44, postcentral gyrus, cerebellum, supramarginal gyrus and rolandic operculum. The left SMA was associated with 11 co-activation clusters spread throughout the brain. Maxima within these areas were seated in posterior medial frontal (pre-SMA), thalamus, precentral gyrus (area 4), inferior occipital gyrus, and cerebellum. The right hemispheric SMA was associated with 13 clusters, within which maxima were located posterior medial frontal (pre-SMA), putamen (medial), precentral gyrus (area 4), putamen, rolandic operculum, and cerebellum (VI). According to the result, it could be found that the area SMA was more likely to co-activate with the ipsilateral areas (details in Table 3.7.2, Table 3.7.3, Fig.3.7.2, Fig. 3.7.3).

Area pre-SMA was associated with six co-activation clusters. Maxima within these areas were located in precentral gyrus (BA 44), thalamus, IFG (p. Opercularis), putamen, inferior parietal lobule, superior parietal lobule, cerebellum, inferior occipital gyrus, and superior temporal gyrus (Area hIP3 (IPS)). The left pre-SMA was related with eight co-activation clusters. The maxima of these clusters were located in precentral gyrus (area 6d2, area 44), thalamus, inferior parietal lobule(area hIP3 (IPs)), cerebellum (vi), supramarginal gyrus, middle occipital gyrus. For the right pre-SMA, there were seven clusters found. The maxima within these clusters were located in precentral gyrus, insula lobe, thalamus, putamen, inferior parietal lobule (area hIP3 (IPS)), IFG (p. opercularis), superior parietal lobule, supramarginal gyrus, cerebellum (VI). The left and right pre-SMA co-activated with bilateral areas, but it seemed that the hemispheric pre-SMA was more likely to connect with the ipsilateral areas (details in Table 3.7.1, Table 3.7.2, Fig.3.7.2, Fig. 3.7.3).
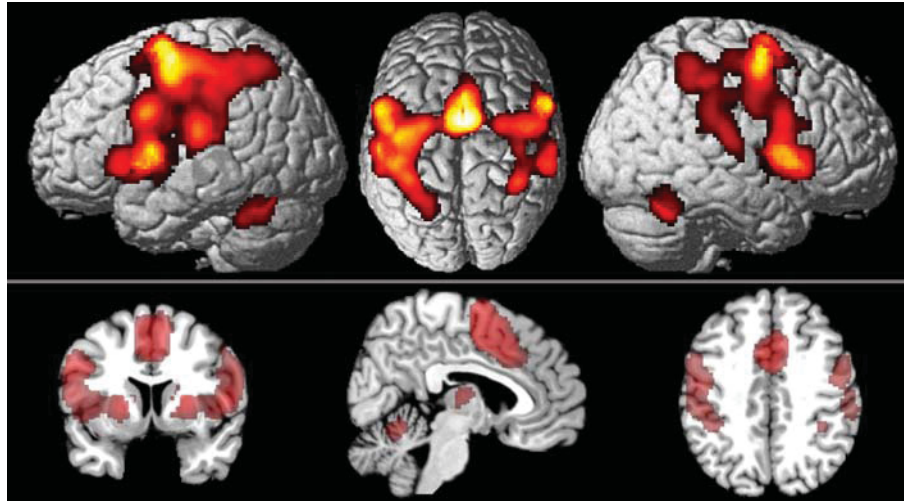
Fig. 3.7.1 Conjunction analysis of functional connectivity patterns for area SMA and pre-SMA with superimposed overview (top row) and section through in MNI template (lower row). Detail cluster assignations are specified in Table 3.7.1.

Table 3.7.1 Conjunction analysis of functional co-activation clusters for areas SMA and pre-SMA.

Macroanatomical location	Hemisphere	Cytoarchitectonic area	Cluster size [Voxel]	Anatomical MNI		
				x	y	z
Thalamus	L	Prefrontal[76%]	354	-12	-20	6
Precentral gyrus	L	Area4a[58%]	122	-38	-24	58
Thalamus	R	Prefrontal[84%]	286	12	-16	6
SupraMarginal gyrus	L	Area OP1[SII][74%]	309	-52	-24	20
Putamen	R	Putamen (medial)[83%]	366	24	2	4
Putamen	L	Putamen (medial)[93%]	440	-26	-4	4
Superior frontal gyrus	L	Area 6d2[46%]	259	-26	-4	60
Rolandic operculum	R	Area44[34%]	490	54	6	8
Superior frontal gyrus	R	Area 6d3[71%]	269	26	-4	56
Cerebellum(VI)	R	Lobule VI(Hem)[94%]	683	20	-54	-22
Cerebellum(VI)	L	Lobule VI(Hem)[95%]	609	-16	-62	-20
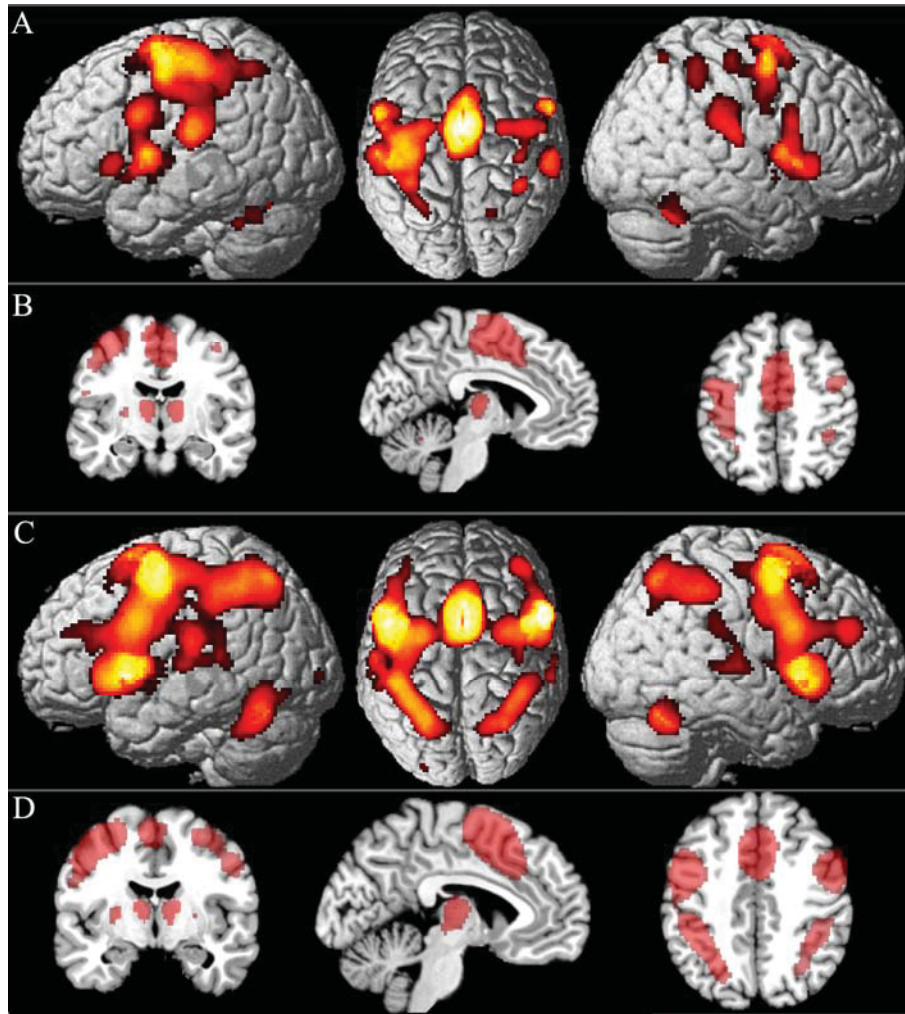
Fig. 3.7.2 Functional connectivity patterns of areas SMA (A, B) and pre-SMA(C, D) displayed on the MNI single subject template. A: the overview functional connectivity of area SMA in the 3D MNI template brain. B: section through the MNI template brain with the functional connectivity pattern of area SMA. C: the overview functional connectivity of area pre-SMA in the 3D MNI template brain. D: section through the MNI template brain with the functional connectivity pattern of area pre-SMA. The cluster assignations area specified in table 3.7.2.

Table 3.7.2 Functional co-activation clusters for areas SMA and pre-SMA. Cluster maxima assigned to the most probable cytoarchitectonic area when present in the SPM Anatomy Toolbox (Eichhoff et al., 2005).

Macroanatomical location	Hemisphere	Cytoarchitectonic area	Cluster size [Voxel]	Anatomical MNI		
				x	y	z
Area SMA						
Posterior-medial frontal	L	Area 6mr / presma [39%]	450	-4	-4	56
Precentral Gyrus	L	Area 4a [58%]	202	-38	-24	58
Supramarginal gyrus	L	Area op1 [sii] [74%]	271	-52	-24	20
Putamen	L	Putamen (medial) [93%]	333	-26	-4	4
Superior frontal gyrus	L	Area 6d2[46%]	196	-26	-4	60
IFG (p.opercularis)	L	Area 44[41%]	321	-48	6	28
Postcentral gyrus	L	Area 2[68%]	393	-36	-40	54
Putamen	R	Putamen(medial) [83%]	282	24	2	4
Rolandic operculum	R	Area 44[34%]	295	54	6	8
Superior frontal gyrus	R	Area 6d3[71%]	162	26	-4	56
Cerebellum (VI)	R	Lobule vi(hem) [94%]	451	20	-54	-22
Cerebellar vermis (4/5)	R	Lobule v(hem) [82%]	191	6	-60	-16
Supramarginal gyrus	R	Area pfcm(IPL) [53%]	121	60	-30	26
Rolandic operculum	R	Area op1[sii] [44%]	165	52	-24	20
Cerebellum (VI)	L	Lobule VI (hem) [93%]	215	-14	-62	-20
Pre-SMA						
Precentral gyrus	L	Area 44 [25%]	733	-48	6	30
Precentral gyrus	L	Area 6d3 [38%]	245	-28	-4	56
Thalamus	L	Thal: Prefrontal[88%]	347	-12	-16	6
Thalamus	R	Thal: Prefrontal[84%]	310	12	-16	6
IFG (p. Opercularis)	R	Area ifj2[32%]	125	50	10	26
Putamen	L	Putamen (medial) [65%]	442	-22	2	4
Inferior parietal lobule	R	Area hIP3(IPS)	362	36	-50	48
Superior parietal lobule	R	Area 7A (SPL)[30%]	248	18	-66	54
Cerebellum (VI)	L	Lobule VI (Hem) [95%]	498	-30	-60	-26
Inferior occipital gyrus	L	Area FG4 [58%]	175	-44	-60	-14
Cerebellum (VI)	R	Lobule VI(Hem) [94%]	644	30	-62	-26
Superior temporal gyrus	R	Area TE2.2[73%]	145	58	-22	6
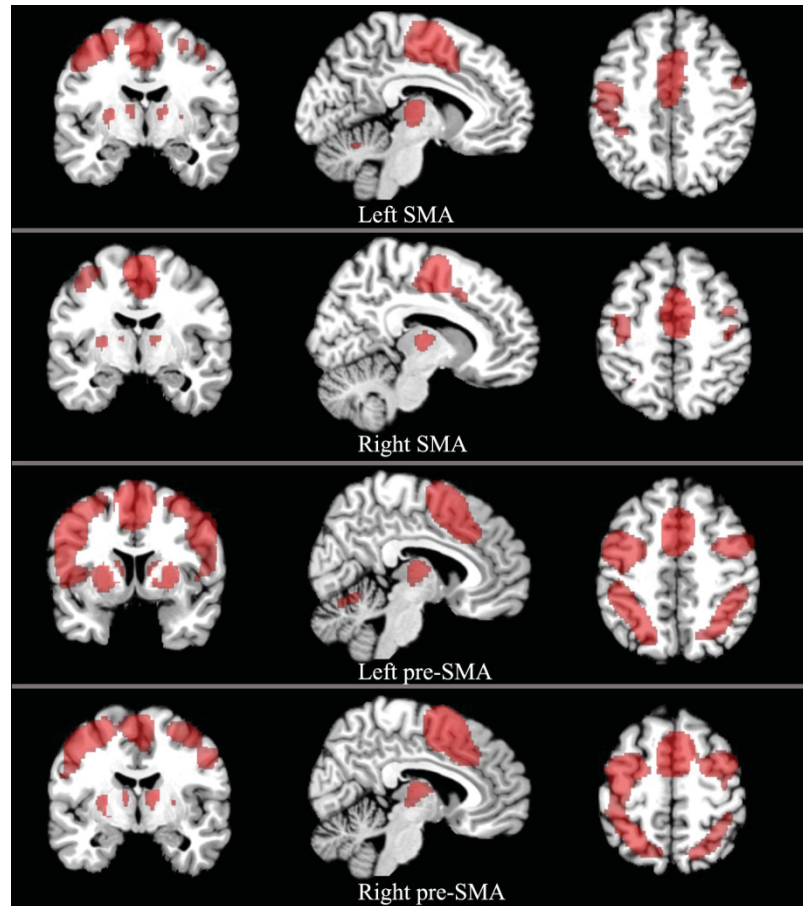
Fig. 3.7.3 Hemispheric showing functional connectivity of areas SMA and pre-SMA. The detail cluster areas are shown in Table 3.7.3.

Table 3.7.3 Functional co-activation clusters for left SMA, right SMA, left pre-SMA, and right pre-SMA.

Macroanatomical location	Hemisphere	Cytoarchitectonic area	Cluster size [Voxel]	Anatomical MNI		
				x	y	z
Left SMA						
Posterior-Medial Frontal	L	Pre-SMA[39%]	451	-4	-4	56
Precentral Gyrus	L	area 4a[43%]	214	-38	-24	60
SupraMarginal Gyrus	L	Area OP1 [SII] [61%]	265	-54	-24	20
Putamen	L	Putamen (medial) [93%]	305	-26	-4	2
Superior Frontal Gyrus	L	Area 6d2[38%]	182	-26	-6	60
IFG (p. Opercularis)	L	Area 44[31%]	275	-48	6	28
Postcentral Gyrus	L	Area 3b[64%]	327	-52	-18	40
Inferior Parietal Lobule	L	Area PFt (IPL) [65%]	180	-46	-32	44
Cerebellum (VI)	R	Lobule VI (Hem) [94%]	470	20	-54	-22
Precentral Gyrus	R	Area 44 [25%]	183	58	8	28
Superior Frontal Gyrus	R	Area 6d3[71%]	153	26	-4	56
Thalamus	L	Prefrontal[79%]	290	-12	-20	4
Putamen	R	Putamen (medial) [83%]	234	24	2	4
Thalamus	R	Prefrontal[48%]	187	14	-16	6
Right SMA						
Posterior-Medial Frontal	R	Pre-SMA[41%]	347	2	-4	56
Pallidum	R	Putamen (medial) [78%]	182	24	0	4
Rolandic Operculum	R	Area 44[42%]	169	54	6	10
Precentral Gyrus	L	Area 4a [47%]	97	-40	-24	58

Putamen	L	Putamen (medial) [93%]	219	-26	-4	4
Rolandic Operculum	R	Area OP1 [SII] [44%]	167	52	-24	20
Rolandic Operculum	L	Area OP1 [SII] [75%]	152	-48	-24	18
SupraMarginal Gyrus	L	Area PFt (IPL) [54%]	101	-52	-28	30
Thalamus	L	Prefrontal[82%]	209	-12	-18	6
Thalamus	R	Prefrontal[84%]	161	12	-16	6
Left pre-SMA						
Insula Lobe	L	Insula Lobe		-34	22	2
Precentral Gyrus	L	Area 44 [25%]	723	-48	6	30
Thalamus	L	Prefrontal [88%]	359	-12	-16	6
Precentral Gyrus	L	Area 6d2 [28%]	151	-28	-4	58
Putamen	R	Putamen (medial) [82%]	331	24	4	4
Thalamus	R	Prefrontal [84%]	307	12	-16	6
Putamen	L	Putamen (medial) [87%]	414	-24	0	4
Inferior Parietal Lobule	R	Area hIP3 (IPS) [57%]	356	36	-50	48
Inferior Parietal Lobule	R	Area 2 [40%]	195	40	-42	54
Superior Parietal Lobule	R	Area 7A (SPL) [48%]	248	20	-66	54
Inferior Occipital Gyrus	L	Area FG4 [58%]	182	-44	-60	-14
Cerebellum (VI)	L	Lobule VI (Hem) [95%]	451	-34	-50	-30
Cerebellum (VI)	R	Lobule VI (Hem) [94%]	642	30	-62	26
SupraMarginal Gyrus	L	Area PFop (IPL) [51%]	98	-56	-24	22
Superior Temporal Gyrus	L	Area TE 2.2 [54%]	125	-58	-22	8
Superior Temporal Gyrus	R	Area TE 2.2 [73%]	105	58	-22	6
Right pre-SMA						
Precentral Gyrus	L	Area 44[21%]	641	-46	6	30
Thalamus	L	Prefrontal[88%]	336	-12	-16	6
Thalamus	R	Prefrontal [84%]	310	12	-16	6
Putamen	R	Putamen (medial) [82%]	329	24	4	4
Inferior Parietal Lobule	L	Area 7PC (SPL) [31%]	128	-30	-52	52
IFG (p. Opercularis)	R	Area ifj2 [32%]	83	50	10	26
Inferior Parietal Lobule	R	Area hIP3 (IPS) [57%]	324	36	-50	48
Superior Parietal Lobule	R	Area 7A (SPL) [38%]	167	30	-60	54
Inferior Parietal Lobule	R	Area 2 [53%]	197	46	-34	48
Cerebellum (VI)	L	Lobule VI (Hem) [96%]	327	-28	-60	-26
Cerebellum (VI)	R	Lobule VI (Hem) [95%]	317	30	-62	-24
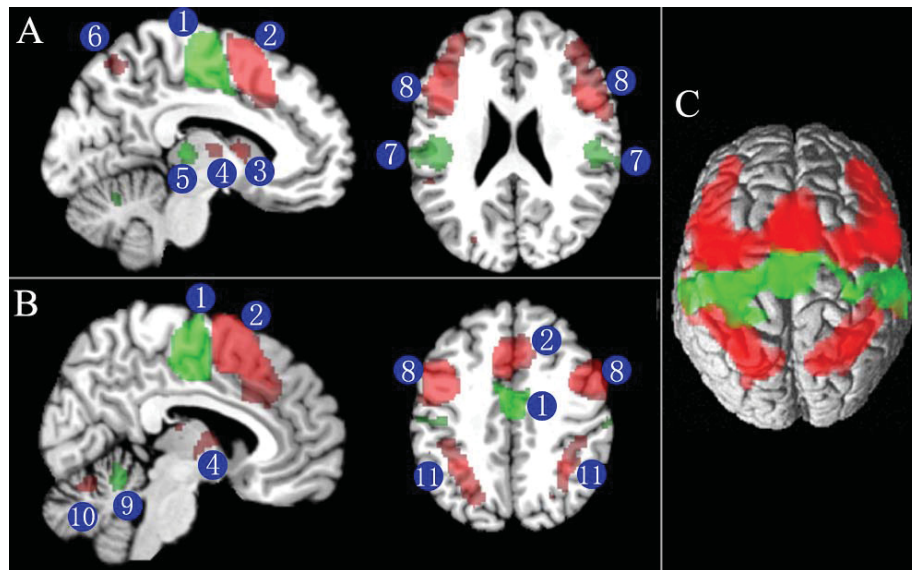
Fig. 3.7.4 Contrast analysis of significant co-activation clusters for area SMA and pre-SMA showing in MNI space. The green colored regions are significantly stronger co-activated with area SMA. However, the red colored regions are significantly stronger co-activated with area pre-SMA. A and B: Section through the MNI template showing the significant stronger co-activation clusters for area SMA and pre-SMA. The numbers indicate the cluster locations: 1 SMA; 2 pre-SMA; 3 caudate; 4 thalamus; 5 putamen; 6 superior parietal lobule; 7 superamarginal gyrus;8 inferior frontal gyrus;9 cerebellar Vemis; 10 cerebulum(VI); 11 inferior parietal lobule. C 3D rendering of the contrast of significant co-activation clusters for areas SMA and pre-SMA in MNI space. Area SMA is significantly stronger co-activated with inferior parietal lobule, precentral gyrus and area 6d1. However, area pre-SMA is significantly stronger co-activated with inferior parietal lobule, and area 6d2.

The contrast analysis between area SMA and pre-SMA revealed that area pre-SMA was more strongly related with the dorsal lateral rostral premotor area 6 and area 4 than area SMA. Area SMA was more highly related with the dorsal lateral caudal premotor area 6 than area pre-SMA (Fig. 3.7.4). Within each area, the hemispheric distinctions of areas SMA and pre-SMA were obviously seen. The hemispheric area of each area was prone to co-activate with ipsilateral areas (Fig. 3.7.5, Fig. 3.7.6).
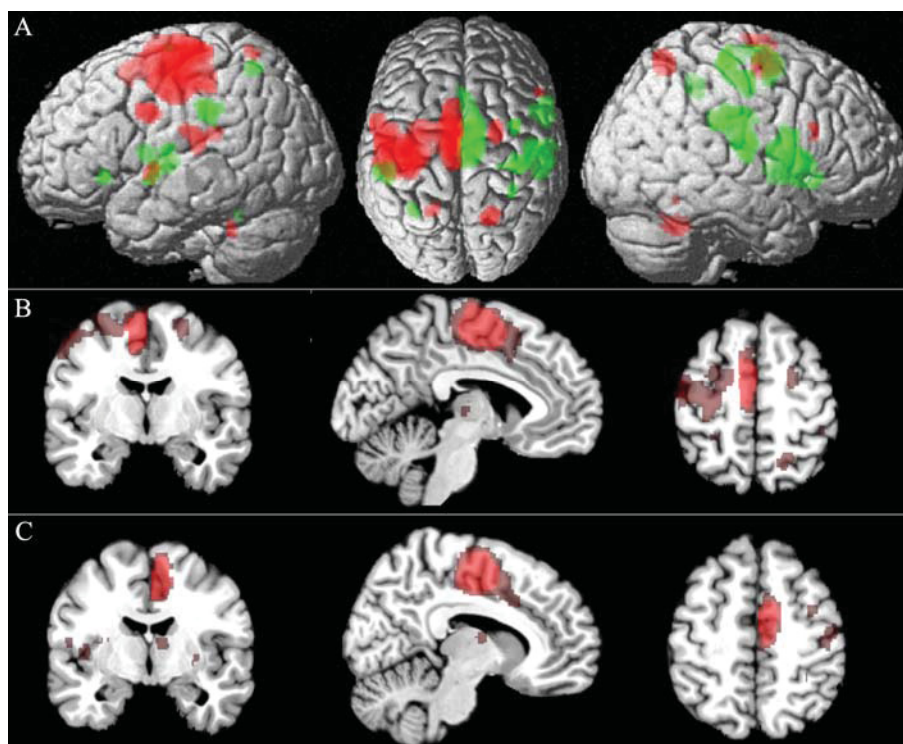
Fig. 3.7.5 Clusters revealed by the contrast analysis between left SMA and right SMA. A: the overview contrast clusters of left SMA and right SMA. The red color indicates the clusters which area left SMA are stronger than right SMA. The clusters in where the right SMA is stronger than left SMA are shown in green color. B: the left SMA is stronger than right SMA. C: The right SMA is stronger than left SMA.

Fig. 3.7.6 Clusters revealed by the contrast analysis between left pre-SMA and right pre-SMA. A: the overview contrast clusters of left pre-SMA and right pre-SMA. The red color indicates the clusters where area left pre-SMA is stronger than right pre-SMA. The clusters in where the right pre-SMA is stronger than left pre-SMA are shown in green color. B: the left pre-SMA is stronger than right pre-SMA. C: The right pre-SMA is stronger than left pre-SMA.
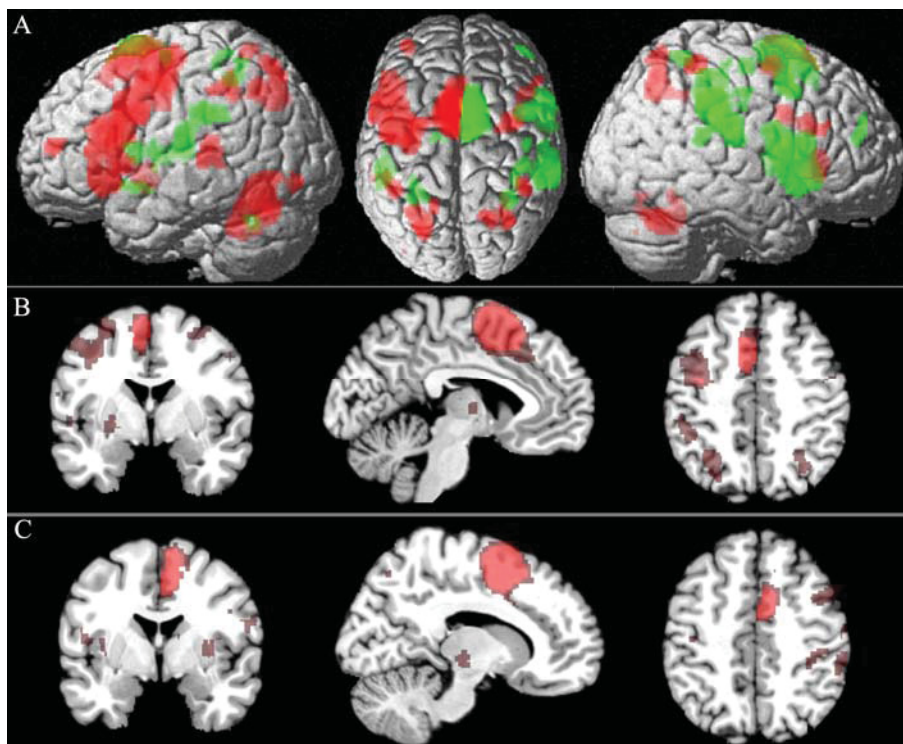
3.7.2 Function characterization of areas SMA and pre-SMA

A functional decoding analysis was carried out based on the BrainMap meta-data to depict the functional features of areas SMA and pre-SMA (Laird, et al. 2009; Laird, et al. 2011). In the present study, the functional domains and paradigm classes within these two areas were identified. The functional conjunction and contrast analysis between area SMA and pre-SMA was performed.

The functional decoding analysis for areas SMA and pre-SMA showed that area SMA was significantly related to functional domains such as action (execution, imagination, and rest), interoception, interoception bladder, and perception somethesis. In contrast, area pre-SMA was significantly correlated with more complex behavioural domains such as action (motor learning, execution, imagination and execution speech), cognition music, and perception vision motion (Fig. 3.7.7). The paradigm classes of areas SMA and pre-SMA were also yielded from the functional decoding analysis. It was noted that area SMA was linked to tasks such as flexion/extension, imagined movement, drawing, sequence recall/learning, grasping, finger tapping/button press. Area pre-SMA was found to be activated in tasks like drawing, sequence recall/learning, saccades, imagined movement, flexion/extension, recitation/repetition (overt), music comprehension, finger tapping/button press (Fig. 3.7.7).

The conjunction analysis of functional clusters for areas SMA and pre-SMA found that these two areas shared some common behavioural domains (action execution, action imagination) and some paradigms clusters (drawing, flextion/extension, imagined movement, finger tapping/button press). The area SMA showed a higher likelihood ratio with action execution than that of area pre-SMA (Fig. 3.7.8). Both left SMA and right SMA were related to the action domain (action/execution and action/imagination) and paradigms such as flexion/extension, imagined movement and finger tapping/button press. Furthermore, left pre-SMA and right pre-SMA were associated with action domain (action/execution, action.imagination), and perception domain (perception.vision.motion) and paradigms classes such as saccades, imagined movement, recitation/repetition(overt), flexion/extension and finger tapping/button press (Fig. 3.7.9, Fig.3.7.10).

The functional segregation between areas SMA and pre-SMA was identified by the contrast analysis. It was found that area pre-SMA was stronger related to functional

domain like emotion, cognition, and perception than that of area SMA. The area SMA, however, was stronger correlated to action/execution and action/rest than area pre-SMA. For the paradigm classes aspect, the area pre-SMA was strongly associated with passive listening, visual object identification, orthographic discrimination, imagined objects/scenes, autobiographical recall, recitation/repetition (overt), deception, anti-saccades, music production, recitation/repetition (covert), visuo-spatial attention. It seemed that the task paradigms of area SMA confined to flexion/extension and rest (Fig.3.7.11). Significant hemispheric divergences in areas SMA and pre-SMA were not detected (Fig. 3.7.12, 3.7.13).
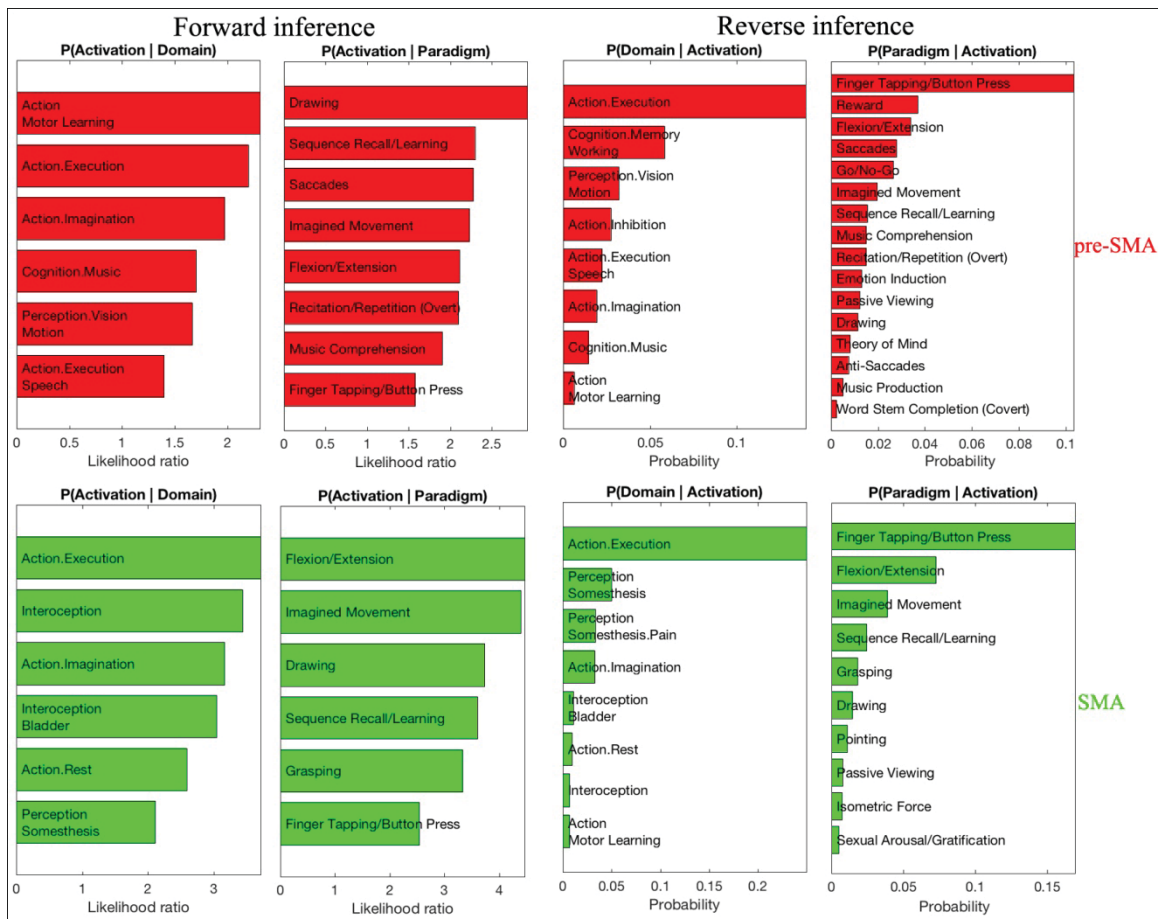
Fig. 3.7.7 Functional decoding of areas SMA and pre-SMA with behavioral domains paradigm classes from BrainMap database (www.brainmap.org; category labeling).Forward inference determines above-chance brain activity given the presence of a functional decoding term, whereas reverse inference determines the above-chance probability of a functional decoding term given observed brain activity.

Fig. 3.7.8 Functional clusters from conjunction analysis of area SMA and area pre-SMA with behavioral domains (top row) and paradigm classes (bottom row of the BrainMap meta-data (www.brainmap.org; category labeling). The left column axis labeling indicates the likelihood ratio values, and the right column axis labeling indicates probability values.
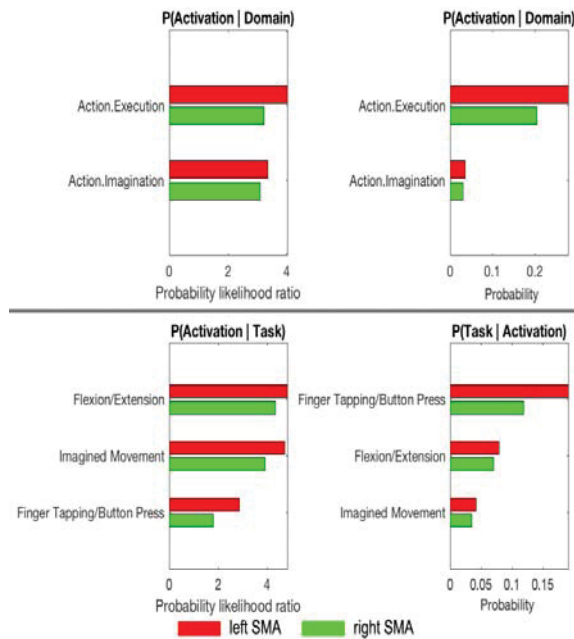
Fig. 3.7.9 Functional clusters from conjunction analysis of left SMA and right SMA with behavioral domains (top row) and paradigm classes (bottom row) of the BrainMap meta-data (www.brainmap.org; category labeling).

Fig. 3.7.10 Functional clusters from conjunction analysis of left pre-SMA and right pre-SMA with behavioral domains (top row) and paradigm classes (bottom row) of the BrainMap meta-data (www.brainmap.org; category labeling).
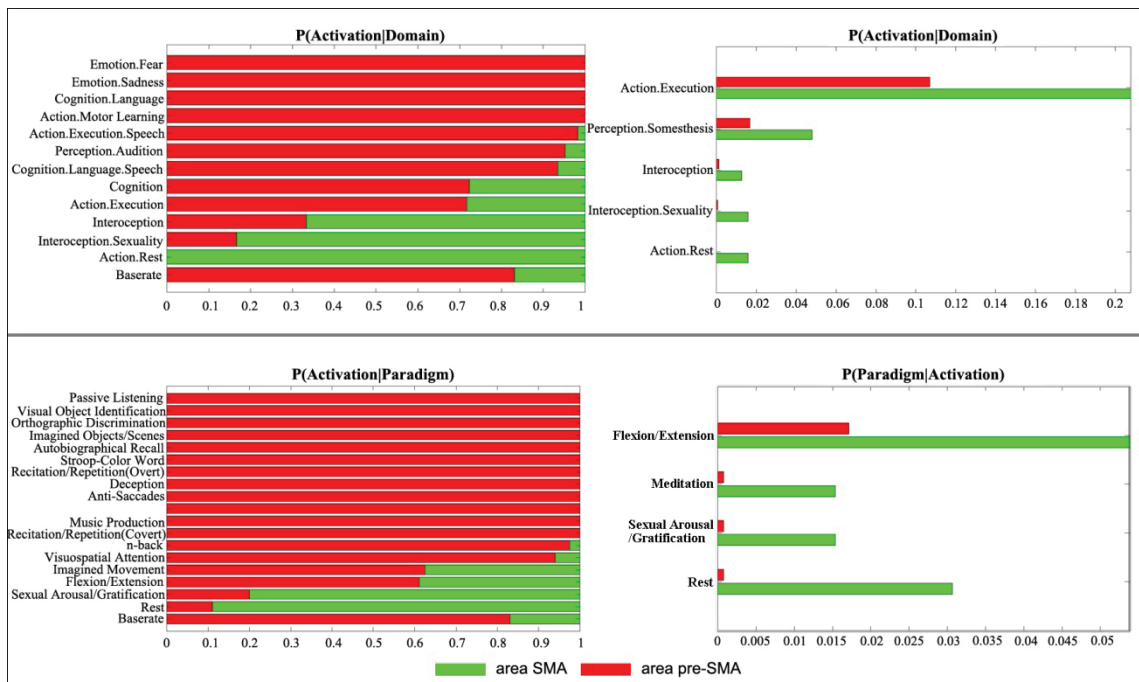
Fig. 3.7.11 Contrast analysis between area SMA and area pre-SMA with behavioral domains (top row) and paradigm classes (bottom row).
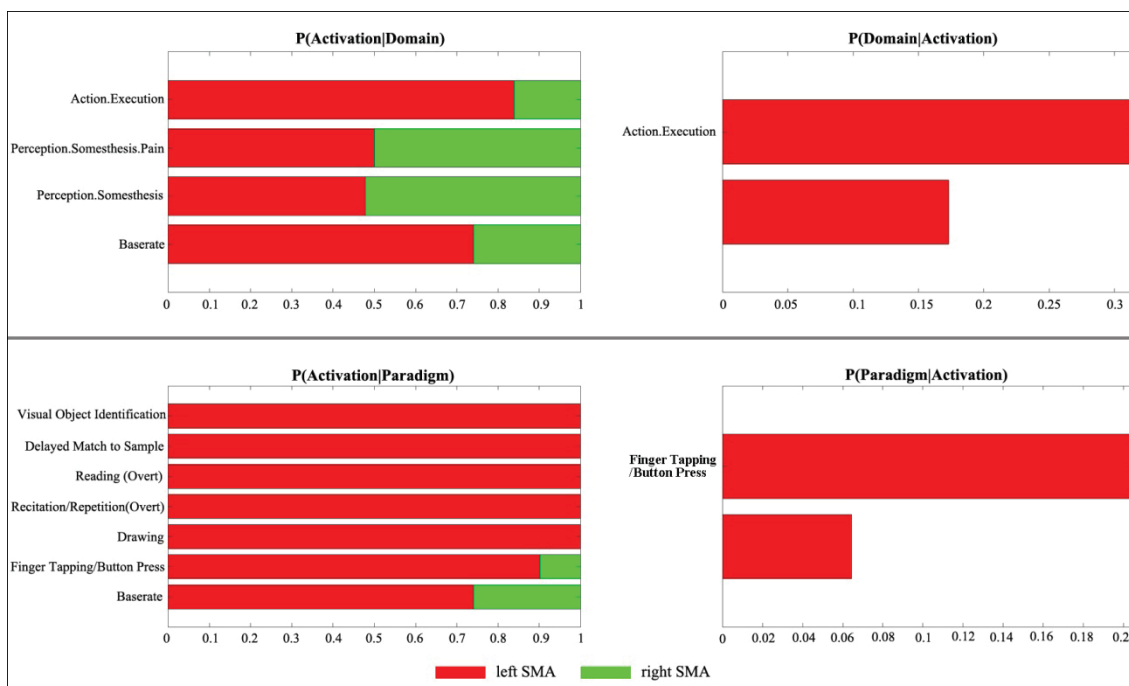
Fig. 3.7.12 Contrast analysis between left SMA and right pre-SMA with behavioral domains (top row) and paradigm classes (bottom row).
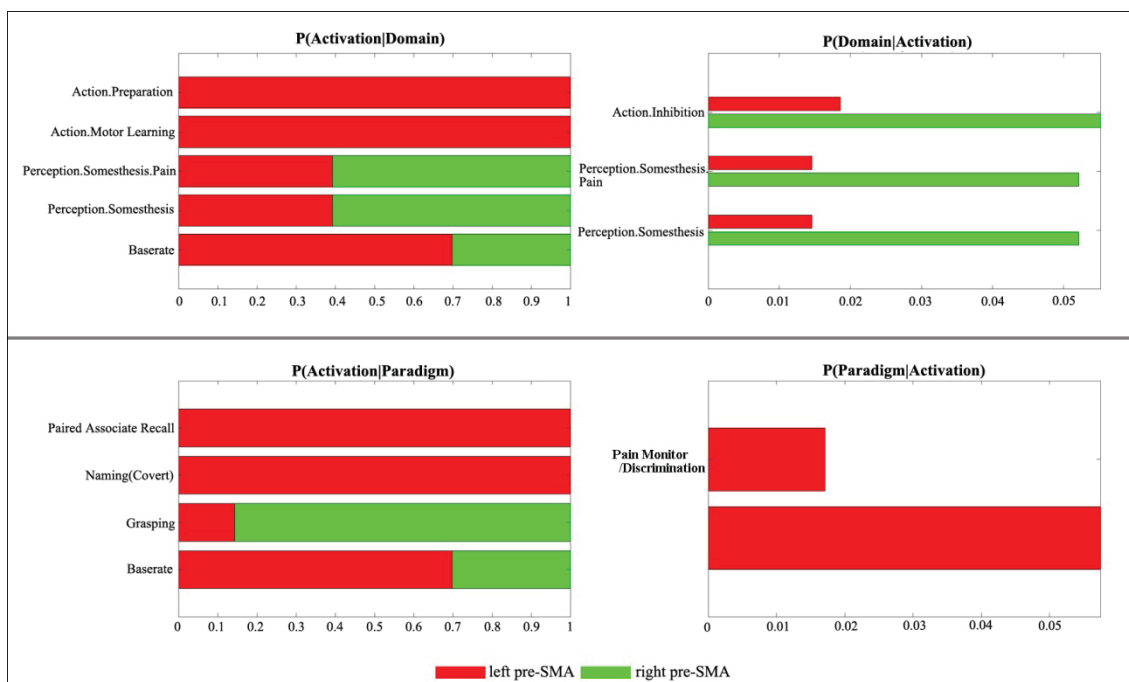
Fig. 3.7.13 Contrast analysis between left pre-SMA and right pre-SMA with behavioral domains (top row) and paradigm classes (bottom row).

4 Discussion

4.1 Cytoarchitecture of areas SMA and pre-SMA

In present study, two agranular areas: area SMA (SMA proper) and area pre-SMA, were identified. Area SMA is characterized both by poor lamination and by densely packed large size pyramidal cells in the lower part of layer III. Area pre-SMA laminates better and has a pronounced layer V. The pyramidal cells in the lower part of layer III are larger in area SMA than in pre-SMA. These findings agree with previous studies (Zilles, et al. 1995; Zilles, et al. 1996; Vorobiev, et al. 1998). Using a microscope to analyse the cytoarchitecture, Vorobiev and co-workers (1998) divided SMA proper into two parts, SMA caudal and SMA rostral. However, we could not confirm this finding with our quantitative cytoarchitectonic analysis. It seems that the photomicrographs of caudal SMA in the study of Vorobiev et al. corresponds to the transition zone between Brodmann area 4 (M1) and Brodmann area 6 (SMA proper). A functional divergence observed in functional imaging studies may explain this. Caudal SMA proper is activated during the execution of a movement, while the rostral SMA proper is more extensively activated by imagining movements (Stephan, et al. 1995; Grafton, et al. 1996; Roth, et al. 1996). Primary motor area was significantly activatedduring the execution of movements, as was the caudal SMA (Stinear, et al. 2009; Miller, et al. 2010). The photomicrographs of caudal SMA shown in Vorobiev's article (1998) were characterized by large pyramidal cells in layer V; their size was between that of Betz cells and the large cells of layer V in rostral SMA. Therefore, more evidence for the existence of a separate caudal SMA is required to demonstrate that it is not the transition zone between Brodmann area 4 and area SMA (or BA6). With quantitative, cytoarchitectural analysis we did not find an area that differed significantly from Brodmann area 4 and the rostral SMA. As discussed below as part of the methodological considerations, the algorithm used in our study can successfully solve the problem of area transitions.

The parcellation of areas SMA and pre-SMA was confirmed by the hierarchical cluster analysis, which suggested that the two areas differed in cell density. To detect this issue, the mean profiles of 10 brains of each area were divided into 10 bins of 10% distance. The significant differences were found at bins 4 (cortical depth: 30%-40%) and 5 (cortical depth: 40%-50%) which were roughly located at the position of lower

part of layer III. This suggested that the most prominent differences between area SMA and pre-SMA were the differences of cell density in the lower part of layer III. Although the cell shape in layer V between area SMA and area pre-SMA was different under microscope inspection, such difference were not significant reflected when using statistics analysis. This is possible considering that the parameter used in our quantitative analysis is gray level index (corresponding with cell density) instead of parameter of cell shape. Notably, in individual brain, the ten feature vectors between the two areas differed significantly. However, because high intersubject variability smoothed the parameter differences of the cytoarchitecture between area SMA and area pre-SMA, the ten mean values of feature vectors of the ten brains between two areas were not found to be different (P＞0.05, Student's t-test).

In this study, it was found that the rostral part (area pre-SMA) laminated better than the caudal part (area SMA). The same trend was found in cingulate cortex and dorsal premotor cortex: areas 24c and PMdr laminated better than areas 24d and PMdc, respectively. The layer V of the three rostral parts including areas pre-SMA, PMdr, and 24c were relatively more pronounced than that of the three caudal parts including areas SMA, PMdc, and 24d, respectively; From caudal parts to rostral parts, the layer III in these areas showed decreased trends in cell density. This kind of continuous and gradual cytoarchitectonic change between those subareas showing high correlated functions may can be thought as "stream" considering about the "Gradationsprinzip" (gradation principle), which was first introduced by Sanides (Sanides 1962; Sanides 1964). From area pre-SMA to area SMA, from area 24c to area 24d, from area PMdr to area PMdc, they shared some common cytoarchitectonic characterizations: the relative cell density in layer II increased, the relative cell density and cell size in layer IIIc increased, the cell density in layer V decreased. This kind of gradation organized pattern enlarges our knowledge about human brain. Not only the gradation of the whole brain as an integrity, but also the gradation of subareas in a functional related entity should be taken into account in the future study.

The cellular patterns within rostral three areas including pre-SMA, PMdr, and 24c are more similar than those cellular patterns between rostral three areas and caudal three areas. Vice versa, the cellular patterns within caudal three areas including areas SMA, PMdc, and 24d are more similar than those cellular patterns between rostral three areas

and caudal three areas. This appearance of the cellular pattern across areas may be related with the anatomical connectivity. The anatomical connectivity within these areas showed similar patterns. Area SMA is strongly linked with PMdc and area 24d, but is relatively modest linked with PMdr and area 24c. On the contrary, area pre-SMA is richly connected with area PMdr and area 24c, but is weakly connected with area PMdc and area 24d (Luppino, et al. 1993). These facts may suggest the notion that cortical areas do not simply form a mosaic, but are hierarchically organized (Amunts and Zilles 2012). The gradual changes of celluar pattern and anatomical connectivity across areas may be the inner mechanism of hierarchical organized cortex.

According to previous study (Matelli, et al. 1991; Zilles, et al. 1995), the architecture of areas SMA and pre-SMA were similar in human and macaque. Moreover, the distribution patterns of many receptors in this area of both species showed many common features (Zilles, et al. 1995). However, there were also some differences in architectonic features of the brain motor cortex between the two species could be found (Zilles, et al. 1995). For example, the cell density of motor areas in monkey is higher than that in human cortex. The Betz cells in human brain cortex were found to be restricted to area 4, while in monkey brain cortex the Betz cells were not so restricted (Zilles, et al. 1995). It is worth mentioning that the shrinkage may affect the brains of two species to different degrees during histological procedures (Amunts, et al. 1999). And it is not clear whether the major compartments (cell bodies and neuropil) shrink to the same degree in the two species.

4.2 Characteristic of areas SMA and pre-SMA detected by different tools

To better understand the distributions of area SMA and pre-SMA, different architectonic tools: cytoarchitecture, myeloarchitectecture, immunoarchitecture, and receptor autoradiography was taken together to make a comparison. From the cytoarchitecture aspect, area SMA is featured by poor lamination; densely packed large size pyramidal cells in the lower part of layer III. Area pre-SMA is characterized by better lamination, pronounced layer V and the small size pyramidal cells of lower part of layer III. The layer scheme of myeloarchitectonics based on tangential and radial was developed by Vogt (Vogt and Vogt 1903), which was similar with the cyroarchitectonic layer scheme. However, comparable measurements between the cyto- and myeo-

architecture of the mesial motor area cortex are still lacking. The myeloarchitectonic researches were widely used in earlier stages (Vogt Cécile 1919; Strasburger 1937; Hopf 1956; Sanides 1962; Sanides 1964). Although these studies did not subdivide the mesial agranular motor area, these works provided much novel knowledge about the brain. For example, by combining myeloarchitectonics with cytoarchitectonics, Sanides proposed the "streams" theory of neocortical regions (Sanides 1962; Sanides 1964). The immunohistochemical staining method was introduced over the last three decades. According to the immunoarchitectonic studies, the area SMA showed an overall homogeneous cortex; And the medium size immunoreactive neurones in the deeper layer III could be found. The area pre-SMA showed a prominent layer V and better distinct layers (Baleydier, et al. 1997; Geyer, et al. 2000; Vogt and Vogt 2003). These observations are consistent with our current studies. For the receptor autoradiography, the changes in receptor densities were found precisely at the borders of the architectonically defined areas (Zilles, et al. 1995). The putative pre-SMA showed higher densities of M2, NMDA, a_1 and 5-HT_2 receptors than the neighbouring premotor cortex. The NMDA, a_1 and 5-HT_2, AMPA receptors in pre-SMA, however, had lower densities than in cingulate sulcus. The 5-HT_1, a_2 receptors showed a lower density in area SMA than in cingulate cortex and primary motor area. The area SMA and area pre-SMA in macaques can be separated by the increases in M2, AMPA, [H^3] kainite, [H^3]MK-801, [H^3] muscimol etc. receptors in area pre-SMA (Zilles, et al. 1995; Geyer, et al. 1998). These characteristics are summarized in table 4.2.1.

116

Table 4.2.1The main characteristics of areas SMA and pre-SMA defined by different protocols.

Analysis tools	Major characteristics of areas in human or macaque		References
	SMA	Pre-SMA	
Cytoarchitecture	Poor lamination; densely packed large size pyramidal cells in the lower part of layer III.	Better lamination; pronounced layer V; The pyramidal cells of lower part of layer III in area SMA are larger than that in area pre-SMA.	
Immunoarchitecture	Absence of any betz cells; some medium size immunoreactive neurones in the deeper layer iii; the overall aspect is very homogeneous cortex.	A prominent layer V; The pyramidal neurones here were small to medium in size and the distinct appearance of layer v is due to its great cellular density. Layer VI seemed to be composed of two sublayers.	(Baleydier, et al. 1997; Geyer, et al. 2000; vogt and vogt 2003)
Receptor autoradiography	Lower densities in 5-HT$_1$, a$_2$ receptors.	Increases in M2, AMPA, [H^3] kainite, [H^3]MK-801, [H^3]muscimol et al. Receptors in area pre-SMA	(Zilles, et al. 1995; Geyer, et al. 1998)

4.3 Comparisons with previous maps of areas SMA and pre-sma

4.3.1 Cytoarchitectonic maps

Woolsey and Penfield introduced the term "supplementary motor area" by using electrical stimulation on monkey cortex or clinical observations (Penfield 1950; Woolsey, et al. 1952). In earlier studies, this entity locating in the mesial frontal motor cortex was considered as a homogeneous area and was investigated as integrity (Brodmann 1909; Von Economo and Koskinas 1925; Bertrand 1956; Orgogozo and Larsen 1979; Smith 1979; Roland, et al. 1980). Now, It has been widely accepted that the traditional supplementary motor area, which has been known as a homogeneous area in the classical characterization (Penfield and Welch 1951; Woolsey, et al. 1952; Tanji and Shima 1996; Geyer, et al. 1998), can be divided into SMA proper(SMA) and pre-SMA, which are homologous to F3,and F6, respectively (Luppino, et al. 1991; Matelli, et al. 1991; Matsuzaka, et al. 1992; Tanji 1994; Rizzolatti, et al. 1996; Geyer, et al. 1998; Nachev, et al. 2008). The cytoarchitectonic evidences was first found by Vogt and Vogt, who divided the area 6 (including the mesial, dorsal lateral area 6) into two parts: 6aα in caudal and 6aβ in rostral (Vogt Cécile 1919). Then, Von Bonin and Bailey subdivided it into areas FB and FC (Bailey 1947), Barbas and Pandya subdivided it into areas 6DC and MII (Barbas and Pandya 1987). Despite the agreement on the principal

subdivion into the mesial frontal surface, the maps of these studies varied from each other, which has been reviewed (Zilles 1990).

These cytoarchitectonic maps of medial frontal motor area differ considerably from each other regarding the number or code of cortical areas, their shape and relationship to macroscopical landmarks or neighbouring areas. For example, the mesial motor surface of area 6 in Brodmann's map had a common border with anterior cingulate: area 24, and almost had no common border with posterior cingulate: area 31 or area 23. In the rostral part, the mesial motor cortex surface bordered with area 8, and border with area 32 in a small corner. In the maps of von Economo and Koskinas, however, the area Fc (corresponding to Brodmann area 6) had no common boder with area La (corresponding to Brodmann area 24), but bordered with area Fcl (corresponding to Brodmann area 32) only (Brodmann 1909; Von Economo and Koskinas 1925; Triarhou 2007). The present study showed that areas SMA and pre-SMA bordered with Broadmann area 24 (area 24d in caudal and area 24c in rostral) at the ventral parts. The transition between area 4 (M1) and area SMA located roughly coincide with the transition between area 23 and area 24, which was corresponding to other studies (Zilles, et al. 1995; Palomero-Gallagher, et al. 2009).

4.3.2 Directed cytoarchitectonic gradations in the areas SMA and pre-SMA

The change of cellular pattern from one to another showed some regulars named streams. Based on earlier observations from the Vogt's (Vogt Cécile 1919) and Brockhaus (Brockhaus 1940), Sanides first introduced the term "gradation" and "Gradationsprinzip" (gradation principle) (Sanides 1962; Sanides 1964). Gradations are spatially directed sequences of cortical areas, which originate, in most cases, in phylogenetically old regions of the cortex. This complex composition makes sense considering the variety of brain functions associated with Brodmann's areas (Amunts and Zilles 2012). In fact, the parcellations obtained from observer-independent procedures reflect the gradation steams and provide insight into the underlying evolution principles of the regional differentiation (Henssen, et al. 2016). According to the gradation principle, from area 6 to area 4, the cell density in layer V gradually decreased (Sanides 1962; Sanides 1964). In present study, it was found that the identical cytoarchitectonic features: from the rostral area pre-SMA to the caudal area SMA, the

cell density in layer V relatively decreased. In addition, as it has been discussed in the part of cytoarchitecture of areas SMA and pre-SMA, from the rostral part to caudal part of mesial frontal cortex, also including the dorsal lateral premotor area and cingulate gyri, the major cytoarchitectonic features in layer II, layer IIIc, layer V showed a similar trend of gradual changes. Thus, it can be confirmed that the gradation streams not only exist between large areas (eg. from Brodmann's area 6 to Brodmann's area 4 to Brodmann's area 1), but also exist between subareas (eg. from area pre-SMA to area SMA), which may suggest that these areas show highly related but different functions.

4.3.3 Myeloarchitectonic maps

The rough locations of areas 6aα and area 6aβ (e.g. anterior to precentral sulcus and above the cingualte sulcus) (Vogt 1910; Vogt Cécile 1919) is identical with the position of areas SMA and pre-SMA in present study. With visual inspection, Vogt and Vogt subdivided the motor agranular area (anterior to the precentral sulcus, corresponding with Brodman area 6) into two parts: 6aα in the caudal, 6aβ in the rostral (Vogt 1910; Vogt Cécile 1919). The mesial frontal surface of area 6aα and area 6aβ were corresponding with area SMA (proper) and pre-SMA, respectively (Matsuzaka, et al. 1992; Picard and Strick 1996). The later studies focusing on the myeloarchitectonic maps of Brodmann area 6 were performed by Strasburg (1937) (Strasburger 1937), Hopf (1956) (Hopf 1956), and Sanides (1962) (Sanides 1962) etc. The Strasburger's map did not divided the area 1 and area 4, the location of mesial area 6 was quite brief (Strasburger 1937). In the Hopf's map, the area 10 located below the mesial area 6 and area 11 located anterior to mesial area 6, which were quite different from the widely accepted map nowadays available (Hopf 1956). These subjective inspection myeloarchitectonic maps provided useful but limited knowledge about the human mesial frontal cortex.

4.3.4 Immunoarchitecture maps

Over the last three decades, one new microstrctural technique was introduced to map areas in the primate cortex. This immunohistochemical staining (SMI-32) of nonphosphorylated epitopes on the neurofilament protein (NFP) revealing the pyramidal

neurons display the laminar distribution patterns with high specificity (Sternberger and Sternberger 1983; Lee, et al. 1988; Mullen, et al. 1992). In present study, it was found the border between area SMA and PMdc, and the border between area pre-SMA and PMdr normally located in the arcuate corner of area 6, which was consistent with the earlier study using immunochemical analysis (SMI-32) on monkeys (Geyer, et al. 2000). In fact, one study performed by Geyer and colleagues has confirmed that the extent of areas defined by the NFP matches well with the areas defined by the cytoarchitecture (Geyer, et al. 2000). So far, the frontal agranular areas including areas SMA and pre-SMA were poorly understood according to immunoarchitecture tools. According to some case studies using immunochemical method (antibody SMI-32 labelled NFP), the roughly locations of areas SMA, and pre-SMA, above the cingulated sulcus in the mesial view, were identical with the current study (Baleydier, et al. 1997; Vogt and Vogt 2003).

4.3.5 Receptor autoradiographic maps

The receptor autoradiography is used to detect the binding patterns of receptors. The cortical area can be featured neurochemically by different ligands. Thus, a "neurochemical fingerprint" can be created. Then, the similar "fingerprint" can be grounded into "neurochemical families" of areas which may indicate functional related areas (Geyer, et al. 1998; Zilles and Amunts 2009). Although not all the receptors are differentially distributed, comprehensive application of many different receptors provides reliable data for cortical parcellation and evaluation of putative areal borders. Compared with previous studies (Zilles, et al. 1995) using receptor autoradiography, the cytoarchitectonic defined border between premotor cortex and area SMA can be well detected by distributions of cholinergic muscarinic M2 receptors; kainate receptors; and α-amino-3-hydroxy-5-methyl-4-isoxazolepropionic acid (AMPA) receptors. The cytoarchitectonic defined border between premotor cortex and area pre-SMA can been detected in the distribution autoradiographs of receptor N-methyl-D-aspartate (NMDA), AMPA, kainate alpha 1, cholinergic muscarinic M2, and serotoninergic $5-HT_2$. However, the border between premotor and area pre-SMA cannot be detected by the distributions of kainate receptor. Overall, the cytoarchitectonic maps of areas SMA and pre-SMA are

in good agreement with the parcellations defined by integrating multiple receptor distributions.

4.3.6 Stimulation and functional imaging studies

The traditional defined supplementary motor area (areas SMA proper and pre-SMA) has been identified by intracortical microstimulation mapping which was based on the basis of somatotopic organizational characteristic of this region (Mitz and Wise 1987; Fried, et al. 1991). However, the somatotopic organization of area SMA is not detected in some studies (Orgogozo and Larsen 1979; Matelli, et al. 1993). Also, it is difficult to evoke movements by stimulation over pre-SMA (Luppino, et al. 1991). Therefore, the stimulation mapping for areas SMA and pre-SMA still needs further studies. Numerous functional imaging studies focusing on the function of human mesial frontal surface, found the functional dissociation between area SMA and area pre-SMA (Ferrandez, et al. 2003; Chainay, et al. 2004; Chung, et al. 2005; Nachev, et al. 2007). Although the maps of areas SMA and pre-SMA from the functional studies are not precisely enough, as the technique developed, it has been verified that the high-resolution MRI reflects myeloarchitecture and cytoarchitecture of human cerebral cortex (Eickhoff, et al. 2005).

Using electrical microstimulation on monkeys, Schlag and colleagues first found a new area in the dorsomedial cortical named supplementary eye field (SEF) responded to photic stimuli and target fixation (Schlag and Schlag-Rey 1987). Then, using electrical stimulation on humans, Matsuzaka and co-workers first defined the areas SMA and pre-SMA in humans which showed a functional dissociation (Matsuzaka, et al. 1992). The supplementary eye field could be defined by functional Magnetic Resonance Imaging and positron emission tomography: a region in the medial frontal cortex, anterior and superior to area SMA, which was activated when subjects executed self-paced horizontal saccades in darkness (Sweeney, et al. 1996; Grosbras, et al. 1999). Supplementary eye field also could be defined by a sulcal landmark: the upper part of the paracentral sulcus (Grosbras, et al. 1999).

In this study, area SEF was not found by cytoarchitectonic analysis. In fact, there is no architectonic evidence for area SEF so far. The previous studies using receptor autoradiographic mapping, myeloarchitecture mapping also did not define the area SEF

(Zilles, et al. 1995; Geyer, et al. 1998). This may be caused by the following reasons: 1. the area SEF, a small size region and located at the border of the SMA and the pre-SMA (Grosbras, et al. 1999; Yamamoto, et al. 2004), this may request a more sensitive method for detecting the borders between the SEF and other areas. Moreover, previous studies has confirmed that the motor representation with hindlimb movements located caudally, forelimb movements located centrally (Mitz and Wise 1987; Luppino, et al. 1991), which may suggest that the representation of occulumotor movements does not necessarily mean a new cytoarchitectonic defined area. This is possible considering that the stimulation studies found supplementary eye field locates rostral to the area of representation for hand and foot movements (area SMA), partly overlaps with area SMA (Yamamoto, et al. 2004).

4.3.7 Anatomical and resting state connectivity, co-activation pattern

The observed cytoarchitectonic border between area SMA and pre-SMA is located close to the vertical line extending from the anterior commissure (Y = 0), which is in good agreement with anatomical connectivity as delineated by diffusion tractography (Johansen-Berg, et al. 2004). Although an inherent limitation exists in anatomical accuracy of brain connections derived from diffusion tractography (Thomas, et al. 2014), this concordance between the two different techniques performed on independent samples is noteworthy considering that diffusion tractography provides an approach to investigate human brain organization in vivo. Despite congruency, it is notable that some differences can be found when taking the anatomical connections of the putative areas SMA and pre-SMA into consideration. The putative area pre-SMA had dense anatomical connections to the medial parietal cortex (Johansen-Berg, et al. 2004), which were not exhibited by the co-activation pattern of area pre-SMA in the present study; Moreover, functional analysis in the present study showed that areas SMA and pre-SMA had significant connections with cerebellum, which were not presented in anatomical connectivity (Johansen-Berg, et al. 2004). These differences may be clarified by the different approaches employed in the two studies. First, the anatomical connectivity and the functional connectivity are conceptual differences: the former is a task-independent property; while the latter is a task-dependent property (Eickhoff, et al. 2011). Moreover, the inherent limitation of diffusion tensor imaging in determining long-range anatomical

projections cannot be overcome, which may cause difficult to identify some anatomical connectivity (Thomas, et al. 2014).

Based on their similarities of functional connections, the parcellations in human medial frontal cortex also be parcellated with resting state functional MRI (Kim, et al. 2010). The observed cytoarchitectonic border (VCA line) of areas SMA and pre-SMA is corresponding to that border between the anterior and posterior clusters derived from resting state functional MRI (Kim, et al. 2010). It was reported that the functional networks in "rest" showed close correspondence with the functional networks in explicit "activation" (Smith, et al. 2009; Simonyan and Fuertinger 2015), which further supported the utilization of functional rest state MRI.

The putative SMA and pre-SMA in medial frontal area has been identified by another feasible approach, co-activation based parcellation (Eickhoff, et al. 2011). The co-activation based parcellation identified the border between the two clusters was located close to VCA line (Eickhoff, et al. 2011), which was identical with the present study. Moreover, the areas defined by co-activation based parcellation and cytoarchitectonic parcellation showed some common co-activation patterns. E.g., the anterior cluster showed significantly higher co-activation probabilities with inferior frontal and posterior parietal cortices while the posterior cluster was significantly stronger co-activated with precentral gyrus, and caudal dorsal premotor cortex (Eickhoff, et al. 2011). Despite the good agreement between co-activation based parcellation and cytoarchitectonic parcellation in determining the rough borders and some co-activation clusters from MACM analysis, differences are still emerged. E.g., the co-activation pattern parcellation defined pre-SMA (Eickhoff, et al. 2011) locates more anterior than the cytoarchitectonic delineated pre-SMA, which is reflected in subsequent MACM analysis using the two method defined areas as seed regions: the saccade task is related to the SMA derived from functional co-activation parcellation, but related to the pre-SMA derived from cytoarchitecture analysis (Eickhoff, et al. 2011). This discrepancy in specific location may be caused by different approaches. Moreover, it should be noted that cytoarchitecture reflects the inner organization of cortical areas which is related but not completely equal to the functional properties of these regions.

4.4 Comparison between the maps in macaque and human

According to previous studies (Luppino, et al.1993; Tanji 1994), the organizations of F3 (identical with SMA in human) and F6 (identical with pre-SMA in human) in monkeys were similar with humans. Area F3 located in the caudal part of mesial frontal cortex and area F6 located in the rostral part of mesial frontal cortex. They both bordered with the dorsal-lateral adjacent areas just in the medial-dorsal-arch, which was similar with the present study in humans.

The human cortex has 10 times the surface area of macaque cortex. Compared with macaque brains, human brains have four basic differences, bigger areas, functional divergence, areas gained or lost, and rearrangements (Stanislas Dehaene 2005). According to the previous stimulation studies, supplementary eye field in human was within the area SMA, located rostral to the area for hand and foot movements (area SMA), partly overlapped with area SMA, or located in the border between the SMA and pre-SMA, close to the paracentral sulcus (Grosbras, et al. 1999; Yamamoto, et al. 2004). The SEF in the macaques, however, lay on the dorsolateral convexity (Schlag and Schlag-Rey 1987; Tehovnik, et al. 2000). So far there is no architectonic evidence available to define supplementary eye field in humans or monkeys.

4.5 Understanding the functional connectivity of areas SMA and pre-SMA

With coordinates based meta-analytic connectivity modelling analysis, the distinct co-activation patterns for area SMA and pre-SMA were investigated. This approach allows us to place the functional aspects of a single area into the context of a neural network.

It was found that areas SMA and pre-SMA share large degree of overlap in co-activation networks involving precentral gyrus, supramarginal gyrus, superior frontal gyrus, rolandic operculum, thalamus, putamen and cerebellum. Some co-activation clusters were supported by previous fibre tracking studies. E.g. the SMA and pre-SMA project to the putamen and cerebellum (Alexander, et al. 1986; Akkal, et al. 2007). The SMA projects to the thalamus in the nucleus ventralis lateralis parsoralis (VLo) part, the pre-SMA connects with thalamus in the nuleus ventralis anterior pars parvocellularis (VApc) (Olszewski 1952; Schell and Strick 1984; Wiesendanger and Wiesendanger

1985; Rouiller, et al. 1999). The anatomical connections between the two areas and precentral gyrus (primary motor cortex), and between the two areas and superior frontal gyrus (premotor cortex) were also found (Luppino, et al. 1993). Although the direct fibre connections between the current areas and rolandic operculum have not been reported, the indirect connections have been found. For example, the functional magnetic resonance imaging study found both supplementary motor area and rolandic operculum connected with inferior parietal lobule (Zhang and Li 2014). On the other hand, functional connectivity does not imply a direct anatomical connection between the respective brain regions (Eickhoff and Grefkes 2011). Therefore, the co-activation clusters between areas SMA, pre-SMA and rolandic operculum is possible, although there are no direct connections found.

4.6 From architectonical gradation to functional gradation

In the present study, the architectonical gradation was found. From caudal areas to rostral areas, the changes of cytoarchitectonic characterizations showed some common trends: the relative cell density and cell size in layer IIIc decreased; the cell density in layer V increased. These findings in these areas are in accordance with the notion that cortical areas do not simply form a mosaic, but are hierarchically organized (Amunts and Zilles 2012). Moreover, the conjunction analysis of functional decoding showed that both areas pre-SMA and SMA are involved to action/execution. In addition, previous studies revealed that the more posterior area primary motor cortex also acts an important role in the execution of body movement (Hlustik, et al. 2001; Schieber 2001). Interestingly, movements are more difficult to elicit from pre-SMA than from SMA or from primary motor cortex (Luppino, et al. 1991). That means the functional related areas from the primary motor area, to area SMA, to area pre-SMA, the function of execution decreased. The function changes between areas might be clarified by the architectonic change.n fact it is extremely difficult to place a simple movement into a single brain area, which may suggest that the functions of human brain present in the form of non-mosaic-like change and the functions across brain areas show subtle functional gradation. This kind of functional gradation may be clarified by the architectonic gradation.

4.7 Functional distinction of mesial frontal cortex and its neighboring areas

The functional segregation of areas SMA and pre-SMA has been found by our contrast analysis of functional decoding. Area SMA was more likely associated with action rest, action execution than area pre-SMA, whereas, area pre-SMA was related to more functions beyond action execution like cognition, emotion, learning, speech and perception. However, there is somewhat confusing regarding the functional distinction between mesial frontal cortex and its neighboring areas: anterior midcingulate cortex (aMCC), dorsomedial prefrontal cortex (dmPFC), dorsal premotor cortex.

4.7.1 Distinction between mesial frontal cortex and a aMCC

In the present study, it was found that the co-activation areas of mesial frontal cortex were mainly located in precentral gyrus, rolandic operculum, supramarginal gyrus, lateral premotor cortex, superior temporal gyrus, superior parietal lobule, inferior frontal gyrus, inferior parietal lobule, inferior occipital gyrus, putamen, cerebellum and thalamus. Previous functional connectivity analyses showed that aMCC co-activated with mesial frontal cortex, rolandic operculum, dorsolateral prefrontal cortex, inferior frontal junction, anterior insula, lateral premotor cortex, inferior parietal lobule, intraparietal sulcus, pallidum, putamen, thalamus and cerebellum (Hoffstaedter, et al. 2014). Despite large overlapping connectivity pattern between mesial frontal and aMCC, it was found that supramarginal gyrus, superior temporal gyrus, superior parietal lobule and inferior occipital gyrus specifically co-activated with mesial frontal cortex. However, dorsolateral prefrontal cortex, BA 45 and intraparietal sulcus more likely co-activated with aMCC (Hoffstaedter, et al. 2014). The different co-activation pattern between mesial frontal cortex and aMCC might be interpreted by the function segregation between the two areas. E.g., mesial frontal cortex contributed to word processing (Chung, et al. 2005; Stoeckel, et al. 2009). However, aMCC was not found to contribute to word processing. This functional difference may be reflected in the individual co-activation pattern of mesial frontal cortex and aMCC.

The aMCC is involved to pain and negative affect including fear-induced activity (Vogt, et al. 2003). Lesions in aMCC can cause impairment in recognizing fear, disgust and anger (Tolomeo, et al. 2016). The negative affect may further contribute to the function of aMCC in cognitive motor control (Shackman, et al. 2011; Tolomeo, et al. 2016). Functional imaging studies showed that a specific part of the aMCC plays an

important role in intentional movement initiation (Hoffstaedter, et al. 2013). These cues do not mean contradictions considering that pain and negative affect normally evoke strong intention to control in order to change the painful situation (Hoffstaedter, et al. 2014). In sum, compared with mesial frontal cortex, the function of aMCC in cognitive motor control was more likely coupled with pain and negative effect.

4.7.2 Distinction between mesial frontal cortex and dmPFC

The functional connectivity of dmPFC was investigated by Eickhoff and co-workers using functional connectivity parcellation (Eickhoff et al. 2016). It was noted that mesial frontal cortex and dmPFC showed overlapping functional connectivity with inferior parietal cortex, inferior frontal gyrus and prefrontal cortex. However, the dmPFC was co-activated specifically with clusters involving emotion like amygdale and hippocampus (Eickhoff et al. 2016). In contrast, the mesial frontal cortex was more strongly co-activated with precentral gyrus, supramarginal gyrus, lateral premotor cortex, superior temporal gyrus, superior parietal lobule, putamen, cerebellum and thalamus. These divergences of functional connectivity networks have been reflected from the functional aspect. The dmPFC is related to emotion and social cognition (Eickhoff et al. 2016), which is not found in the functional coding analysis of mesial frontal cortex in present study.

4.7.3 Distinction between mesial frontal cortex and dorsal premotor cortex

Co-activation clusters of dorsal premotor areas identified by MACM were located in dorsal prefrontal cortex, precentral gyrus, rostral intraparietal sulcus, anterior insula, secondary somatosensory cortex, Broca's region, thalamus, putamen and cerebellum (Benjamin et al. 2016). It could be found that extensive overlapped co-activation areas between dorsal premotor cortex and mesial frontal cortex. Compared with mesial frontal cortex, the dorsal premotor was more likely to co-activate with dorsal prefrontal cortex. In addition, the mesial frontal cortex connected with cerebellum at lobule VI, while the dorsal premotor connected with dorsal surface of cerebellum (Benjamin et al. 2016).

From functional coding aspect, both dorsal premotor cortex and mesial frontal cortex were related to action (execution, imagination), interoception, cognition/space, but the

functional segregations between the two regions still could be found. The mesial frontal cortex was associated with action motor learning, action execution speech and cognition music. The dorsal premotor cortex, however, showed high activation probability for working memory (Benjamin et al. 2016).

4.8 Methodological consideration

The evidence from hierarchical clustering analysis in present study supported the distribution of areas SMA and pre-SMA. The method used in the present study calculates the gray level index (GLI), an estimate of the cell density of neurons, which is not interfered by the anisotropy and the cutting direction of histological serial sections. This quantitative cytoarchitectural analysis tool is especially important, because the borders between areas are not clearly defined in vast majority of cytoarchitectonic areas by pure visual inspection under microscope. For example, the cytoarchitectonic borders between area M1 (primary motor cortex) and area SMA cannot be easily defined by microscope checking. The cytoarchitectonic features (Betz cells in layer Vb of area M1, prominent layer IIIc in area SMA) change gradually at the transition area between the two areas. In such cases, some authors using qualitative analysis marked the transition area as an independent transition area (Von Economo and Koskinas 1925) or even put the border in the middle of this "transitional" zone (White, et al. 1997), which might cause biased or irreproducible result due to subjective evaluation. The observer-independent algorithm can position the precise border where the program finds significant peak in multivariate distance function (Fig. 4.8.1). This procedure allows one to recognize a transition as a distinct cytoarchitectonic unit with observer-independent reproducibly borders (Amunts, et al. 1999). According to the objective analysis, one can define the degree of similarity between the cytoarchitecture of the transition area and the neighbouring area with unbiased estimate. This algorithm-based mapping procedures has been successfully applied for more than 40 areas (Schleicher, et al. 2009) of the human isocortex such as area Brodmann's 44 and 45 (Amunts, et al. 1999), human medial orbitofrontal cortex (Henssen, et al. 2016), human frontal pole (Bludau, et al. 2014), human posterior insular cortex (Kurth, et al. 2010), human anterior cingulated cortex (Palomero-Gallagher, et al. 2008), human primary somatosensory

cortex (Geyer, et al. 1999). These applications have successfully introduced the mapping procedures.
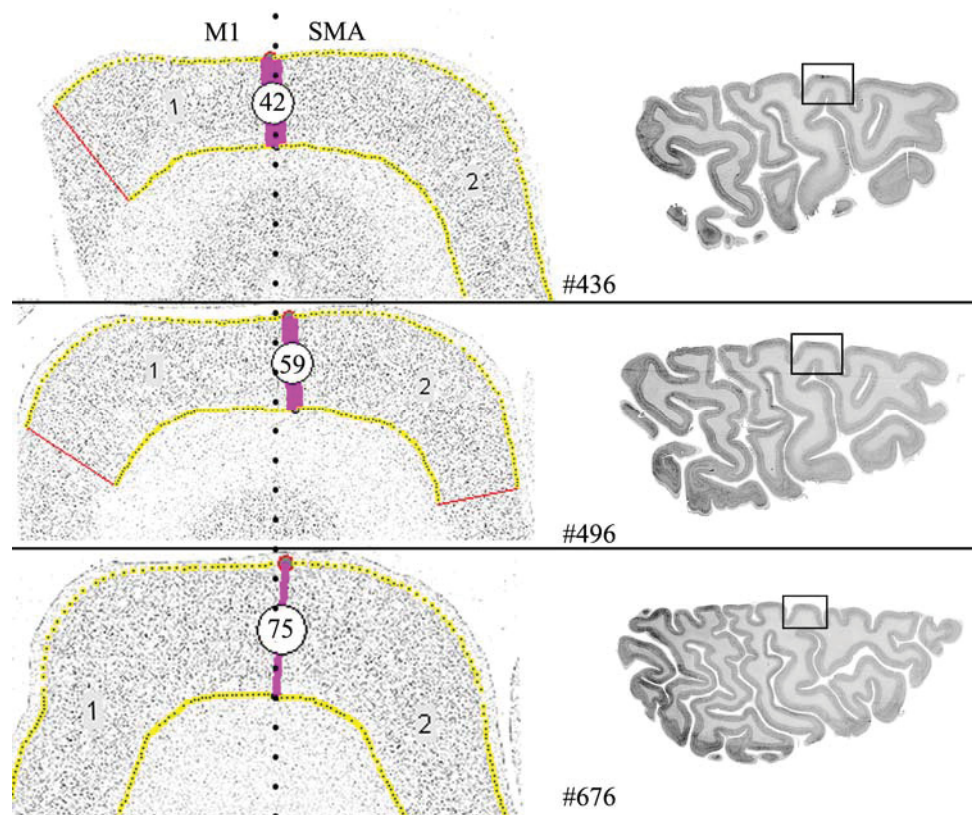
Fig. 4.8.1 The quantitative cytoarchitectonic analysis on the three adjacent sections in brain case 17. It can be noted that this algorithm defined the borders stably and reproducibly across the neighboring sections.

The present cytoarchitectural analysis tools cannot identify the cell morphometric parameters. Beside the differences in cell density, it has been found some differences in cell shape between area SMA and pre-SMA. The neurons in layer III and V is more homologous in area SMA than those in area pre-SMA. The pyramidal in lower part of layer III and layer V of area SMA are elongated. However, in area pre-SMA those cells in layer III are smaller and the cells in layer V are relative squat. This leads to the poor lamination and difficult to demarcate layer III and V in area SMA. More information or subareas may be found in future when one algorithm including cell shape analysis is introduced.

5 Conclusions and outlooks

In present study, it was demonstrated that the mesial frontal motor cortex comprised of two structurally and functionally heterogeneous brain regions: area SMA and pre-SMA. The probability maps of areas SMA and pre-SMA are a step toward a complete map of the human motor cortex, which is based on observer-independent mapping. Using the maximum probabilistic maps of areas SMA and pre-SMA as seed regions for the coordinate based neuroimaging meta-analysis, a functional segregation between areas SMA and pre-SMA was revealed. These results supported the microstructural, and functional segregation of areas SMA and pre-SMA.

These findings of the present study may contribute to understanding of the correlation between the microstructural parcellation and its functional segregation of mesial frontal area. The cytoarchitectonic parcellation of area SMA and pre-SMA can be used as anatomical constraints for a precise mapping for the interpretation of functional neuroimaging studies. How brain activity allows behaviour and produces mental activity is one of the overarching grand challenges of neuroscience for the twenty-first century (Hougan2008). Integrating novel multiple approaches to distinguish cortical modules may contribute to the understanding of the brain on multiple levels (Amunts and Zilles 2015).

6 Reference

Aizawa, H., M. Inase, et al. (1991). "Reorganization of activity in the supplementary motor area associated with motor learning and functional recovery." Exp Brain Res **84**(3): 668-671.

Akkal, D., R. P. Dum, et al. (2007). "Supplementary motor area and presupplementary motor area: targets of basal ganglia and cerebellar output." J Neurosci **27**(40): 10659-10673.

Alexander, G. E., M. R. DeLong, et al. (1986). "Parallel organization of functionally segregated circuits linking basal ganglia and cortex." Annu Rev Neurosci **9**: 357-381.

Amick, M. M., H. E. Schendan, et al. (2006). "Frontostriatal circuits are necessary for visuomotor transformation: mental rotation in Parkinson's disease." Neuropsychologia **44**(3): 339-349.

Amunts, K., E. Armstrong, et al. (2007). "Gender-specific left-right asymmetries in human visual cortex." J Neurosci **27**(6): 1356-1364.

Amunts, K., O. Kedo, et al. (2005). "Cytoarchitectonic mapping of the human amygdala, hippocampal region and entorhinal cortex: intersubject variability and probability maps." Anat Embryol (Berl) **210**(5-6): 343-352.

Amunts, K., A. Malikovic, et al. (2000). "Brodmann's areas 17 and 18 brought into stereotaxic space-where and how variable?" Neuroimage **11**(1): 66-84.

Amunts, K., G. Schlaug, et al. (1996). "Asymmetry in the human motor cortex and handedness." Neuroimage **4**(3 Pt 1): 216-222.

Amunts, K., A. Schleicher, et al. (1999). "Broca's region revisited: cytoarchitecture and intersubject variability." J Comp Neurol **412**(2): 319-341.

Amunts, K., F. Schmidt-Passos, et al. (1997). "Postnatal development of interhemispheric asymmetry in the cytoarchitecture of human area 4." Anat Embryol (Berl) **196**(5): 393-402.

Amunts, K. and K. Zilles (2001). "Advances in cytoarchitectonic mapping of the human cerebral cortex." Neuroimaging Clin N Am **11**(2): 151-169, vii.

Amunts, K. and K. Zilles (2012). "Architecture and organizational principles of Broca's region." Trends Cogn Sci **16**(8): 418-426.

Amunts, K. and K. Zilles (2015). "Architectonic Mapping of the Human Brain beyond Brodmann." Neuron **88**(6): 1086-1107.

Ariani, G., M. F. Wurm, et al. (2015). "Decoding Internally and Externally Driven Movement Plans." J Neurosci **35**(42): 14160-14171.

Assal, F., S. Schwartz, et al. (2007). "Moving with or without will: functional neural correlates of alien hand syndrome." Ann Neurol **62**(3): 301-306.

Axel Schleicher, K. A., Stephan Geyer, Tilo Kowalski, Karl Zilles (1998). "An observer-independent cytoarchitectonic mapping of the human cortex using a stereological approach." Acta Stereologica **17**.

Bailey., G. V. B. E. P. (1947). The Neocortex of Macaca mulatta. Urbana, Illionois, The University of Illinois Press.

Baleydier, C., P. Achache, et al. (1997). "Neurofilament architecture of superior and mesial premotor cortex in the human brain." Neuroreport **8**(7): 1691-1696.

Bannur, U. and V. Rajshekhar (2000). "Post operative supplementary motor area syndrome: clinical features and outcome." Br J Neurosurg **14**(3): 204-210.

Barbas, H. and D. N. Pandya (1987). "Architecture and frontal cortical connections of the premotor cortex (area 6) in the rhesus monkey." J Comp Neurol **256**(2): 211-228.

Benjamin Sigl, Caspers S, Mohlberg H, Cieslik E, Eickhoff S, Amunts K. 2016. The human dorsal premotor cortex – cytoarchitecture, maps and function. In.

Bertrand, G. (1956). "Spinal efferent pathways from the supplementary motor area." Brain **79**(3): 461-473.

Bludau, S., S. B. Eickhoff, et al. (2014). "Cytoarchitecture, probability maps and functions of the human frontal pole." Neuroimage **93 Pt 2**: 260-275.

Braak, H. and E. Braak (1976). "The pyramidal cells of Betz within the cingulate and precentral gigantopyramidal field in the human brain. A Golgi and pigmentarchitectonic study." Cell Tissue Res **172**(1): 103-119.

Braak, H. (1980). Architectonics of the Human Telencephalic Cortex. Germany, Springer-Verlag.

Brinkman, C. (1981). "Lesions in supplementary motor area interfere with a monkey's performance of a bimanual coordination task." Neurosci Lett **27**(3): 267-270.

Brockhaus, H. (1940). "Die Cyto- und Myeloarchitektonik des Cortex claustralis und des Claustrum beim Menschen." J. Psychol. Neurol. **49**: 249-348.

Brodmann, K. (1909). Vergleichende Lokalisationslehre der Grosshirnrinde in ihren Prinzipien dargestellt auf Grund des Zellenbaues. Leipzig, Johann Ambrosius Barth.

Chainay, H., A. Krainik, et al. (2004). "Foot, face and hand representation in the human supplementary motor area." Neuroreport **15**(5): 765-769.

Chao, H. H., X. Luo, et al. (2009). "Activation of the pre-supplementary motor area but not inferior prefrontal cortex in association with short stop signal reaction time--an intra-subject analysis." BMC Neurosci **10**: 75.

Chen, X. and V. Stuphorn (2015). "Sequential selection of economic good and action in medial frontal cortex of macaques during value-based decisions." Elife **4**.

Chin-shoou Lin, J. L. L., Frank Berkowitz (2007). "Somatotopic Identification of Language-SMA in Language Processing via fMRI." Journal of Scientific and Practical Computing **1**(2): 3-8.

Chung, G. H., Y. M. Han, et al. (2005). "Functional heterogeneity of the supplementary motor area." AJNR Am J Neuroradiol **26**(7): 1819-1823.

Chung, G. H., Y. M. Han, et al. (2000). "Functional MRI of the supplementary motor area: comparison of motor and sensory tasks." J Comput Assist Tomogr **24**(4): 521-525.

Cona, G., G. Marino, et al. (2016). "TMS of supplementary motor area (SMA) facilitates mental rotation performance: Evidence for sequence processing in SMA." Neuroimage.

Coull, J. T., F. Vidal, et al. (2004). "Functional anatomy of the attentional modulation of time estimation." Science **303**(5663): 1506-1508.

Crucian, G. P., S. Armaghani, et al. (2014). "Dopamine does not appear to affect mental rotation in Parkinson's disease." J Mov Disord **7**(2): 77-83.

Crucian, G. P., A. M. Barrett, et al. (2003). "Mental object rotation in Parkinson's disease." J Int Neuropsychol Soc **9**(7): 1078-1087.

Cui, R. Q., D. Huter, et al. (2000). "High resolution DC-EEG mapping of the Bereitschaftspotential preceding simple or complex bimanual sequential finger movement." Exp Brain Res **134**(1): 49-57.

Cunnington, R., C. Windischberger, et al. (2002). "The preparation and execution of self-initiated and externally-triggered movement: a study of event-related fMRI." Neuroimage **15**(2): 373-385.

Cunnington, R., C. Windischberger, et al. (2003). "The preparation and readiness for voluntary movement: a high-field event-related fMRI study of the Bereitschafts-BOLD response." Neuroimage **20**(1): 404-412.

Deecke, L. and H. H. Kornhuber (1978). "An electrical sign of participation of the mesial 'supplementary' motor cortex in human voluntary finger movement." Brain Res **159**(2): 473-476.

Deecke, L., W. Lang, et al. (1987). "Bereitschaftspotential in patients with unilateral lesions of the supplementary motor area." J Neurol Neurosurg Psychiatry **50**(11): 1430-1434.

Deecke, L., P. Scheid, et al. (1969). "Distribution of readiness potential, pre-motion positivity, and motor potential of the human cerebral cortex preceding voluntary finger movements." Exp Brain Res **7**(2): 158-168.

Defebvre, L., J. L. Bourriez, et al. (1994). "Spatiotemporal study of Bereitschaftspotential and event-related desynchronization during voluntary movement in Parkinson's disease." Brain Topogr **6**(3): 237-244.

Deiber, M. P., M. Honda, et al. (1999). "Mesial motor areas in self-initiated versus externally triggered movements examined with fMRI: effect of movement type and rate." J Neurophysiol **81**(6): 3065-3077.

Della Sala, S., A. Francescani, et al. (2002). "Gait apraxia after bilateral supplementary motor area lesion." J Neurol Neurosurg Psychiatry **72**(1): 77-85.

Dick, J. P., J. C. Rothwell, et al. (1989). "The Bereitschaftspotential is abnormal in Parkinson's disease." Brain **112 (Pt 1)**: 233-244.

Dixon, W. J., Brown, M. B., Engelman, L., Hill, M. A., and Jennrich, R. I (1988). BMDP Statistical Software Manual. Berkeley, Univ. of California Press.

Draganski, B., F. Kherif, et al. (2008). "Evidence for segregated and integrative connectivity patterns in the human Basal Ganglia." J Neurosci **28**(28): 7143-7152.

Dreher, J. C., W. Trapp, et al. (1999). "Planning dysfunction in schizophrenia: impairment of potentials preceding fixed/free and single/sequence of self-initiated finger movements." Exp Brain Res **124**(2): 200-214.

Dum, R. P. and P. L. Strick (1991). "The origin of corticospinal projections from the premotor areas in the frontal lobe." J Neurosci **11**(3): 667-689.

Dum, R. P. and P. L. Strick (1996). "Spinal cord terminations of the medial wall motor areas in macaque monkeys." J Neurosci **16**(20): 6513-6525.

Durston, S., K. M. Thomas, et al. (2002). "The effect of preceding context on inhibition: an event-related fMRI study." Neuroimage **16**(2): 449-453.

Eickhoff, S. B., A. R. Laird, et al. (2016). "Functional Segregation of the Human Dorsomedial Prefrontal Cortex." Cereb Cortex **26**(1): 304-321.

Eickhoff, S., N. B. Walters, et al. (2005). "High-resolution MRI reflects myeloarchitecture and cytoarchitecture of human cerebral cortex." Hum Brain Mapp **24**(3): 206-215.

Eickhoff, S. B., D. Bzdok, et al. (2012). "Activation likelihood estimation meta-analysis revisited." Neuroimage **59**(3): 2349-2361.

Eickhoff, S. B., D. Bzdok, et al. (2011). "Co-activation patterns distinguish cortical modules, their connectivity and functional differentiation." Neuroimage **57**(3): 938-949.

Eickhoff, S. B. and C. Grefkes (2011). "Approaches for the integrated analysis of structure, function and connectivity of the human brain." Clin EEG Neurosci **42**(2): 107-121.

Eickhoff, S. B., S. Heim, et al. (2006). "Testing anatomically specified hypotheses in functional imaging using cytoarchitectonic maps." Neuroimage **32**(2): 570-582.

Eickhoff, S. B., A. Schleicher, et al. (2007). "Analysis of neurotransmitter receptor distribution patterns in the cerebral cortex." Neuroimage **34**(4): 1317-1330.

Eickhoff, S. B., K. E. Stephan, et al. (2005). "A new SPM toolbox for combining probabilistic cytoarchitectonic maps and functional imaging data." Neuroimage **25**(4): 1325-1335.

Emeric, E. E., M. Leslie, et al. (2010). "Performance monitoring local field potentials in the medial frontal cortex of primates: supplementary eye field." J Neurophysiol **104**(3): 1523-1537.

Evans, A. C., A. L. Janke, et al. (2012). "Brain templates and atlases." Neuroimage **62**(2): 911-922.

Evans, A. C., S. Marrett, et al. (1992). "Anatomical mapping of functional activation in stereotactic coordinate space." Neuroimage **1**(1): 43-53.

Feinberg, T. E., R. J. Schindler, et al. (1992). "Two alien hand syndromes." Neurology **42**(1): 19-24.

Ferrandez, A. M., L. Hugueville, et al. (2003). "Basal ganglia and supplementary motor area subtend duration perception: an fMRI study." Neuroimage **19**(4): 1532-1544.

Fontaine, D., L. Capelle, et al. (2002). "Somatotopy of the supplementary motor area: evidence from correlation of the extent of surgical resection with the clinical patterns of deficit." Neurosurgery **50**(2): 297-303; discussion 303-295.

Fox, P. T. and J. L. Lancaster (2002). "Opinion: Mapping context and content: the BrainMap model." Nat Rev Neurosci **3**(4): 319-321.

Fox, P. T., J. L. Lancaster, et al. (2014). "Meta-analysis in human neuroimaging: computational modeling of large-scale databases." Annu Rev Neurosci **37**: 409-434.

Fried, I., A. Katz, et al. (1991). "Functional organization of human supplementary motor cortex studied by electrical stimulation." J Neurosci **11**(11): 3656-3666.

Fulton, J. F. (1935). "A note on the definition of the "motor" and "premotor" areas." Brain **58**: 311-316.

Galaburda, A. M., J. Corsiglia, et al. (1987). "Planum temporale asymmetry, reappraisal since Geschwind and Levitsky." Neuropsychologia **25**(6): 853-868.

Garraux, G., P. Peigneux, et al. (2007). "Task-related interaction between basal ganglia and cortical dopamine release." J Neurosci **27**(52): 14434-14441.

Gaymard, B., S. Rivaud, et al. (1993). "Role of the left and right supplementary motor areas in memory-guided saccade sequences." Ann Neurol **34**(3): 404-406.

Geyer, S., A. Ledberg, et al. (1996). "Two different areas within the primary motor cortex of man." Nature **382**(6594): 805-807.

Geyer, S., M. Matelli, et al. (1998). "Receptor autoradiographic mapping of the mesial motor and premotor cortex of the macaque monkey." J Comp Neurol **397**(2): 231-250.

Geyer, S., M. Matelli, et al. (2000). "Functional neuroanatomy of the primate isocortical motor system." Anat Embryol (Berl) **202**(6): 443-474.

Geyer, S., A. Schleicher, et al. (1999). "Areas 3a, 3b, and 1 of human primary somatosensory cortex." Neuroimage **10**(1): 63-83.

Geyer, S., K. Zilles, et al. (2000). "Neurofilament protein distribution in the macaque monkey dorsolateral premotor cortex." Eur J Neurosci **12**(5): 1554-1566.

Geyer, S. and R. Turner (2015). Microstructural parcellation of the human cerebral cortex, Springer.

Grafton, S. T., M. A. Arbib, et al. (1996). "Localization of grasp representations in humans by positron emission tomography. 2. Observation compared with imagination." Exp Brain Res **112**(1): 103-111.

Grosbras, M. H., E. Lobel, et al. (1999). "An anatomical landmark for the supplementary eye fields in human revealed with functional magnetic resonance imaging." Cereb Cortex **9**(7): 705-711.

Gundersen, H. J., T. F. Bendtsen, et al. (1988). "Some new, simple and efficient stereological methods and their use in pathological research and diagnosis." APMIS **96**(5): 379-394.

Gyung Ho Chung, Y. M. H., Su-Hyun Jeong, Heon Lee, Gong Yong Jin, and Sang Yong Lee, (2004). "Somatotopic Mapping of the Supplementary Motor Area." Journal of the Korean Society of Magnetic Resonance in Medicine **8**(1): 9-16.

Hömke, L. (2006). "A multigrid method for anisotropic PDEs in elastic image registration." Numerical Linear Algebra with Applications **13**(2-3): 215-229.

Hans-Joachim. Kretschmann, F. W. (1971). Computeranwendungen bei Wachstumsproblemen in Biologie und Medizin. Berlin, Springer.

Halsband, U., N. Ito, et al. (1993). "The role of premotor cortex and the supplementary motor area in the temporal control of movement in man." Brain **116 (Pt 1)**: 243-266.

Hammond, G. (2002). "Correlates of human handedness in primary motor cortex: a review and hypothesis." Neurosci Biobehav Rev **26**(3): 285-292.

Hassan, A. and K. A. Josephs (2016). "Alien Hand Syndrome." Curr Neurol Neurosci Rep **16**(8): 73.

He, S. Q., R. P. Dum, et al. (1995). "Topographic organization of corticospinal projections from the frontal lobe: motor areas on the medial surface of the hemisphere." J Neurosci **15**(5 Pt 1): 3284-3306.

Heinrichs-Graham, E., D. J. Arpin, et al. (2016). "Cue-related Temporal Factors Modulate Movement-related Beta Oscillatory Activity in the Human Motor Circuit." J Cogn Neurosci **28**(7): 1039-1051.

Hertrich, I., S. Dietrich, et al. (2016). "The role of the supplementary motor area for speech and language processing." Neurosci Biobehav Rev **68**: 602-610.

Henn S, S. T., Engler K, Zilles K, Witsch K (1997). Elastische Anpassung in der digitalen Bildverarbeitung auf mehreren Auflösungsstufen mit Hilfe von Mehrgitterverfahren. In: Paulus E, Wahl FM (eds) Mustererkennung. Berlin, Springer.

Henssen, A., K. Zilles, et al. (2016). "Cytoarchitecture and probability maps of the human medial orbitofrontal cortex." Cortex **75**: 87-112.

Hikosaka, O., K. Sakai, et al. (1996). "Activation of human presupplementary motor area in learning of sequential procedures: a functional MRI study." J Neurophysiol **76**(1): 617-621.

Hlustik, P., A. Solodkin, et al. (2001). "Somatotopy in human primary motor and somatosensory hand representations revisited." Cereb Cortex **11**(4): 312-321.

Hodgson, T. L., W. H. Dittrich, et al. (1999). "Eye movements and spatial working memory in Parkinson's disease." Neuropsychologia **37**(8): 927-938.

Hoffstaedter, F., C. Grefkes, et al. (2014). "The role of anterior midcingulate cortex in cognitive motor control: evidence from functional connectivity analyses." Hum Brain Mapp 35(6): 2741-2753.

Hoffstaedter, F., C. Grefkes, et al. (2013). "The "what" and "when" of self-initiated movements." Cereb Cortex 23(3): 520-530.

Holmes, C. J., R. Hoge, et al. (1998). "Enhancement of MR images using registration for signal averaging." J Comput Assist Tomogr **22**(2): 324-333.

Hopf, A. (1956). "Über die Verteilung myeloarchitektonischer Merkmale in der Stirnhirnrinde beim Menschen." J Hirnforsch **2**(4): 311-333.

Hoshi, E. and J. Tanji (2004). "Differential roles of neuronal activity in the supplementary and presupplementary motor areas: from information retrieval to motor planning and execution." J Neurophysiol **92**(6): 3482-3499.

Hougan M, A. B. (2008). From molecules to minds—challenges for the 21st century: workshop summary. Washington, DC, National Academies.

Huerta, M. F. and J. H. Kaas (1990). "Supplementary eye field as defined by intracortical microstimulation: connections in macaques." J Comp Neurol **293**(2): 299-330.

Husain, M., A. Parton, et al. (2003). "Self-control during response conflict by human supplementary eye field." Nat Neurosci **6**(2): 117-118.

Hupfeld, K. E., C. J. Ketcham, et al. (2016). "Transcranial direct current stimulation (tDCS) to the supplementary motor area (SMA) influences performance on motor tasks." Exp Brain Res.

Iansek, R., J. L. Bradshaw, et al. (1995). Chapter 3 Interaction of the basal ganglia and supplementary motor area in the elaboration of movement. Advances in Psychology. J. G. Denis and P. P. Jan, North-Holland. **Volume 111:** 37-59.

Inase, M., S. T. Sakai, et al. (1996). "Overlapping corticostriatal projections from the supplementary motor area and the primary motor cortex in the macaque monkey: an anterograde double labeling study." J Comp Neurol **373**(2): 283-296.

Inase, M., H. Tokuno, et al. (1999). "Corticostriatal and corticosubthalamic input zones from the presupplementary motor area in the macaque monkey: comparison with the input zones from the supplementary motor area." Brain Res **833**(2): 191-201.

Iseki, K. and T. Hanakawa (2010). "[The functional significance of the basal ganglia-thalamo-cortical loop in gait control in humans: a neuroimaging approach]." Brain Nerve **62**(11): 1157-1164.

Jahanshahi, M., I. H. Jenkins, et al. (1995). "Self-initiated versus externally triggered movements. I. An investigation using measurement of regional cerebral blood flow with PET and movement-related potentials in normal and Parkinson's disease subjects." Brain **118 (Pt 4)**: 913-933.

Jenkins, I. H., W. Fernandez, et al. (1992). "Impaired activation of the supplementary motor area in Parkinson's disease is reversed when akinesia is treated with apomorphine." Ann Neurol **32**(6): 749-757.

Jenkins, I. H., M. Jahanshahi, et al. (2000). "Self-initiated versus externally triggered movements. II. The effect of movement predictability on regional cerebral blood flow." Brain **123 (Pt 6)**: 1216-1228.

Johansen-Berg, H., T. E. Behrens, et al. (2004). "Changes in connectivity profiles define functionally distinct regions in human medial frontal cortex." Proc Natl Acad Sci U S A **101**(36): 13335-13340.

Johnston, S., E. C. Leek, et al. (2004). "Functional contribution of medial premotor cortex to visuo-spatial transformation in humans." Neurosci Lett **355**(3): 209-212.

Joliot, M., G. Jobard, et al. (2015). "AICHA: An atlas of intrinsic connectivity of homotopic areas." J Neurosci Methods **254**: 46-59.

Jones, S. E., B. R. Buchbinder, et al. (2000). "Three-dimensional mapping of cortical thickness using Laplace's equation." Hum Brain Mapp **11**(1): 12-32.

Judaš, M. and M. Cepanec (2010). "Oskar Vogt: The first myeloarchitectonic map of the human frontal cortex." Translational Neuroscience **1**(1): 72-94.

Jurgens, U. (1984). "The efferent and afferent connections of the supplementary motor area." Brain Res **300**(1): 63-81.

Karl Zilles. (1990). In The Human Nervous System. Cortex. G. Paxinos. San Diego, Academic Press**:** 757-802.

Kasasbeh, A. S., C. K. Yarbrough, et al. (2012). "Characterization of the supplementary motor area syndrome and seizure outcome after medial frontal lobe resections in pediatric epilepsy surgery." Neurosurgery **70**(5): 1152-1168; discussion 1168.

Kazennikov, O., B. Hyland, et al. (1998). "Effects of lesions in the mesial frontal cortex on bimanual co-ordination in monkeys." Neuroscience **85**(3): 703-716.

Kennerley, S. W., K. Sakai, et al. (2004). "Organization of action sequences and the role of the pre-SMA." J Neurophysiol **91**(2): 978-993.

Kim, J. H., J. M. Lee, et al. (2010). "Defining functional SMA and pre-SMA subregions in human MFC using resting state fMRI: functional connectivity-based parcellation method." Neuroimage **49**(3): 2375-2386.

Kim, Y. K. and S. H. Shin (2014). "Comparison of effects of transcranial magnetic stimulation on primary motor cortex and supplementary motor area in motor skill learning (randomized, cross over study)." Front Hum Neurosci **8**: 937.

Klein, J. C., T. E. J. Behrens, et al. (2007). "Connectivity-based parcellation of human cortex using diffusion MRI: Establishing reproducibility, validity and observer independence in BA 44/45 and SMA/pre-SMA." Neuroimage **34**(1): 204-211.

Kornhuber, H. H. and L. Deecke (1965). "Hirnpotentialänderungen bei Willkürbewegungen und passiven Bewegungen des Menschen: Bereitschaftspotential und reafferente Potentiale." Pflüger's Archiv für die gesamte Physiologie des Menschen und der Tiere **284**(1): 1-17.

Constantin von Economo; Georg N Koskinas. (1925). Die cytoarchitektonik der hirnrinde des erwachsenen menschen. Wien, Springer.

Kotz, S. A. and M. Schwartze (2011). "Differential input of the supplementary motor area to a dedicated temporal processing network: functional and clinical implications." Front Integr Neurosci **5**: 86.

Krainik, A., H. Duffau, et al. (2004). "Role of the healthy hemisphere in recovery after resection of the supplementary motor area." Neurology **62**(8): 1323-1332.

Krainik, A., S. Lehericy, et al. (2003). "Postoperative speech disorder after medial frontal surgery: role of the supplementary motor area." Neurology **60**(4): 587-594.

Krainik, A., S. Lehericy, et al. (2001). "Role of the supplementary motor area in motor deficit following medial frontal lobe surgery." Neurology **57**(5): 871-878.

Krings, T., R. Topper, et al. (2000). "Cortical activation patterns during complex motor tasks in piano players and control subjects. A functional magnetic resonance imaging study." Neurosci Lett **278**(3): 189-193.

Kunieda, T., A. Ikeda, et al. (2000). "Different activation of presupplementary motor area, supplementary motor area proper, and primary sensorimotor area,

depending on the movement repetition rate in humans." Exp Brain Res **135**(2): 163-172.

Kurth, F., S. B. Eickhoff, et al. (2010). "Cytoarchitecture and probabilistic maps of the human posterior insular cortex." Cereb Cortex **20**(6): 1448-1461.

Laird, A. R., S. B. Eickhoff, et al. (2011). "The BrainMap strategy for standardization, sharing, and meta-analysis of neuroimaging data." BMC Res Notes **4**: 349.

Laird, A. R., S. B. Eickhoff, et al. (2009). "ALE Meta-Analysis Workflows Via the Brainmap Database: Progress Towards A Probabilistic Functional Brain Atlas." Front Neuroinform **3**: 23.

Laird, A. R., P. M. Fox, et al. (2005). "ALE meta-analysis: controlling the false discovery rate and performing statistical contrasts." Hum Brain Mapp **25**(1): 155-164.

Lamm, C., C. Windischberger, et al. (2001). "Evidence for premotor cortex activity during dynamic visuospatial imagery from single-trial functional magnetic resonance imaging and event-related slow cortical potentials." Neuroimage **14**(2): 268-283.

Langner, R., C. Rottschy, et al. (2014). "Meta-analytic connectivity modeling revisited: Controlling for activation base rates." Neuroimage **99**: 559-570.

Laplane, D., J. Talairach, et al. (1977). "Clinical consequences of corticectomies involving the supplementary motor area in man." J Neurol Sci **34**(3): 301-314.

Lau, H. C., R. D. Rogers, et al. (2004). "Attention to intention." Science **303**(5661): 1208-1210.

Lee, A. C., J. P. Harris, et al. (1998). "Impairments of mental rotation in Parkinson's disease." Neuropsychologia **36**(1): 109-114.

Lee, D. and S. Quessy (2003). "Activity in the supplementary motor area related to learning and performance during a sequential visuomotor task." J Neurophysiol **89**(2): 1039-1056.

144

Lee, V. M., L. Otvos, Jr., et al. (1988). "Identification of the major multiphosphorylation site in mammalian neurofilaments." Proc Natl Acad Sci U S A **85**(6): 1998-2002.

Leek, E. C. and S. J. Johnston (2009). "Functional specialization in the supplementary motor complex." Nat Rev Neurosci **10**(1): 78; author reply 78.

Li, C. S., C. Huang, et al. (2006). "Imaging response inhibition in a stop-signal task: neural correlates independent of signal monitoring and post-response processing." J Neurosci **26**(1): 186-192.

Liddle, P. F., K. A. Kiehl, et al. (2001). "Event-related fMRI study of response inhibition." Hum Brain Mapp **12**(2): 100-109.

Lima, C. F., S. Krishnan, et al. (2016). "Roles of Supplementary Motor Areas in Auditory Processing and Auditory Imagery." Trends Neurosci **39**(8): 527-542.

Linden, D. E., R. A. Bittner, et al. (2003). "Cortical capacity constraints for visual working memory: dissociation of fMRI load effects in a fronto-parietal network." Neuroimage **20**(3): 1518-1530.

Luppino, G., M. Matelli, et al. (1993). "Corticocortical connections of area F3 (SMA-proper) and area F6 (pre-SMA) in the macaque monkey." J Comp Neurol **338**(1): 114-140.

Luppino, G., M. Matelli, et al. (1994). "Corticospinal projections from mesial frontal and cingulate areas in the monkey." Neuroreport **5**(18): 2545-2548.

Luppino, G., M. Matelli, et al. (1991). "Multiple representations of body movements in mesial area 6 and the adjacent cingulate cortex: an intracortical microstimulation study in the macaque monkey." J Comp Neurol **311**(4): 463-482.

Luppino, G. and G. Rizzolatti (2000). "The Organization of the Frontal Motor Cortex." News Physiol Sci **15**: 219-224.

Luppino, G., S. Rozzi, et al. (2003). "Prefrontal and agranular cingulate projections to the dorsal premotor areas F2 and F7 in the macaque monkey." Eur J Neurosci **17**(3): 559-578.

Maier, M. A., J. Armand, et al. (2002). "Differences in the corticospinal projection from primary motor cortex and supplementary motor area to macaque upper limb motoneurons: an anatomical and electrophysiological study." Cereb Cortex **12**(3): 281-296.

Manocha, S. (1970). Macaca Mulatta: Enzyme Histochemistry of the Nervous System. United States of America, Academic Press,INC.

Marsden, C. D. (1989). "Slowness of movement in Parkinson's disease." Mov Disord **4 Suppl 1**: S26-37.

Matelli, M., G. Luppino, et al. (1985). "Patterns of cytochrome oxidase activity in the frontal agranular cortex of the macaque monkey." Behav Brain Res **18**(2): 125-136.

Matelli, M., G. Luppino, et al. (1991). "Architecture of superior and mesial area 6 and the adjacent cingulate cortex in the macaque monkey." J Comp Neurol **311**(4): 445-462.

Matelli, M., G. Rizzolatti, et al. (1993). "Activation of precentral and mesial motor areas during the execution of elementary proximal and distal arm movements: a PET study." Neuroreport **4**(12): 1295-1298.

Matsuzaka, Y., H. Aizawa, et al. (1992). "A motor area rostral to the supplementary motor area (presupplementary motor area) in the monkey: neuronal activity during a learned motor task." J Neurophysiol **68**(3): 653-662.

Matsuzaka, Y. and J. Tanji (1996). "Changing directions of forthcoming arm movements: neuronal activity in the presupplementary and supplementary motor area of monkey cerebral cortex." J Neurophysiol **76**(4): 2327-2342.

Mendez, M. F. (2004). "Aphemia-like syndrome from a right supplementary motor area lesion." Clin Neurol Neurosurg **106**(4): 337-339.

Merker, B. (1983). "Silver staining of cell bodies by means of physical development." J Neurosci Methods **9**(3): 235-241.

Michely, J., L. J. Volz, et al. (2015). "Dopaminergic modulation of motor network dynamics in Parkinson's disease." Brain **138**(Pt 3): 664-678.

Miller, K. J., G. Schalk, et al. (2010). "Cortical activity during motor execution, motor imagery, and imagery-based online feedback." Proc Natl Acad Sci U S A **107**(9): 4430-4435.

Mita, A., H. Mushiake, et al. (2009). "Interval time coding by neurons in the presupplementary and supplementary motor areas." Nat Neurosci **12**(4): 502-507.

Mitz, A. R. and S. P. Wise (1987). "The somatotopic organization of the supplementary motor area: intracortical microstimulation mapping." J Neurosci **7**(4): 1010-1021.

Mullen, R. J., C. R. Buck, et al. (1992). "NeuN, a neuronal specific nuclear protein in vertebrates." Development **116**(1): 201-211.

Nachev, P., C. Kennard, et al. (2008). "Functional role of the supplementary and pre-supplementary motor areas." Nat Rev Neurosci **9**(11): 856-869.

Nachev, P., G. Rees, et al. (2005). "Volition and conflict in human medial frontal cortex." Curr Biol **15**(2): 122-128.

Nachev, P., H. Wydell, et al. (2007). "The role of the pre-supplementary motor area in the control of action." Neuroimage **36 Suppl 2**: T155-163.

Nakamura, K., K. Sakai, et al. (1998). "Neuronal activity in medial frontal cortex during learning of sequential procedures." J Neurophysiol **80**(5): 2671-2687.

Nakamura, K., K. Sakai, et al. (1999). "Effects of local inactivation of monkey medial frontal cortex in learning of sequential procedures." J Neurophysiol **82**(2): 1063-1068.

Nambu, A., M. Takada, et al. (1996). "Dual somatotopical representations in the primate subthalamic nucleus: evidence for ordered but reversed body-map transformations from the primary motor cortex and the supplementary motor area." J Neurosci **16**(8): 2671-2683.

Nambu, A., H. Tokuno, et al. (2002). "Functional significance of the cortico-subthalamo-pallidal 'hyperdirect' pathway." Neurosci Res **43**(2): 111-117.

Nirkko, A. C., C. Ozdoba, et al. (2001). "Different ipsilateral representations for distal and proximal movements in the sensorimotor cortex: activation and deactivation patterns." Neuroimage **13**(5): 825-835.

Northoff, G., A. Pfennig, et al. (2000). "Delayed onset of late movement-related cortical potentials and abnormal response to lorazepam in catatonia." Schizophr Res **44**(3): 193-211.

Obhi, S. S., P. Haggard, et al. (2002). "rTMS to the supplementary motor area disrupts bimanual coordination." Motor Control **6**(4): 319-332.

Ohara, S., A. Ikeda, et al. (2000). "Movement-related change of electrocorticographic activity in human supplementary motor area proper." Brain **123 (Pt 6)**: 1203-1215.

Ohmae, S., T. Takahashi, et al. (2015). "Decoding the timing and target locations of saccadic eye movements from neuronal activity in macaque oculomotor areas." J Neural Eng **12**(3): 036014.

Olszewski, J. (1952). he thalamus of the Macaca Mulatta. Basel and New York, S. Karger.

Orgogozo, J. M. and B. Larsen (1979). "Activation of the supplementary motor area during voluntary movement in man suggests it works as a supramotor area." Science **206**(4420): 847-850.

P. C. Mahalanobis, D. N. M., M. W. M. Yeatts and C. Radhakrishna Rao (1949). Anthropometric Survey of the United Provinces, 1941: A Statistical Study. Sankhyā, the Indian Statistical Institute.

Pai, M. C. (1999). "Supplementary motor area aphasia: a case report." Clin Neurol Neurosurg **101**(1): 29-32.

Palomero-Gallagher, N., H. Mohlberg, et al. (2008). "Cytology and receptor architecture of human anterior cingulate cortex." J Comp Neurol **508**(6): 906-926.

Palomero-Gallagher, N., B. A. Vogt, et al. (2009). "Receptor architecture of human cingulate cortex: evaluation of the four-region neurobiological model." Hum Brain Mapp **30**(8): 2336-2355.

Park, H., J. S. Kim, et al. (2013). "Differential beta-band event-related desynchronization during categorical action sequence planning." PLoS One **8**(3): e59544.

Parton, A., P. Nachev, et al. (2007). "Role of the human supplementary eye field in the control of saccadic eye movements." Neuropsychologia **45**(5): 997-1008.

Pastor, M. A., B. L. Day, et al. (2004). "The functional neuroanatomy of temporal discrimination." J Neurosci **24**(10): 2585-2591.

Penfield, W. (1950). "The supplementary motor area in the cerebral cortex of man." Arch Psychiatr Nervenkr Z Gesamte Neurol Psychiatr **185**(6-7): 670-674.

Penfield, W. and E. Boldrey (1937). "Somatic motor and sensory representation in the cerebral cortex of man as studied by electrical stimulation." Brain **60**(4): 389-443.

Penfield, W. and K. Welch (1951). "The supplementary motor area of the cerebral cortex; a clinical and experimental study." AMA Arch Neurol Psychiatry **66**(3): 289-317.

Pfurtscheller, G., M. Woertz, et al. (2003). "Early onset of post-movement beta electroencephalogram synchronization in the supplementary motor area during self-paced finger movement in man." Neurosci Lett **339**(2): 111-114.

Picard, N. and P. L. Strick (1996). "Motor areas of the medial wall: a review of their location and functional activation." Cereb Cortex **6**(3): 342-353.

Playford, E. D., I. H. Jenkins, et al. (1992). "Impaired mesial frontal and putamen activation in Parkinson's disease: a positron emission tomography study." Ann Neurol **32**(2): 151-161.

Pollmann, S. and D. Y. von Cramon (2000). "Object working memory and visuospatial processing: functional neuroanatomy analyzed by event-related fMRI." Exp Brain Res **133**(1): 12-22.

Potgieser, A. R., B. M. de Jong, et al. (2014). "Insights from the supplementary motor area syndrome in balancing movement initiation and inhibition." Front Hum Neurosci **8**: 960.

Purcell, B. A., P. K. Weigand, et al. (2012). "Supplementary eye field during visual search: salience, cognitive control, and performance monitoring." J Neurosci **32**(30): 10273-10285.

Rascol, O., U. Sabatini, et al. (1994). "Normal activation of the supplementary motor area in patients with Parkinson's disease undergoing long-term treatment with levodopa." J Neurol Neurosurg Psychiatry **57**(5): 567-571.

Ray, S. and S. J. Heinen (2015). "A mechanism for decision rule discrimination by supplementary eye field neurons." Exp Brain Res **233**(2): 459-476.

Richter, W., R. Somorjai, et al. (2000). "Motor area activity during mental rotation studied by time-resolved single-trial fMRI." J Cogn Neurosci **12**(2): 310-320.

Rizzolatti, G., G. Luppino, et al. (1996). "The classic supplementary motor area is formed by two independent areas." Adv Neurol **70**: 45-56.

Rizzolatti, G., G. Luppino, et al. (1998). "The organization of the cortical motor system: new concepts." Electroencephalogr Clin Neurophysiol **106**(4): 283-296.

Roberts, R. E. and M. Husain (2015). "A dissociation between stopping and switching actions following a lesion of the pre-supplementary motor area." Cortex **63**: 184-195.

Robinson, J. L., A. R. Laird, et al. (2012). "The functional connectivity of the human caudate: an application of meta-analytic connectivity modeling with behavioral filtering." Neuroimage **60**(1): 117-129.

Robinson, J. L., A. R. Laird, et al. (2010). "Metaanalytic connectivity modeling: delineating the functional connectivity of the human amygdala." Hum Brain Mapp **31**(2): 173-184.

Roland, P. E., B. Larsen, et al. (1980). "Supplementary motor area and other cortical areas in organization of voluntary movements in man." J Neurophysiol **43**(1): 118-136.

Roland, P. E. and K. Zilles (1994). "Brain atlases - a new research tool." Trends in Neurosciences **17**(11): 458-467.

Roland, P. E. and K. Zilles (1996). "The developing European computerized human brain database for all imaging modalities." Neuroimage **4**(3 Pt 2): S39-47.

Roland, P. E. and K. Zilles (1998). "Structural divisions and functional fields in the human cerebral cortex." Brain Res Brain Res Rev **26**(2-3): 87-105.

Roth, M., J. Decety, et al. (1996). "Possible involvement of primary motor cortex in mentally simulated movement: a functional magnetic resonance imaging study." Neuroreport **7**(7): 1280-1284.

Rouiller, E. M., J. Tanne, et al. (1999). "Origin of thalamic inputs to the primary, premotor, and supplementary motor cortical areas and to area 46 in macaque monkeys: a multiple retrograde tracing study." J Comp Neurol **409**(1): 131-152.

Rushworth, M. F., K. A. Hadland, et al. (2002). "Role of the human medial frontal cortex in task switching: a combined fMRI and TMS study." J Neurophysiol **87**(5): 2577-2592.

Sakai, K., O. Hikosaka, et al. (1999). "Presupplementary motor area activation during sequence learning reflects visuo-motor association." J Neurosci **19**(10): RC1.

Sampaio-Baptista, C., A. A. Khrapitchev, et al. (2013). "Motor skill learning induces changes in white matter microstructure and myelination." J Neurosci **33**(50): 19499-19503.

Sanides, F. (1962). Die Architektonik des Menschlichen Gehirns, Springer-Verlag (in German), Springer-Verlag.

Sanides, F. (1964). "The Cyto-Myeloarchitecture of the Human Frontal Lobe and Its Relation to Phylogenetic Differentiation of the Cerebral Cortex." J Hirnforsch **7**: 269-282.

Sarkisov SA, F. I., Preobrashenskaya NS. (1949). Cytoarchitecture of the Human Cortex Cerebri. Moscow, Medgiz.

Scepkowski, L. A. and A. Cronin-Golomb (2003). "The alien hand: cases, categorizations, and anatomical correlates." Behav Cogn Neurosci Rev **2**(4): 261-277.

Schaefer, M., H. J. Heinze, et al. (2010). "Alien hand syndrome: neural correlates of movements without conscious will." PLoS One **5**(12): e15010.

Schell, G. R. and P. L. Strick (1984). "The origin of thalamic inputs to the arcuate premotor and supplementary motor areas." J Neurosci **4**(2): 539-560.

Schieber, M. H. (2001). "Constraints on somatotopic organization in the primary motor cortex." J Neurophysiol **86**(5): 2125-2143.

Schlag, J. and M. Schlag-Rey (1987). "Evidence for a supplementary eye field." <u>J Neurophysiol</u> **57**(1): 179-200.

Schleicher, A., K. Amunts, et al. (2000). "A stereological approach to human cortical architecture: identification and delineation of cortical areas." <u>J Chem Neuroanat</u> **20**(1): 31-47.

Schleicher, A., K. Amunts, et al. (1999). "Observer-independent method for microstructural parcellation of cerebral cortex: A quantitative approach to cytoarchitectonics." <u>Neuroimage</u> **9**(1): 165-177.

Schleicher, A., P. Morosan, et al. (2009). "Quantitative architectural analysis: a new approach to cortical mapping." <u>J Autism Dev Disord</u> **39**(11): 1568-1581.

Schleicher, A., N. Palomero-Gallagher, et al. (2005). "Quantitative architectural analysis: a new approach to cortical mapping." <u>Anat Embryol (Berl)</u> **210**(5-6): 373-386.

Schleicher, A. and K. Zilles (1990). "A quantitative approach to cytoarchitectonics: analysis of structural inhomogeneities in nervous tissue using an image analyser." <u>J Microsc</u> **157**(Pt 3): 367-381.

Schleicher, A., K. Zilles, et al. (1986). "A quantitative approach to cytoarchitectonics: software and hardware aspects of a system for the evaluation and analysis of structural inhomogeneities in nervous tissue." <u>J Neurosci Methods</u> **18**(1–2): 221-235.

Scholz, J., M. C. Klein, et al. (2009). "Training induces changes in white-matter architecture." <u>Nat Neurosci</u> **12**(11): 1370-1371.

Schormann, T., A. Dabringhaus, et al. (1995). "Statistics of deformations in histology and application to improved alignment with MRI." <u>IEEE Trans Med Imaging</u> **14**(1): 25-35.

Schormann, T., S. Henn, et al. (1996). A new approach to fast elastic alignment with applications to human brains. <u>Visualization in Biomedical Computing: 4th</u>

International Conference, VBC'96 Hamburg, Germamy, September 22–25, 1996 Proceedings. K. H. Höhne and R. Kikinis. Berlin, Heidelberg, Springer Berlin Heidelberg**:** 337-342.

Schormann, T., M. von Matthey, et al. (1993). "Alignment of 3-D brain data sets originating from MR and histology." Bioimaging **1**(2): 119-128.

Schormann, T. and K. Zilles (1997). "Limitations of the principal-axes theory." IEEE Trans Med Imaging **16**(6): 942-947.

Schormann, T. and K. Zilles (1998). "Three-dimensional linear and nonlinear transformations: an integration of light microscopical and MRI data." Hum Brain Mapp **6**(5-6): 339-347.

Schultze-Kraft, M., D. Birman, et al. (2016). "The point of no return in vetoing self-initiated movements." Proc Natl Acad Sci U S A **113**(4): 1080-1085.

Schwartze, M., K. Rothermich, et al. (2012). "Functional dissociation of pre-SMA and SMA-proper in temporal processing." Neuroimage **60**(1): 290-298.

Shackman, A. J., T. V. Salomons, et al. (2011). "The integration of negative affect, pain and cognitive control in the cingulate cortex." Nat Rev Neurosci **12**(3): 154-167.

Shima, K., H. Mushiake, et al. (1996). "Role for cells in the presupplementary motor area in updating motor plans." Proc Natl Acad Sci U S A **93**(16): 8694-8698.

Shima, K. and J. Tanji (1998). "Both supplementary and presupplementary motor areas are crucial for the temporal organization of multiple movements." J Neurophysiol **80**(6): 3247-3260.

Shima, K. and J. Tanji (2006). "Binary-coded monitoring of a behavioral sequence by cells in the pre-supplementary motor area." J Neurosci **26**(9): 2579-2582.

Shirota, Y., H. Ohtsu, et al. (2013). "Supplementary motor area stimulation for Parkinson disease: a randomized controlled study." Neurology **80**(15): 1400-1405.

Shook, B. L., M. Schlag-Rey, et al. (1990). "Primate supplementary eye field: I. Comparative aspects of mesencephalic and pontine connections." J Comp Neurol **301**(4): 618-642.

Shook, B. L., M. Schlag-Rey, et al. (1991). "Primate supplementary eye field. II. Comparative aspects of connections with the thalamus, corpus striatum, and related forebrain nuclei." J Comp Neurol **307**(4): 562-583.

Simonyan, K. and S. Fuertinger (2015). "Speech networks at rest and in action: interactions between functional brain networks controlling speech production." J Neurophysiol **113**(7): 2967-2978.

Smith, A. M. (1979). "The activity of supplementary motor area neurons during a maintained precision grip." Brain Res **172**(2): 315-327.

Smith, E. E., J. Jonides, et al. (1998). "Components of verbal working memory: evidence from neuroimaging." Proc Natl Acad Sci U S A **95**(3): 876-882.

Smith, S. M., P. T. Fox, et al. (2009). "Correspondence of the brain's functional architecture during activation and rest." Proc Natl Acad Sci U S A **106**(31): 13040-13045.

So, N. and V. Stuphorn (2016). "Supplementary Eye Field Encodes Confidence in Decisions Under Risk." Cereb Cortex **26**(2): 764-782.

Stanislas Dehaene, J.-R. D., Marc D. Hauser, Giacomo Rizzolatti (2005). From Monkey Brain to Human Brain A Fyssen Foundation Symposium. Cambridge Massachusetts, MIT Press.

Stanton, G. B., C. J. Bruce, et al. (1993). "Topography of projections to the frontal lobe from the macaque frontal eye fields." J Comp Neurol **330**(2): 286-301.

Steinmetz, H., J. Rademacher, et al. (1990). "Total surface of temporoparietal intrasylvian cortex: diverging left-right asymmetries." Brain Lang **39**(3): 357-372.

Stephan, K. M., G. R. Fink, et al. (1995). "Functional anatomy of the mental representation of upper extremity movements in healthy subjects." J Neurophysiol **73**(1): 373-386.

Sternberger, L. A. and N. H. Sternberger (1983). "Monoclonal antibodies distinguish phosphorylated and nonphosphorylated forms of neurofilaments in situ." Proc Natl Acad Sci U S A **80**(19): 6126-6130.

Stinear, C. M., J. P. Coxon, et al. (2009). "Primary motor cortex and movement prevention: where Stop meets Go." Neurosci Biobehav Rev **33**(5): 662-673.

Strasburger, E. H. (1937). "Die myeloarchitektonische Gliederung des Stirnhirns beim Menschen und Schimpansen." Journal fur psychologie und neurologie **47**(6): 565-606.

Stoeckel, C., P. M. Gough, et al. (2009). "Supramarginal gyrus involvement in visual word recognition." Cortex **45**(9): 1091-1096.

Stuphorn, V. (2015). "The role of supplementary eye field in goal-directed behavior." J Physiol Paris **109**(1-3): 118-128.

Stuphorn, V., J. W. Brown, et al. (2010). "Role of supplementary eye field in saccade initiation: executive, not direct, control." J Neurophysiol **103**(2): 801-816.

Sumner, P., P. Nachev, et al. (2007). "Human medial frontal cortex mediates unconscious inhibition of voluntary action." Neuron **54**(5): 697-711.

Sweeney, J. A., M. A. Mintun, et al. (1996). "Positron emission tomography study of voluntary saccadic eye movements and spatial working memory." J Neurophysiol **75**(1): 454-468.

Talairach, J. T., P. (1988). Coplanar Stereotaxic Atlas of the Human Brain. Stuttgart, Thieme.

Tanji, J. (1985). "Comparison of neuronal activities in the monkey supplementary and precentral motor areas." Behav Brain Res **18**(2): 137-142.

Tanji, J. (1994). "The supplementary motor area in the cerebral cortex." Neurosci Res **19**(3): 251-268.

Tanji, J. (1996). "New concepts of the supplementary motor area." Curr Opin Neurobiol **6**(6): 782-787.

Tanji, J. (2001). "Sequential organization of multiple movements: involvement of cortical motor areas." Annu Rev Neurosci **24**: 631-651.

Tanji, J. and K. Kurata (1979). "Neuronal activity in the cortical supplementary motor area related with distal and proximal forelimb movements." Neurosci Lett **12**(2-3): 201-206.

Tanji, J. and K. Kurata (1982). "Comparison of movement-related activity in two cortical motor areas of primates." J Neurophysiol **48**(3): 633-653.

Tanji, J. and K. Kurata (1985). "Contrasting neuronal activity in supplementary and precentral motor cortex of monkeys. I. Responses to instructions determining motor responses to forthcoming signals of different modalities." J Neurophysiol **53**(1): 129-141.

Tanji, J. and K. Shima (1994). "Role for supplementary motor area cells in planning several movements ahead." Nature **371**(6496): 413-416.

Tanji, J. and K. Shima (1996). "Supplementary motor cortex in organization of movement." Eur Neurol **36 Suppl 1**: 13-19.

Tankus, A., Y. Yeshurun, et al. (2009). "Encoding of speed and direction of movement in the human supplementary motor area." J Neurosurg **110**(6): 1304-1316.

Tehovnik, E. J., M. A. Sommer, et al. (2000). "Eye fields in the frontal lobes of primates." Brain Res Brain Res Rev **32**(2-3): 413-448.

Tellmann, S., S. Bludau, et al. (2015). "Cytoarchitectonic mapping of the human brain cerebellar nuclei in stereotaxic space and delineation of their co-activation patterns." Front Neuroanat **9**: 54.

Thaler, D. E., E. T. Rolls, et al. (1988). "Neuronal activity of the supplementary motor area (SMA) during internally and externally triggered wrist movements." Neurosci Lett **93**(2-3): 264-269.

Thickbroom, G. W., M. L. Byrnes, et al. (2000). "The role of the supplementary motor area in externally timed movement: the influence of predictability of movement timing." Brain Res **874**(2): 233-241.

Thomas, C., F. Q. Ye, et al. (2014). "Anatomical accuracy of brain connections derived from diffusion MRI tractography is inherently limited." Proc Natl Acad Sci U S A **111**(46): 16574-16579.

Tolomeo, S., D. Christmas, et al. (2016). "A causal role for the anterior mid-cingulate cortex in negative affect and cognitive control." Brain **139**(6): 1844-1854.

Triarhou, L. C. (2007). "A proposed number system for the 107 cortical areas of Economo and Koskinas, and Brodmann area correlations." Stereotact Funct Neurosurg **85**(5): 204-215.

Uhl, F., A. W. Kornhuber, et al. (1996). "Supplementary motor area in spatial coordination of bilateral movements: a new aspect to 'the SMA debate'?" Electroencephalogr Clin Neurophysiol **101**(6): 469-477.

Ulu, M. O., N. Tanriover, et al. (2008). "Surgical treatment of lesions involving the supplementary motor area: clinical results of 12 patients." Turk Neurosurg **18**(3): 286-293.

Vergani, F., L. Lacerda, et al. (2014). "White matter connections of the supplementary motor area in humans." J Neurol Neurosurg Psychiatry **85**(12): 1377-1385.

Vogt, B. A. and L. Vogt (2003). "Cytology of human dorsal midcingulate and supplementary motor cortices." J Chem Neuroanat **26**(4): 301-309.

Vogt, B. A., G. R. Berger, et al. (2003). "Structural and functional dichotomy of human midcingulate cortex." Eur J Neurosci **18**(11): 3134-3144.

Vogt Cécile , V. O. (1919). "Allgemeine Ergebnisse unserer Hirnforschung." J Psychol Neurol **25**: 277-462.

Vogt, O. (1906). "Der Wert der myelogenetischen Felder der Grosshirnrinde (Cortex pallii)." Anat. Anz **29**: 273.

Vogt, O. (1910). "Die myeloarchitektonische Felderung des menschlichen Stirnhirns." J Psychol Neurol **15**(4/5): 221-232.

Vogt, O. and C. Vogt (1903). "Zur anatomischen Gliederung des Cortex cerebri." J Psychol Neurol **2**: 160-180.

Vorobiev, V., P. Govoni, et al. (1998). "Parcellation of human mesial area 6: cytoarchitectonic evidence for three separate areas." Eur J Neurosci **10**(6): 2199-2203.

Walter, C. A. (1905). Histological studies on the localisation of cerebral function, Cambridge, University Press.

Ward, J. H. (1963). "Hierarchical Grouping to Optimize an Objective Function." Journal of the American Statistical Association 58(301): 236-244.

White, L. E., T. J. Andrews, et al. (1997). "Structure of the human sensorimotor system. I: Morphology and cytoarchitecture of the central sulcus." Cereb Cortex **7**(1): 18-30.

Wiesendanger, R. and M. Wiesendanger (1985). "The thalamic connections with medial area 6 (supplementary motor cortex) in the monkey (macaca fascicularis)." Exp Brain Res **59**(1): 91-104.

Windischberger, C., C. Lamm, et al. (2003). "Human motor cortex activity during mental rotation." Neuroimage **20**(1): 225-232.

Wise, S. P. (1996). "Corticospinal efferents of the supplementary sensorimotor area in relation to the primary motor area." Adv Neurol **70**: 57-69.

Wise, S. P. and J. Tanji (1981). "Supplementary and precentral motor cortex: contrast in responsiveness to peripheral input in the hindlimb area of the unanesthetized monkey." J Comp Neurol **195**(3): 433-451.

Woolsey, C. N., P. H. Settlage, et al. (1952). "Patterns of localization in precentral and "supplementary" motor areas and their relation to the concept of a premotor area." Res Publ Assoc Res Nerv Ment Dis **30**: 238-264.

Wree, A., A. Schleicher, et al. (1982). "Estimation of volume fractions in nervous tissue with an image analyzer." J Neurosci Methods **6**(1-2): 29-43.

Wriessnegger, S. C., D. Steyrl, et al. (2014). "Short time sports exercise boosts motor imagery patterns: implications of mental practice in rehabilitation programs." Front Hum Neurosci **8**: 469.

Yamamoto, J., A. Ikeda, et al. (2004). "Human eye fields in the frontal lobe as studied by epicortical recording of movement-related cortical potentials." Brain **127**(Pt 4): 873-887.

Yang, S. N. and S. Heinen (2014). "Contrasting the roles of the supplementary and frontal eye fields in ocular decision making." J Neurophysiol **111**(12): 2644-2655.

Yazawa, S., A. Ikeda, et al. (1998). "Human supplementary motor area is active in preparation for both voluntary muscle relaxation and contraction: subdural recording of Bereitschaftspotential." Neurosci Lett **244**(3): 145-148.

Yeo, S. S., P. H. Chang, et al. (2013). "The cortical activation differences between proximal and distal joint movements of the upper extremities: a functional NIRS study." NeuroRehabilitation **32**(4): 861-866.

Zhang, S. and C. S. Li (2014). "Functional clustering of the human inferior parietal lobule by whole-brain connectivity mapping of resting-state functional magnetic resonance imaging signals." Brain Connect **4**(1): 53-69.

Zilles, K. and K. Amunts (2009). "Receptor mapping: architecture of the human cerebral cortex." Curr Opin Neurol **22**(4): 331-339.

Zilles, K., N. Palomero-Gallagher, et al. (2002). "Architectonics of the human cerebral cortex and transmitter receptor fingerprints: reconciling functional neuroanatomy and neurochemistry." Eur Neuropsychopharmacol **12**(6): 587-599.

Zilles, K., M. Qu, et al. (1993). "Regional distribution and heterogeneity of alpha-adrenoceptors in the rat and human central nervous system." J Hirnforsch **34**(2): 123-132.

Zilles, K., G. Schlaug, et al. (1996). "Anatomy and transmitter receptors of the supplementary motor areas in the human and nonhuman primate brain." Adv Neurol **70**: 29-43.

Zilles, K., G. Schlaug, et al. (1995). "Mapping of human and macaque sensorimotor areas by integrating architectonic, transmitter receptor, MRI and PET data." J Anat **187 (Pt 3)**: 515-537.

Zilles, K. Palomero-Gallagher N, Amunts, K. (2015). Myeloarchitecture and maps of the cerebral cortex. Brain Mapping: An Encyclopedic Reference. A. W.Toga, Academic Press: Elsevier. 2: 137-156.

Zilles, K., Schlaug, G., Geyer, S., Luppino, G., Matelli, M., Que, M., et al. (1996). Anatomy and transmitter receptors of the supplementary motor areas in the human and nonhuman primate brain. In H. O. Lueders (Ed.), Supplementary Sensorimotor Area. Philadelphia, Lippincott-Raven.

Zilles, K., A. Schleicher, et al. (1997). "Quantitative analysis of sulci in the human cerebral cortex: development, regional heterogeneity, gender difference, asymmetry, intersubject variability and cortical architecture." Hum Brain Mapp **5**(4): 218-221.

Zilles, K., A. Schleicher, et al. (1988). "Quantitative receptor autoradiography in the human brain." Histochemistry **90**(2): 129-137.

Zilles, K., A. Schleicher, et al. (1986). "Quantitative autoradiography of transmitter binding sites with an image analyzer." J Neurosci Methods **18**(1-2): 207-220.

Curriculum Vitae

Name: Jianghai Ruan

Address: Cécile and Oskar Vogt Institute of Brain Research

Heinrich-Heine-Universitaet,

40225, Duesseldorf

E-mail: Jianghai.Ruan@hhu.de

Educational background:

12. 2015 - present: Ph.D student in Cécile and Oskar Vogt Institute of Brain Research at Heinrich-Heine University, Duesseldorf, Germany

12. 2012 - 12. 2015: Ph.D student in Centre of Neurology and Neuropsychiatry, LVR-Klinikum Duesseldorf, Hospital of the Heinrich-Heine-University Duesseldorf

07.2010 - 07.2012: Master of Clinical Medicine, Beijing University of Chinese Medicine, Beijing, China

09.2007 - 7.2010: Bachelor of Traditional Chinese Medicine, Beijing University of Chinese Medicine, Beijing, China

07.2005 - 07.2007: College of Biology, in Nankai University, Tianjin, China

Publications:

J Ruan & RJ Seitz. Impaired Sleep and Reduced Spontaneous Movement Activity in Acute Stroke: An Exploratory Study. J J Neur Neurosci. 2014, 1(2): 008.

Ruan, J., G. Wang, et al. (2014). "[Clinical-diffusion mismatch and short-term clinical outcomes among patients with acute ischemic stroke]." Zhonghua Yi Xue Za Zhi 94(9): 678-683.[Article in Chinese]

Patent:

Ruan Jianghai,An Intelligent Control System for Household Electrical Apparatus Based on Human Brain EEG Signal Detection.Patent number: CN104914727A

Honors:

Granted a full scholarship from Program of Governmental Graduate students Scholarship launched by China Scholarship Council (2012).